AFML-TR-72-199

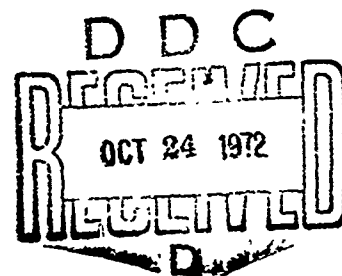# RESEARCH ON SYNTHESIS OF
HIGH-STRENGTH ALUMINUM ALLOYS

J. D. Boyd, D. C. Drennen, C. J. Martin, C. W. Price,
A. R. Rosenfield, and D. N. Williams

BATTELLE
Columbus Laboratories

D. S. Thompson
Reynolds Metals Company

D D C

RECEIVED

OCT 24 1972

D

NOTICE

When Government drawings, specifications, or other data are used for any purpose other than in connection with a definitely related Government procurement operation, the United States Government thereby incurs no responsibility nor any obligation whatsoever; and the fact that the government may have formulated, furnished, or in any way supplied the said drawings, specifications, or other data, is not to be regarded by implication or otherwise as in any manner licensing the holder or any other person or corporation, or conveying any rights or permission to manufacture, use, or sell any patented invention that may in any way be related thereto.

DOCUMENT CONTROL DATA - R & D

(Security classification of title, body of abstract and indexing annotation must be entered when the overall report is classified)

1 ORIGINATING ACTIVITY *(Corporate author)*	2a. REPORT SECURITY CLASSIFICATION
Battelle's Columbus Laboratories 505 King Avenue Columbus, Ohio 43201	Unclassified
	2b. GROUP N/A

3 REPORT TITLE

Research on Synthesis of High Strength Aluminum Alloys

4. DESCRIPTIVE NOTES *(Type of report and inclusive dates)*

First Annual Progress Report

5. AUTHOR(S) *(First name, middle initial, last name)*

I. D. Boyd	C. W. Price	D. N. Williams
D. C. Drennen	A. R. Rosenfield	
C. J. Martin	D. S. Thompson	

6. REPORT DATE	7a. TOTAL NO. OF PAGES	7b. NO. OF REFS
July 1972	97	26

8a. CONTRACT OR GRANT NO F33615-71-C-1805	9a. ORIGINATOR'S REPORT NUMBER(S)
b. PROJECT NO. 7353	
c. Task No. 735302	9b. OTHER REPORT NO(S) *(Any other numbers that may be assigned this report)* AFML-TR-72-199
d.	

10 DISTRIBUTION STATEMENT

Approved for public release; distribution unlimited.

11 SUPPLEMENTARY NOTES	12. SPONSORING MILITARY ACTIVITY
	Air Force Materials Laboratory Air Force Systems Command Wright-Patterson Air Force Base, Ohio 45433

13. ABSTRACT

The objective of Task A is to provide increased strength and fracture resistance in aluminum alloys by optimizing the precipitate microstructure. To control the size and distribution of the intermediate precipitates in some high-strength 7000 and 2000 series alloys, several alloys were cast and their precipitate microstructures characterized by microscopy after homogenization treatments at various times and temperatures. Homogenization treatments were selected to produce a fine and a coarse intermediate precipitate. The objective of Task B is to develop a recrystallized microstructure in wrought high-strength aluminum alloys during hot working. Recrystallization occurred along the grain boundaries in the 2024 alloy only at the highest upset rate (8.8 inch/sec) and the highest temperature (925 F). Preliminary microscopy results indicate that the intermediate precipitate in 2024 may not be stable during hot working. Recrystallization appeared to be complete in the Al-4.6Cu alloy upset at 8.8 inch/sec at 925 F, but recrystallization only along grain boundaries was observed at a slower rate of 0.016 inch/sec at the same temperature. Preliminary work on an Al-5.6Zn-2.4Mg-1.4Cu alloy has shown that the alloy resists recrystallization during hot working and recrystallizes to a moderately fine grain size on subsequent solution heat treatment.

DD FORM 1 NOV 65 1473

14 KEY WORDS	LINK A		LINK B		LINK C	
	ROLE	WT	ROLE	WT	ROLE	WT
Aluminum Alloys						
Homogenization						
Stress Corrosion Cracking						
Fine Grained Aluminum Alloys						
Fracture Toughness						
Precipitate Characteristics						
Recrystallization/Up-setting						
Thermomechanical - Gleeble						
Processing Aluminum Alloys						

RESEARCH ON SYNTHESIS OF HIGH-STRENGTH
ALUMINUM ALLOYS

J. D. Boyd, D. C. Drennen, C. J. Martin, C. W. Price,
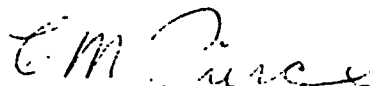A. R. Rosenfield, and D. N. Williams

BATTELLE
Columbus Laboratories

D. S. Thompson
Reynolds Metals Company

Approved for public release: distribution unlimited.

FOREWORD

This report was prepared by the Department of Physics and Metallurgy, Battelle's Columbus Laboratories, Columbus, Ohio, under USAF Contract No. F33615-71-C-1805. The contract represents Task A - The Relation Between Precipitate Microstructure and Mechanical Properties in Aluminum Alloys - prepared by the Metal Science Group in Collaboration with the Metallurgical Research Division of the Reynolds Metals Company and Task B - The Control of Grain Structure During Hot Working - prepared by the Nonferrous Metallurgy Division at Battelle. The contract was initiated under Project No. 7353, "Research on Metals and Ceramics", Task No. 735302, "Correlation of Structure and Properties". The program was administered under the direction of the Air Force Materials Laboratory, Air Force Systems Command, United States Air Force, with 1/Lt David P. Voss, LLS, as Project Engineer.

This report covers the period from 1 July 1971 through 31 July 1972. The manuscript was released by the authors in July 1972 for publication as an AFML Technical Report.

This technical report has been reviewed and is approved.

C. M. PIERCE
Metal & Ceramic Synthesis Branch
Metals and Ceramics Division
Air Force Materials Laboratory

ii

❀ Battelle

C........ ....
... . .
. . . . .
.. ..
.. ..

October 11, 1972

Air Force Materials Laboratory/LLS
Attention Lt. D. P. Voss
Code: FY 1457
Contract: F33615-81-C-1805
Item No. 0002, Sequence No. A001
Wright-Patterson Air Force Base
Ohio   45433 .

Dear Lt. Voss:

<u>Contract No. F33615-71-C-1805</u>

Enclosed are twenty-five (25) copies of the first annual progress report on
the subject contract entitled "Research on Synthesis of High-Strength
Aluminum Alloys". The report covers the period July 1, 1971 – June 30,
1972. Additional copies have been distributed in accordance with the dis-
tribution list appended to this report.

Very truly yours,

C. W. Price

CWP/mz
Enc.

ABSTRACT

The objective of Task A is to provide increased strength and fracture resistance in aluminum alloys by optimizing the precipitate microstructure. To control the size and distribution of the intermediate precipitates in some high-strength 7000 and 2000 series alloys, several alloys were cast and their precipitate microstructures characterized by microscopy after homogenization treatments at various times and temperatures. Homogenization treatments were selected to produce a fine and a coarse intermediate precipitate. The objective of Task B is to develop a recrystallized microstructure in wrought high-strength aluminum alloys during hot working. Recrystallization occurred along the grain boundaries in the 2024 alloy only at the highest upset rate (8.8 inch/sec) and the highest temperature (925 F). Preliminary microscopy results indicate that the intermediate precipitate in 2024 may not be stable during hot working. Recrystallization appeared to be complete in the Al-4.6Cu alloy upset at 8.8 inch/sec at 925 F, but recrystallization only along grain boundaries was observed at a slower rate of 0.016 inch/sec at the same temperature. Preliminary work on an Al-5.6Zn-2.4Mg-1.4Cu alloy has shown that the alloy resists recrystallization during hot working and recrystallizes to a moderately fine grain size on subsequent solution heat treatment.

TABLE OF CONTENTS

LIST OF ILLUSTRATIONS

LIST OF ILLUSTRATIONS
(Continued)

LIST OF ILLUSTRATIONS
(Continued)

LIST OF TABLES

LIST OF TABLES
(Continued)

I

SUMMARY

The objectives of both tasks of this project are concerned with studies of various aspects of processing aluminum alloys. In Task A, the size and distribution of all three types of second-phase particles that occur in aluminum alloys will be controlled. The three types are the large insoluble phases (iron and silicon bearing), the intermediate size particles (chromium, manganese, or zirconium bearing) and the hardening precipitates. There are indications that the amount and distribution of each of these phases can affect final properties, particularly fracture toughness. The present work is designed to produce material containing controlled amounts of these second phases and to determine their influence on final properties. Control of the large particles is achieved by choice of composition, control of the intermediate particles is by suitable homogenization, and control of the hardening precipitates is by choice of aging practice. So far, both 7000 (Al-Zn-Mg-Cu) and 2000 (Al-Cu-Mg) alloys have been cast, and a homogenization study is nearly complete. Two homogenization practices will be chosen for each alloy, one to produce a fine distribution of the intermediate particles and the other to produce a coarse distribution. The effect of such homogenization practices on grain structure is shown for two Al-Cu-Mg alloys.

The Task B research studies have as their objective the development of a recrystallized microstructure in wrought high-strength aluminum alloys during hot-working operations. Studies are under way to determine the effects of strain rate and temperature on the recrystallization behavior of 2024 and high-purity Al-4.6Cu alloy samples upset 50 percent in one deformation operation.

Initial studies have shown 2024 alloy to be extremely resistant to recyrstallization. After upsetting at a fast rate (8.8 inch/sec) at 925 F, some areas along grain boundaries appeared recrystallized, but little recrystallization was observed after upsetting at a slow rate (0.016 inch/sec) at 925 F or at lower temperatures. No obvious change in microstructure occurred during solution heat treatment of the upset samples. Recrystallization appeared complete in some areas of Al-4.6Cu upset at a fast rate at 925 F, and grain boundary recrystallization was observed after upsetting at a slow rate at 925 F. At lower temperatures, no recrystallization was apparent. These samples were held either 23 or 33 seconds at temperature following upsettings and were then subjected to a moderately rapid cooling between the upset dies (~10 F/sec). Work is being started to examine the importance of postupset annealing in which variable annealing times, both at and above the upset temperature, followed by water quenching will be examined.

Transmission electron microscopy is being used to examine subgrain size, dislocation structure, and changes in precipitate morphology accompanying upsetting. Preliminary results suggest that subgrain size varies with position in the original grains (i.e., smaller near grain boundaries). The presence of helical dislocations in 2024 will apparently permit subgrains to be readily distinguished from recrystallized material. Additional studies should permit the effects of

deformation temperature and strain rate on subgrain size to be determined. Preliminary results suggest that the intermediate precipitate in 2024 may not be entirely stable during hot working. Conformation of this unexpected observation is planned.

Two high-purity Al-Zn-Mg-Cu alloys included in the Task A studies are being processed so as to provide a fine-grained recrystallized microstructure. The possibility exists that the use of multiple deformation recrystallization steps may produce the desired microstructure in this material. These fine-grained materials will be evaluated to determine the effects of microstructural control on tensile, toughness, fatigue, and stress corrosion properties. Preliminary investigation has shown that one of the alloys, Al-5.6Zn-2.4Mg-1.4Cu, although resistant to recrystallization during hot working, recrystallizes quite readily to a moderately fine grain size on subsequent solution heat treatment.

II

INTRODUCTION

There is a continuing need for improved reliability of air frame structural materials. To achieve this, improved or more consistent toughness, fatigue, and corrosion resistance are essential. These parameters are increasingly being included in new specifications because of the more reliable test procedures developed over the last decade. The influence of such metallurgical variables as composition, heat treatment and aging have long been recognized as important, but little systematic attention has been given to other stages of processing. The present work, the first year's results of which are reported here, is concerned with interaction of processing with composition on the final properties of the product. The work is divided into two tasks which are based on different premises to achieve improved properties. These are:

Task A "The Relation Between Precipitate Microstructure and Mechanical Properties in Aluminum Alloys"

Task B "A Fundamental Study of the Control of Grain Structure of Aluminum Alloys During Primary Working"

The Task A research is being carried out in the Metal Science Group at Battelle, in close collaboration (via a subcontract) with the Metallurgical Research Division of the Reynolds Metals Company. The objective of this task is to determine the optimum combinations of small, intermediate, and large precipitates consistent with high strength and a good resistance to fracture under unidirectional or cyclic loading and stress corrosion. A series of 13 experimental alloys has been prepared. The concentrations of major alloy elements are based on the commercial 7075 and 2024 compositions, and the effects of alloy chemistry and ingot homogenization treatment on the character and size distribution of intermediate precipitates are being investigated. Alloys containing Cr, Mn, or Zr as the minor alloy element have been subjected to different homogenization treatments, and the resulting distributions of intermediate precipitates are being characterized by transmission electron microscopy. In addition, the relation between precipitate microstructure and slip character is being studied in a high-purity Al-Zn-Mg-Cu alloy.

The Task B research is being carried out in the Nonferrous Metallurgy Division at Battelle. The objective of this task is to determine the primary working conditions of wrought aluminum alloys which produce a fine-grained, recrystallized grain structure. It is expected that such a grain structure will effect a greater resistance to stress-corrosion cracking than that associated with the elongated, highly polygonized grain structure common to conventionally processed aluminum alloys. Initially, the recrystallization behavior of two alloys, 2024 and a high-purity Al-4.6 Cu, will be studied as a function of hot-working conditions. Hot working will be simulated by means of a programmed thermal-mechanical testing machine (Gleeble).

3

TASK A. THE RELATION BETWEEN PRECIPITATE MICROSTRUCTURE AND MECHANICAL PROPERTIES OF ALUMINUM ALLOYS

Background

Since the mechanical properties of a heat-treated aluminum alloy are determined largely by the character and size distributions of second-phase particles, it is logical to look to the origins and effects of microstructure for possible routes to improved mechanical properties. Accordingly, the objective of this task is to investigate how certain steps in processing affect the final precipitate microstructure and to evaluate the effects of various precipitate size distributions on ambient-temperature mechanical properties. A more detailed background to this project was presented in the first semi-annual report[1]*.

The various second-phase particles or precipitates which occur in high-strength aluminum alloys can be conveniently divided into three groups according to size and origin, as follows: (1) large precipitates (1-100 μ) are mainly iron- and silicon-rich compounds which form during casting, (2) intermediate precipitates (500 A-0.5 μ) are chromium-, manganese-, or zirconium-rich compounds which precipitate during ingot homogenization, and (3) small precipitates (<0.1 μ) are compounds such as $MgZn_2$, $CuAl_2$, and Al_2CuMg, and their respective metasable forms (η', θ', and S'), which precipitate during aging in the final heat treatment.

Each of the three types of precipitates in aluminum alloys exerts a powerful influence on specific mechanical properties. The large precipitates influence toughness[2-4] and fatigue strength[5-7]. The intermediate precipitates control grain size and morphology, and in certain alloys they stabilize the dislocation substructure. They also have a direct influence on toughness since their character and size distribution determine the critical strain required for microvoid coalescence[3-4]. In addition, the nondeformable intermediate precipitates should promote homogeneous slip, which is expected to increase an alloy's resistance to the initiation of cracks by fatigue[8-9] or stress corrosion[10-11]. The small precipitates interact with glide dislocations and hence determine an alloy's yield strength and slip character. As a result of years of development work the presently attainable room-temperature yield strengths are probably near the practicable maximum for most alloys. However, in order to improve the resistance of high-strength alloys to fatigue and stress-corrosion cracking, some attention should be given to the problem of achieving a homogeneous slip character at a high strength level. It is also important to control the density of grain-boundary precipitates for improved toughness[12] and resistance to stress-corrosion cracking[13].

---

*References appear on page 36.

Thus, the mechanical behavior of high-strength aluminum alloys is determined by the total precipitate microstructure. In order to arrive at the optimum combination of small, intermediate, and large precipitates for a particular application, it is necessary to control the size distribution of each type of precipitate at all stages of processing. This is the overall objective of Task A of this program. However, at present the work under Task A is concentrating on two areas of investigation: (1) controlling the type and size distribution of intermediate precipitates by alloy chemistry and ingot-homogenization treatment and (2) determining the relation between precipitate microstructure and slip character.

Controlling the Size Distribution of Intermediate Precipitates

The intermediate precipitates are compounds of aluminum with elements such as Cr, Mn, and Zr. These minor alloy elements are added to commercial alloys to control recrystallization. Generally, the Mn-rich phases have the largest particle sizes followed by the Cr-rich phases and the Zr-rich phase. The last exists as very small particles (300-700 A) which exhibit strain-contrast effects in transmission electron microscopy, indicating that they are partially coherent with the matrix.

The elements which form the intermediate precipitates have exceedingly low solid solubilities and diffusivities in aluminum[14]. Consequently, these minor-alloy elements are retained in solid solution during casting and form regions of supersaturation at the centers of the primary dendrites. During ingot homogenization the intermediate precipitates form in these regions of supersaturation. Because of the low solubilities and diffusivities of their constituent elements, they are thought to be stable with respect to coarsening or dissolution during subsequent thermal and mechanical treatments. Since the intermediate precipitates tend to form at the center of the primary dendrites, their distribution throughout a given piece of material can be nonuniform. This nonuniform distribution persists during working and heat-treatment operations and results in microstructural patterns in certain wrought products which are known as "banding".

Thus, any effort to control the character or size distribution of the intermediate precipitates must take the following factors into consideration:

(1) Alloy chemistry (minor alloy elements and impurity elements)

(2) Solidification conditions (cooling rate, degree of agitation, etc.)

(3) Diffusivities of minor-alloy elements

(4) Distribution of large precipitates

(5) Ingot homogenization treatment.

In the present research, only the effects of alloy chemistry and ingot homogenization treatment are being investigated systematically. However, the effects of the other variables are being considered when necessary (e.g., the nonuniform distribution of particles due to segregation during solidification).

Experimental Program

The experimental program is concerned initially with fabrication of materials, documentation of microstructure and a testing program to evaluate strength, fracture toughness, fatigue, and corrosion resistance. Before final material processing, a homogenization study is being carried out to determine the effect of time and temperature on intermediate particle size and spacing. From this study, two homogenization practices will be chosen for each group of alloys so that a coarse and a fine distribution of the intermediate particles can be achieved. A flow chart for the homogenization study and fabrication portions of the program is shown in Figure 1.

All the alloys for Task A have been cast. Macroetched half slices are shown in Figure 2. All are porosity free and fine grained, though alloys B and O contain some "feathered" grains. This condition is the result of casting twins[15], but for the present application, which is primarily the production of sheet, it is not expected that the effects of this cast structure will be obvious in the final product. Thus, these ingots will not be recast and will represent another minor variation which can be followed through processing.

The analyses of all the ingots are given in Table I. For convenience, two methods of describing alloys are used; one is an arbitrary letter and the other is the closest Aluminum Association alloy designation together with any element substitution. Since, with the exception of Alloy O, only one element of the group Cr, Zr, Mn, or V is added to an alloy, then a designation 7475+Zr means the substitution of Cr by Zr in Alloy 7475.

Alloy J was intended to be Alloy D. Since it was cast early in the program, it has been used for expediency in those portions of the work which would not be affected by the minor deviation in chemistry. This alloy will not be included in any further work.

Homogenization Study

The objective of this study is to determine two homogenization practices for each type of alloy, i.e., for Cr-bearing 7000 series alloys, Zr-bearing 7000 series alloys, Mn-bearing 2000 series alloys, and the Zr- and V-bearing 2000 series alloy. The selected practices are to produce a fine and coarse distribution of the

```
┌──────────────┐      ┌────────────────────────┐      ┌──────────────────┐
│ Homogenization│─────│ Investigate 750 F (400 C),│─────│ Determine minimum │
│ Study         │      │ 850 F (454 C) and T_max for│      │ SHT practices     │
└──────────────┘      │ 6, 72, 240, and 670 hours │      │ that will dissolve│
                      └────────────────────────┘      │ soluble phases    │
                                  │                    │ without affecting │
                                  │                    │ intermediate      │
                                  │                    │ precipitates      │
                                  │                    └──────────────────┘
                      ┌────────────────────────┐
                      │   Electron Microscopy   │
                      └────────────────────────┘
                                  │
                      ┌────────────────────────────────┐
                      │ Select high and low homogenization│
                      │ practices to produce coarse and fine│
                      │ distribution of intermediate particles│
                      └────────────────────────────────┘
                                  │
                      ┌────────────────────────────────┐
                      │ Apply these homogenization practices, then scalp│
                      │ and roll material to various gages (1, 1/2, 1/4,│
                      │ 1/8 and 1/16")│
                      └────────────────────────────────┘
                                  │
                 ┌────────────────────────────────────────┐
                 │ After SHT and aging determine volume fraction and distribution│
                 │ of coarse second-phase particles, intermediate particles, and│
                 │ age-hardening precipitates│
                 └────────────────────────────────────────┘
                                  │
                      ┌────────────────────────┐
                      │      Test Program       │
                      └────────────────────────┘
```

FIGURE 1.   PROGRAM FLOW CHART
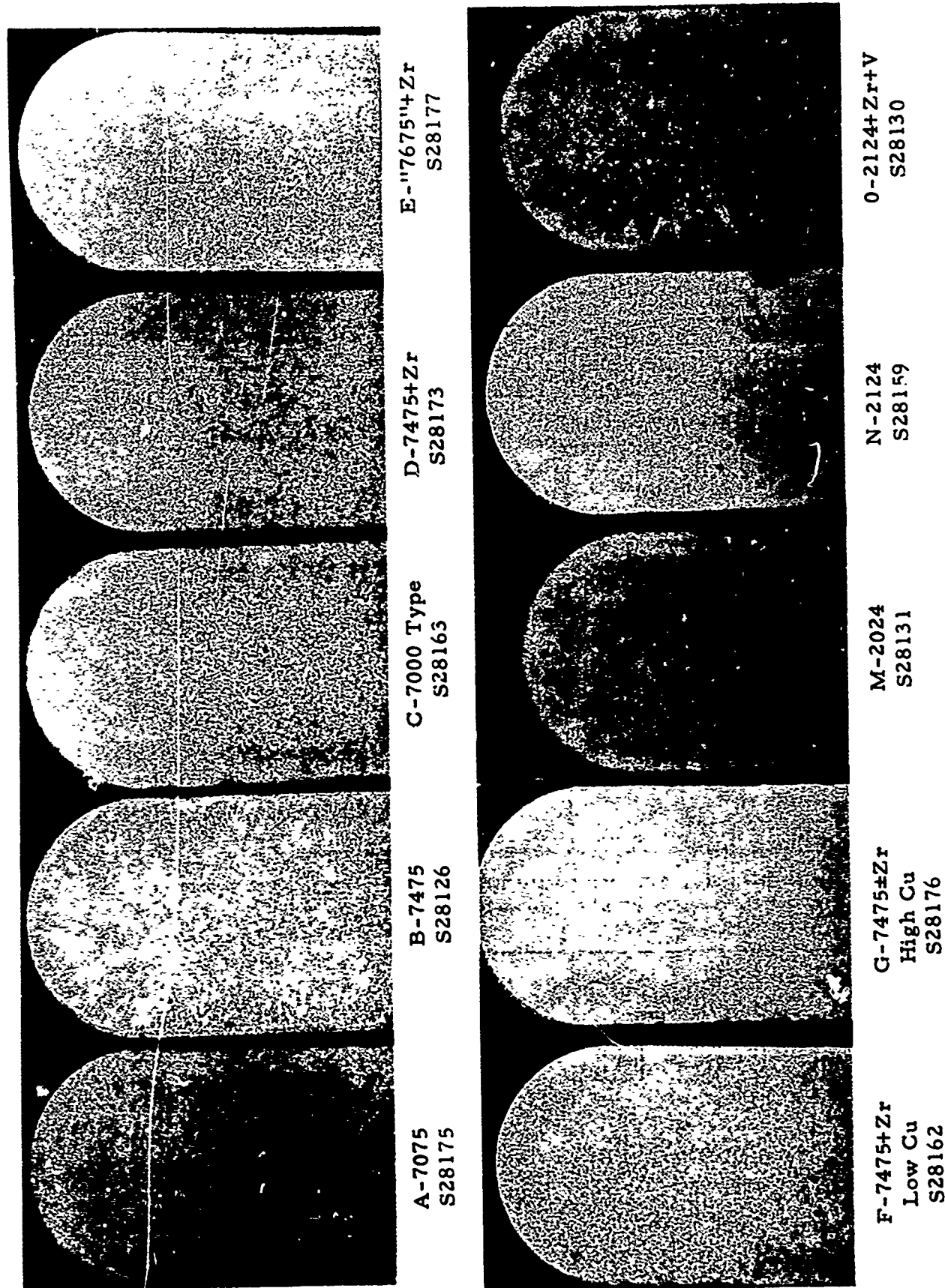
FIGURE 2. CAST STRUCTURES OF EXPERIMENTAL ALLOYS

Note feathered structure of Alloys B & O.

8

TABLE I. CHEMICAL ANALYSES OF EXPERIMENTAL ALLOYS

Alloy	Approximate Aluminum Association Designation	Casting Sample No.	Zn	Mg	Cu	Fe	Si	Cr	Zr	Mn	V	Ti
A	7075	28175	5.79	2.50	1.42	0.20	0.13	0.18	ND(a)	< 0.01		< 0.01
B	7475	28126	5.60	2.40	1.48	0.06	0.04	0.16	ND(a)	< 0.01	ND(a)	< 0.01
C	7000 Type	28163	5.68	2.36	1.48	0.02	0.01	0.18	ND(a)	< 0.01	ND(a)	< 0.01
D	7475+Zr	28173	5.81	2.46	1.54	0.08	0.05	< 0.01	0.12	< 0.01	ND(a)	< 0.01
E	"7675"+Zr	28177	5.52	2.41	1.42	0.01	< 0.01	< 0.01	0.11	< 0.01	ND(a)	< 0.01
F	7475+Zr Low Cu	28162	5.56	2.32	1.22	0.06	0.04	< 0.01	0.11	< 0.01	ND(a)	< 0.01
G	7475+Zr High Cu	28176	5.54	2.37	2.13	0.06	0.04	< 0.01	0.11	< 0.01	ND(a)	< 0.01
X	Al-Zn-Mg-Cu	26983	5.60	2.44	1.43	< 0.01	< 0.01	< 0.01	ND(a)	< 0.01	ND(a)	< 0.01
J(b)		28157	5.48	2.37	1.52	0.07	0.15	< 0.01	0.12	< 0.01	ND(a)	< 0.01
M	2024	28131	0.02	1.34	4.36	0.33	0.19	< 0.01	ND(a)	0.46	ND(a)	< 0.01
N	2124	28159	< 0.01	1.17	3.92	0.07	0.04	< 0.01	ND(a)	0.28	ND(a)	< 0.01
O	2024+Zr+V	28130	0.07	1.50	4.40	0.33	0.23	< 0.01	0.16	< 0.01	0.10	< 0.01

(a) Element not determined, but there is no reason to expect it to be present at a level greater than 0.01 percent.

(b) Alloy J, an off-analysis version of Alloy D, was used in the homogenization study.

9

appropriate intermediate particles. It is presumed that all Cr-bearing 7000 ser-
ies alloys will behave in a similar manner so that only one need be considered.
Therefore, Alloy B was chosen. Similarly, for the Zr-bearing 7000 series,
Alloy J was selected; Alloys M and O were selected for the other two alloy types.
There is some evidence[16, 17] that the level of Si or Fe can accelerate the precip-
itation of Zr-bearing particles in an Al-Zr binary; however, the effect of Fe and
Si are not expected to have a critical effect on the distribution of intermediate
precipitates.

Samples from these four ingots were subjected to 12 different time-
temperature combinations. After the determination of a suitable solution heat
treatment (SHT) practice for each condition, these samples were examined by
transmission electron microscopy (TEM) to determine the size and distribution of
the intermediate particles. Since only a coarse and a fine distribution were
desired, it was not necessary to carry out accurate quantitative metallography.
If differences are not readily apparent, then the precise homogenization selected
will not be critical.

After homogenization the specimens were still-air cooled and hence contained
dense, coarse precipitates of soluble phases which would obscure the intermediate
particles in TEM. Thus, it was necessary to apply a SHT to return the matrix
precipitates to solid solution. Some caution had to be used in selecting a SHT
practice for the material homogenized at low temperatures in order that significant
growth of the intermediate particles does not occur. It was found that a few
minutes at conventional SHT temperatures was sufficient to dissolve the soluble
phases without appreciable growth of the intermediate particles[1].

The homogenization practices which were applied to small full-thickness
sections cut from Ingots B, J*, M, and O are listed in Table II. The above tem-
peratures span the entire feasible range and the times cover the most practical two
orders of magnitude. All metallography samples were taken at a depth approxi-
mately one quarter of the way through the thickness.

TABLE II. EXPERIMENTAL HOMOGENIZATION TREATMENTS

Alloys	Homogenization Temperature	Homogenization Time, hr
B, J, M & O	750 F (400 C)	
B, J, M & O	850 F (454 C)	
M & O	925 F (496 C)	6, 72, 240 & 670
B, J	16 hr @ 860 F (460 C) + 960 F (515 C)	

---

*Alloy J was used for this part of the program since it was not discovered to be an out-of-specification version of Alloy D
until the homogenization study was under way. Since only the Si level was too high, its use was continued for the
homogenization study.

So far, the homogenization study has been completed for Alloys M and B. The work on Alloy J is nearly finished and for Alloy O it is hindered by intermediate particle identification problems. In Alloy O the presence of typical Zr-bearing particles is readily evident; however, identification of V-bearing particles with either transmission electron microscopy or the electron microprobe has not been possible. Further work will be carried out in an effort to choose the two homogenization practices.

## Homogenization Study of Alloys M (2024) and O (2024+Zr+V)

Some typical transmission electron micrographs of homogenized samples of Alloy M (2024) are shown in Figure 3 and of Alloy O (2124) in Figure 4. In Figure 3a two areas of the "as-cast" material are shown. The micrograph on the left shows platelets of θ and S phase. The area shown in the right-hand micrograph is somewhat unusual inasmuch as it appears to consist of an array of small plates following common boundaries. Whatever their structure, all these plates disappear after a short (10 min.) SHT at 925 F (496 C). The bulk of the solution-heat-treated material looked like the left-hand side of Figure 3b. A few areas did contain small particles as shown in the right-hand micrograph of Figure 3b. As expected, particle coarsening occurs with increasing homogenization time or temperature (Figure 3c). A summary of the lath length and width ranges seen in these particles is given in Table III. The same size data are shown plotted on a log-log plot as a function of reciprocal temperature in Figure 5 and time in Figure 6a and b. Since only approximate size ranges were measured on a few micrographs, it is difficult to draw conclusions. For a diffusion-controlled coarsening mechanism of spherical particles it would be expected that coarsening be governed by

$$(\bar{r})^3 - (\bar{r}_o)^3 \propto \frac{Kt}{T} \quad , \tag{1}$$

where $\bar{r}$ is the average particle size after coarsening from an initial average size of $\bar{r}_o$, t is time, T is temperature, and K is a function of the coefficient of diffusion, D, molar volume of the particle, equilibrium solute concentration, and the interfacial free energy of the particle-matrix interface. Thus, if r_o is negligibly small and K is regarded as a constant, then a logarithm plot of r against t or 1/T should have a slope of one-third. Equation (1) emerged from extensions of the Lifschitz-Wagner theory to coarsening of particles in a solid matrix[18,19]. This equation takes no account of the effect of volume fraction[20] or particle shapes other than spherical[21] nor the dependence of D on solute concentration[22]. The effect of shape is particularly important; the exponent of Equation (1) can vary from unity in the case of lengthening of plates[23] to numbers greater than 3[21]. Thus, we rewrite Equation (1) as

$$(\bar{r})^n - (\bar{r}_o)^n \propto \frac{Kt}{T} \quad . \tag{2}$$

11
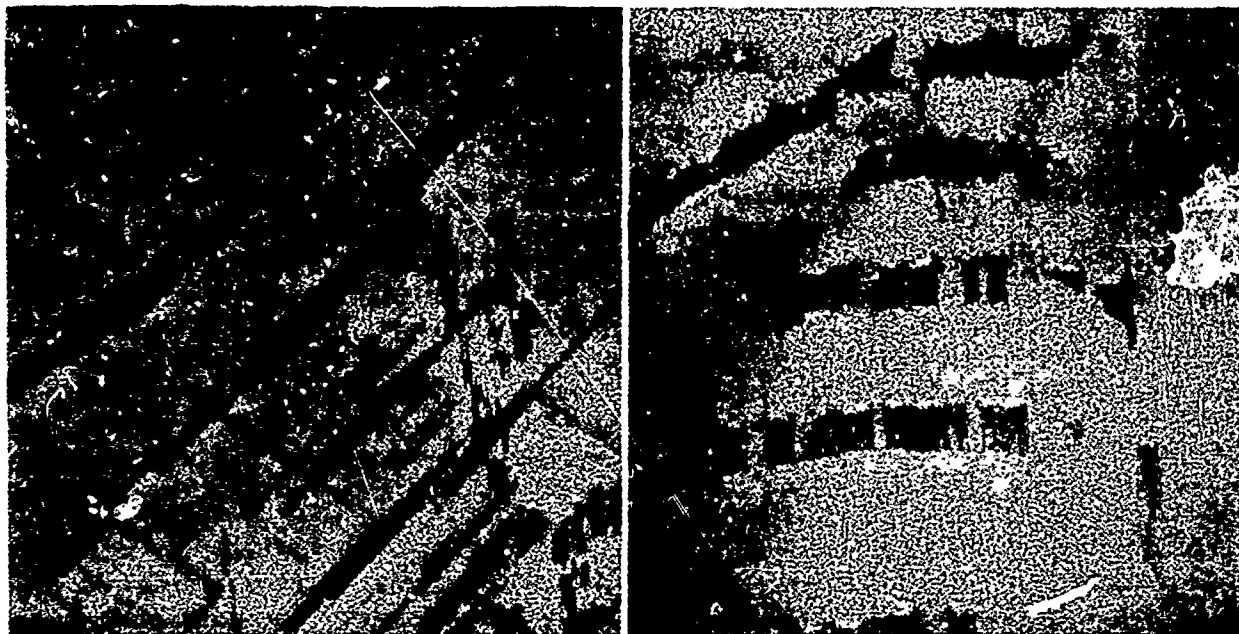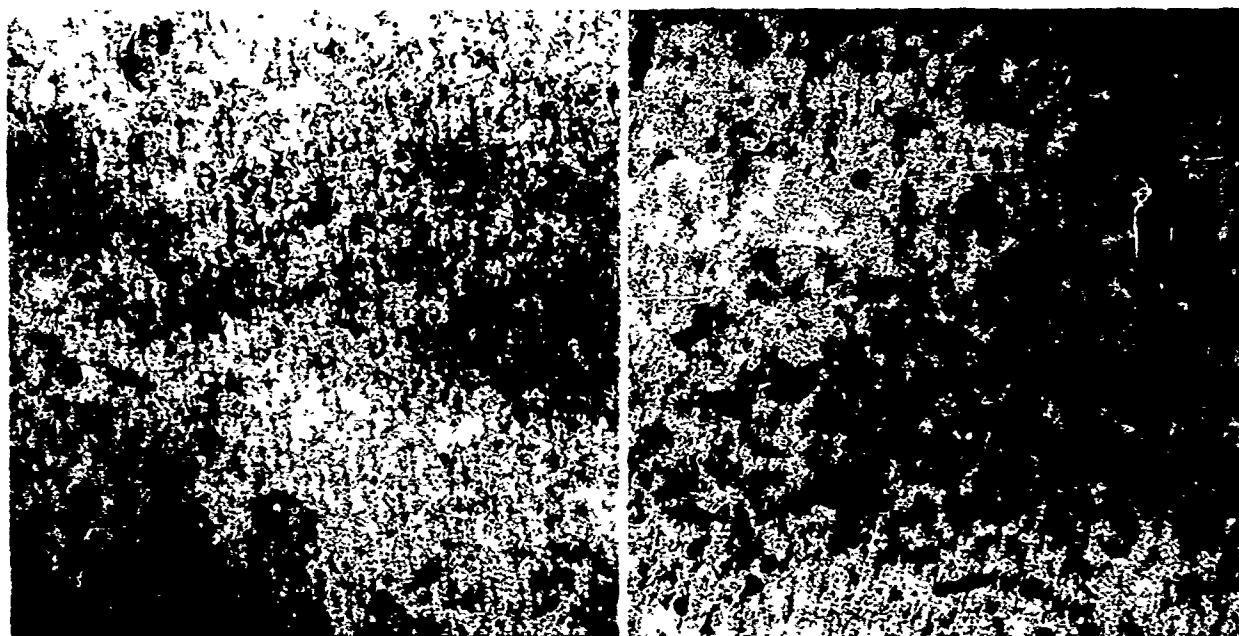
50,000X

a. As-Cast

50,000X

b. As-Cast + Short Solution Heat Treatment and Quenched

FIGURE 3. ALLOY M (2024)

12

Time, hr	Homogenization Temperature		
	750 F (400 C)	850 F (454 C)	925 F (496 C)
6			
72			
240			
670			
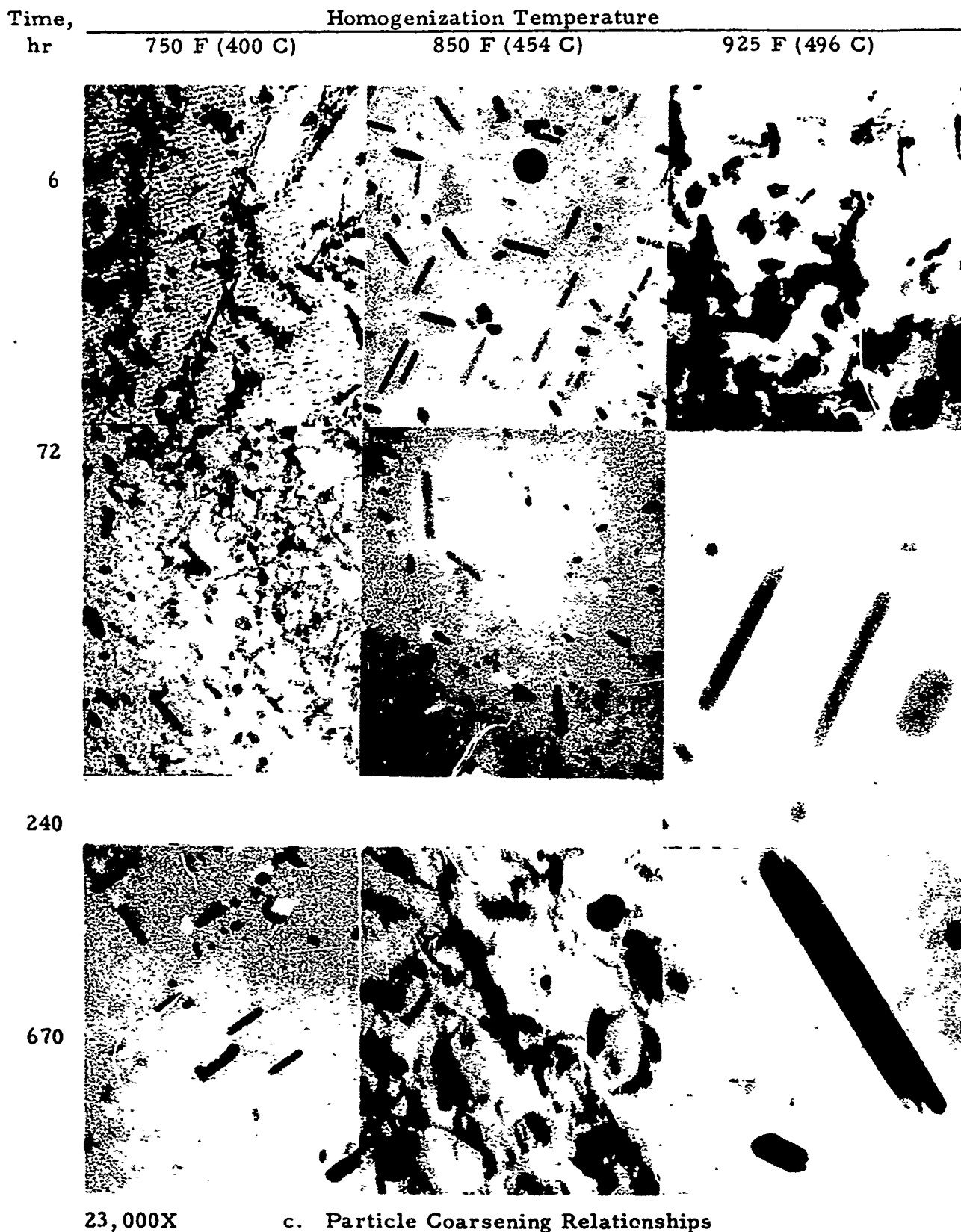
23,000X   c.   Particle Coarsening Relationships

FIGURE 3. (CONTINUED)

13
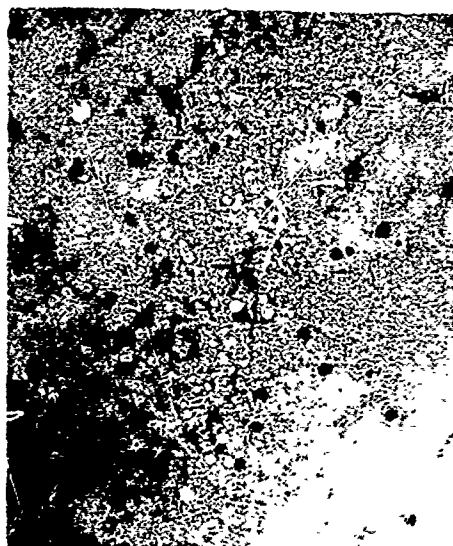
72,000X   50,000X
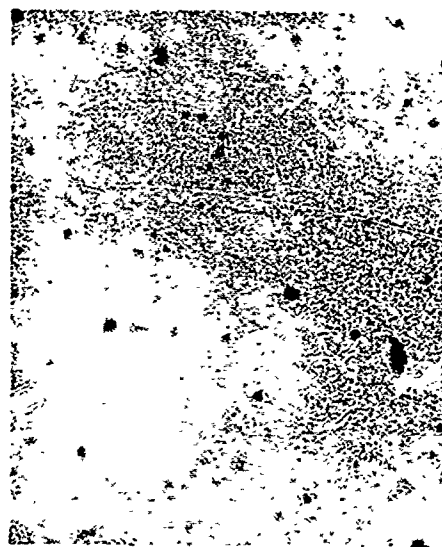
240 Hr at 750 F (400 C)   670 Hr at 850 F (454 C)

a.   Zr-Bearing Particles

50,000X   25,000X   25,000X

670 Hr at 750 F (400 C)   72 Hr at 850 F (454 C)   670 Hr at 925 F (496 C)

b.   Unidentified Large Particles

FIGURE 4.   TRANSMISSION ELECTRON MICROGRAPHS OF ALLOY 0 (2024 + Zr + V) AFTER VARIOUS HOMOGENIZATION PRACTICES FOLLOWED BY SOLUTION HEAT TREATING AND QUENCHING
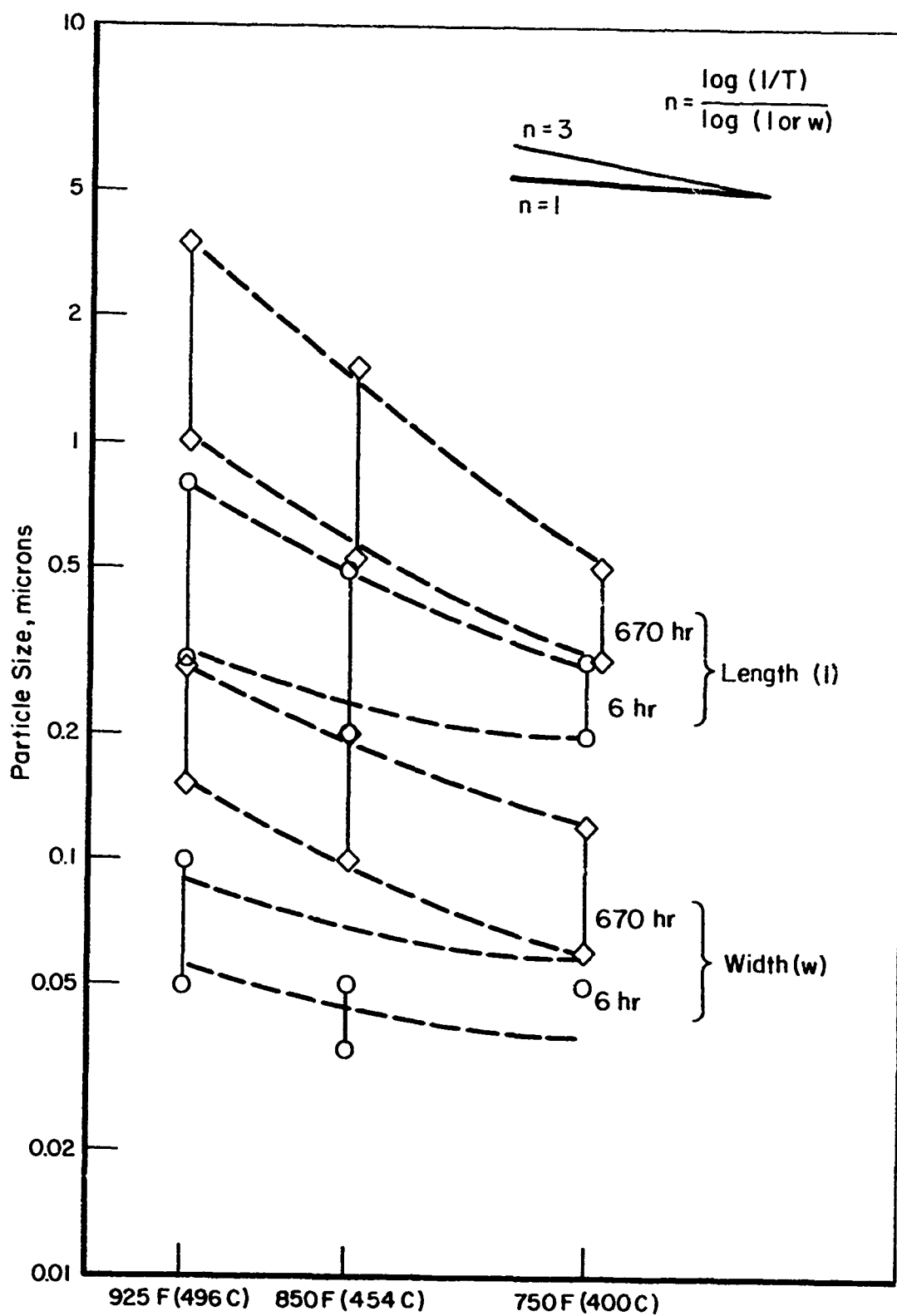
FIGURE 5.   PARTICLE LENGTH AND WIDTH RANGES IN ALLOY M (2024)
AS A FUNCTION OF 1/T

15
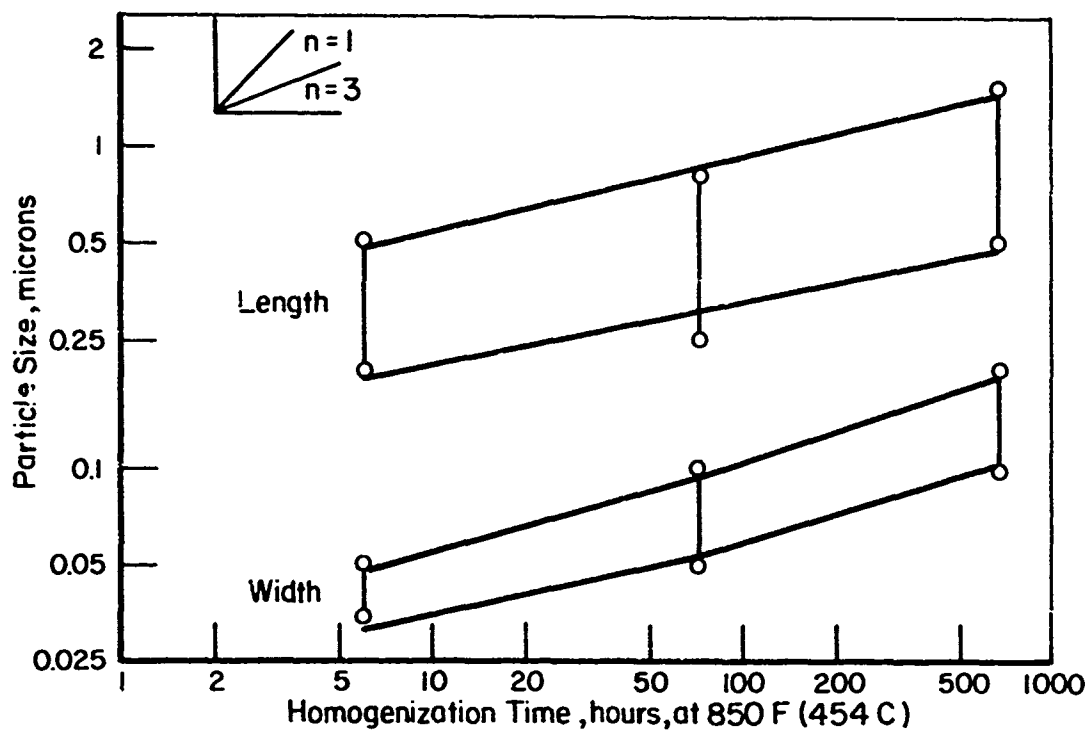
FIGURE 6a.   ALLOY M (2024) Mn-PARTICLE COARSENING AS A FUNCTION
OF TIME AT 850 F (454 C)
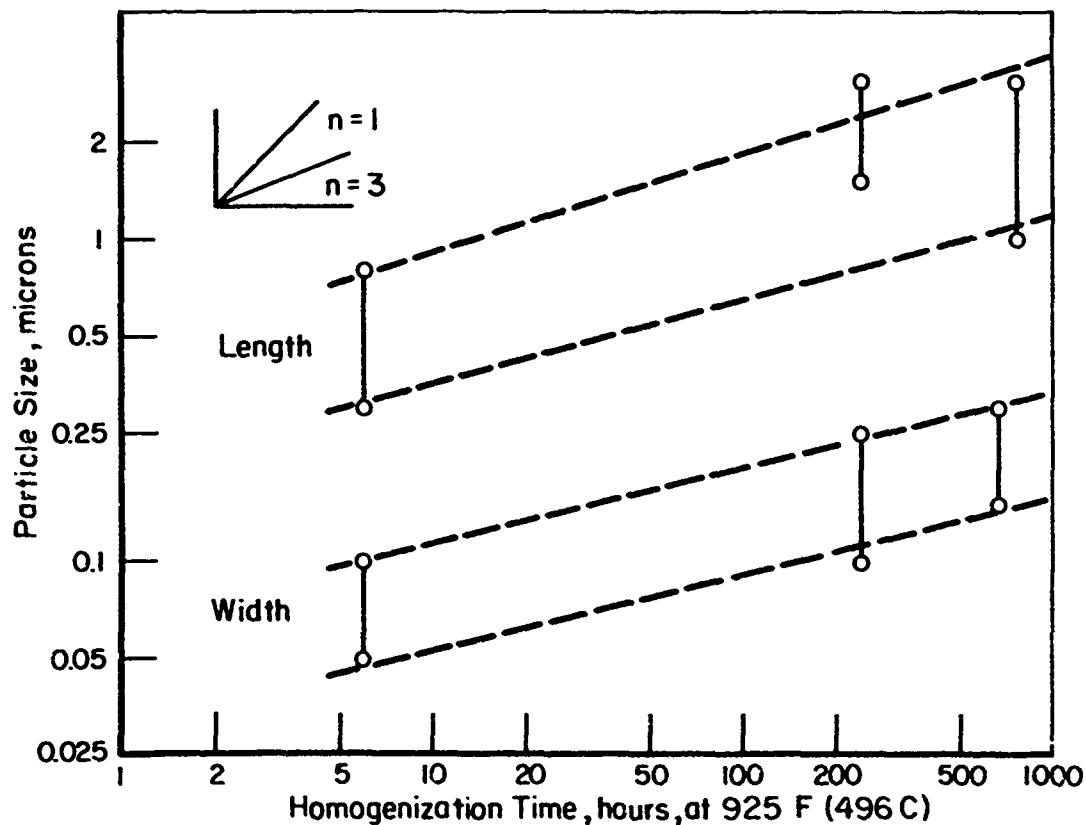
FIGURE 6b.   ALLOY M (2024) Mn-PARTICI E COARSENING AS A FUNCTION
OF TIME AT 925 F (496 C)

While it is not possible to derive a value of n in Figures 5 and 6, at least the value of n = 1 and n = 3 can be compared with the present data. From Figure 6 it seems that n is approximately 3, which is in agreement with Equation (1). As a function of 1/T (Figure 5), however, n is much higher than 3, probably due to the fact that K varies with temperature or because of changes in the nucleation rate with temperature. It is also of interest that the aspect ratios of these particles remained approximately constant during homogenization.

TABLE III. MANGANESE-BEARING PARTICLE SIZE IN ALLOY M
AS A FUNCTION OF HOMOGENIZATION PRACTICE

| Homogenization Time, hr	Dimension	Particle Length (l) and Width (w) Ranges, in Microns, at Indicated Homogenization Temperatures		
		750 F (400 C)	850 F (454 C)	925 F (496 C)
6	l	0.2-0.3	0.2-0.5	0.3-0.8
	w	0.05	0.035-0.5	0.05-0.1
72	l	0.2-0.4	0.025-0.8	
	w	0.05-0.09	0.05-0.10	
240	l			1.5-3
	w			0.1-0.25
670	l	0.3-0.5	0.1-0.2	0.15-0.3

The two homogenization practices for Alloy M were 6 hours at 850 F (454 C) and 240 hours at 925 F (496 C). The lower temperature practice was chosen since it led to a particle distribution similar to the 670-hour treatment and was therefore more convenient.

As mentioned earlier, some problem has been experienced in detecting the presence of vanadium in Alloy O. Some typical TEM micrographs are shown in Figure 4. The small round particles in the material homogenized at 750 F (400 C) or 850 F (454 C) appear to be Zr-bearing phases. It can be seen that some size difference can be achieved, such as between 72 hours at 850 F (454 C) and 670 hours at 850 F (454 C). Some unidentified coarse particles were seen, such as those shown in Figure 4 – 670 hours at 925 F (496 C), however, it was not possible to obtain diffraction patterns.

The final practices for the Zr-bearing 7000 series alloys and Alloy O have not been selected, although a homogenization of 6 or 72 hours at 850 F (454 C) along with 240 hours at 960 F (515 C) is expected to be employed for the 7000 series.

Homogenization Study of Alloys B (7475) and J (7475+Zr)

The characterization of Alloy B by TEM and optical microscopy is shown in Figures 7 and 8, respectively. The composition of Alloy B corresponds approximately to Aluminum Association Designation 7475. The composition is given in Table I. The homogenization and solution heat treatments studied for Alloy B are listed in Table IV. B-72/750* (Figure 7a) and B-6/850 (Figure 7c) do not appear to show much difference in the TEM structure. The dislocation density appears to be about the same, but on reverting to low magnification (Figure 8a-f) it would appear that B-72/750 had the superior homogenizing treatment. However, on viewing all the alloys there is definite shape progression from B-72/750 (Figure 7a), which has a majority of small, basically round particles, up to B-670/960 (Figure 7m), which has very large particles with a greater tendency to angularity. When viewing B-670/960 optically, it would appear that the particles had grown to the extent that they become visible at 500X (Figure 8f). On comparing B-72/750 with B-670/960 in the electron microscope, Figures 7a and 7m, we find evidence of Ostwald ripening, since the more extended homogenization treatment produced a smaller number of larger particles. One alloy that showed a drastic difference was B-72/850 (Figure 7g). It would appear that it contained some form of planar defect. This "defect" had a certain orientation preference as can be seen from Figure 7g. This alloy was the only one that gave a variation in diffraction patterns (Figure 7h); on analysis it shows that the intersection of the "defects" with the foil surface is along [001] and that the "planar defects" probably are along ($\bar{1}$10) or (1$\bar{1}$0) planes. An analysis of particle size variation showed a general increase as the homogenization treatments became longer and the temperatures were increased (Table IV). The "planar defects" in B-72/850 did not appear to affect the particle size. All particles other than the "planar defects" observed during this characterization would be termed intermediate precipitates.

Alloy J was also characterized by TEM and optical microscopy as is shown in Figures 9 and 10, respectively. This alloy is of similar composition to Alloy B but with added Si and Zr. One objective in this alloy was to determine the homogenization treatments required to produce a uniform distribution of Zr-rich particles. The alloys characterized are listed in Table V. J-72/750 (Figure 9a) showed similar "planar defects" to those found in B-72/850. They appeared far denser and also smaller in overall size. The only connection between B-72/850 and J-72/750 was that their homogenization treatment was for 72 hours, but B-72/850 was at 850 F (454 C) and J-72/750 was at 750 F (399 C), which could explain the variation and difference in distribution of the defects between the alloys. J-72/750 also showed extra diffracted spots superimposed on the (001) matrix diffraction pattern (Figure 9d). There was some evidence of small clusters that were assumed to be Zr particles (Figure 9a) in the matrix between the "planar defects". Figure 9e shows J-6/850 to have a clear matrix with a reasonably low dislocation

*In the terminology used in this report for specimen number, "B" is the alloy designation, 72 is time in hours, and 750 is temperature, F.
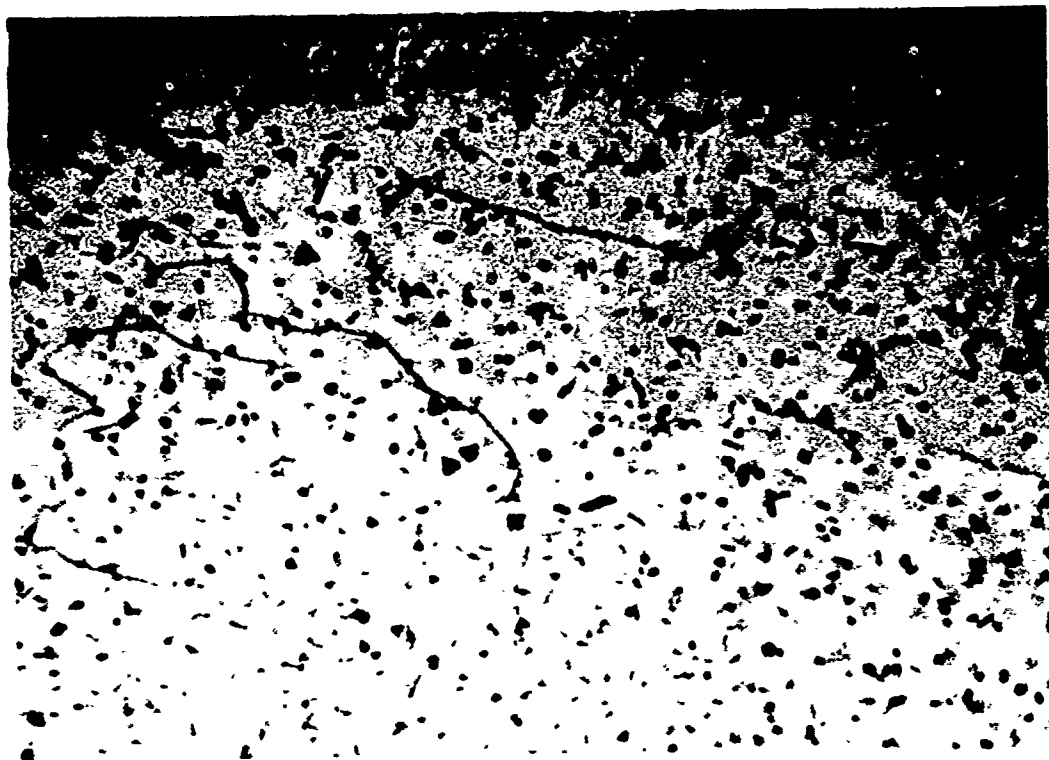
29,000X

a. B-72/750
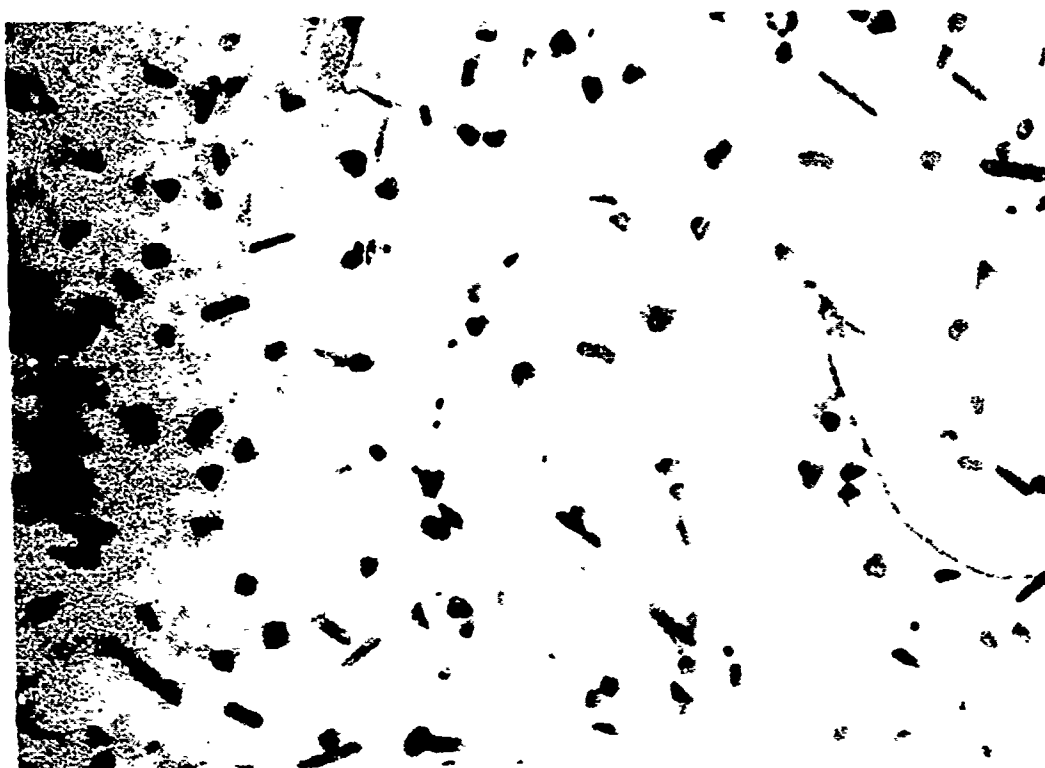
60,000X

b. B-72/750

FIGURE 7. TRANSMISSION ELECTRON MICROSCOPY OF ALLOY B
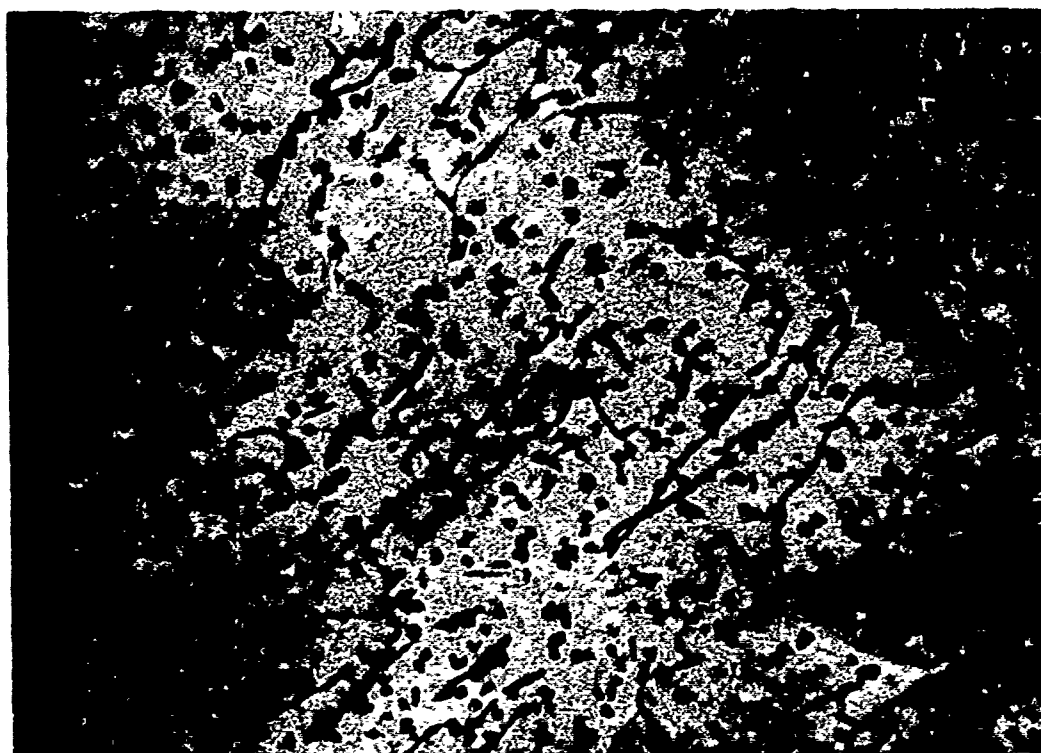
30,000X

c. B-6/850
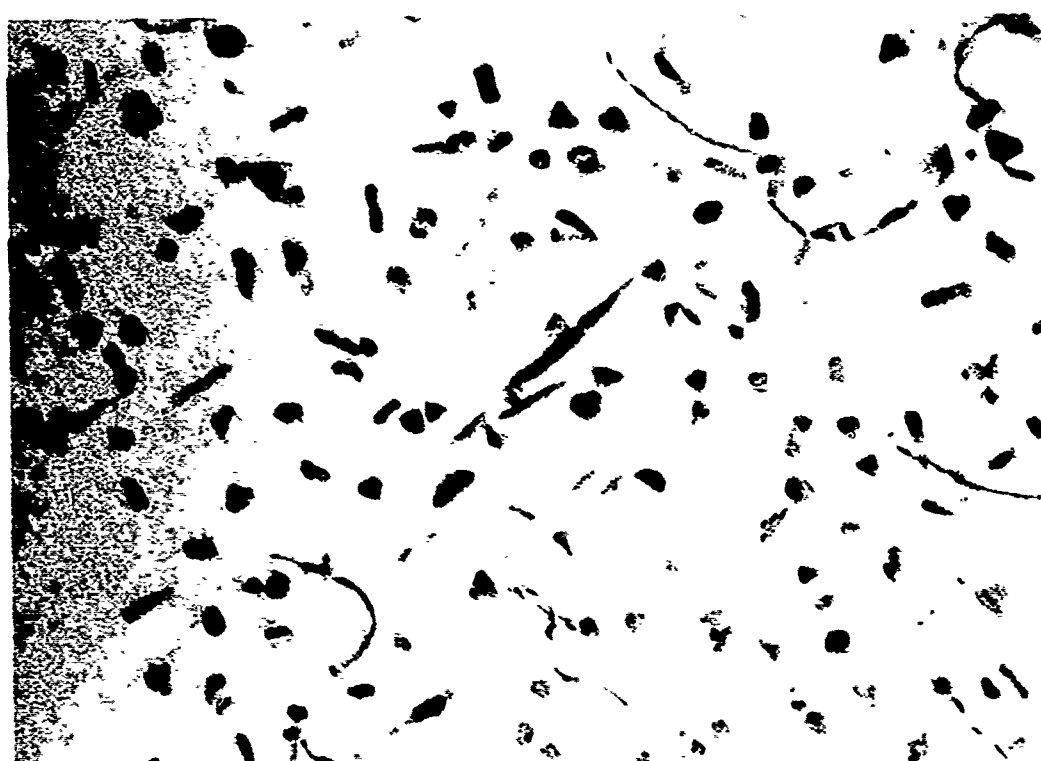
60,000X

d. B-6/850

FIGURE 7. (CONTINUED)

20
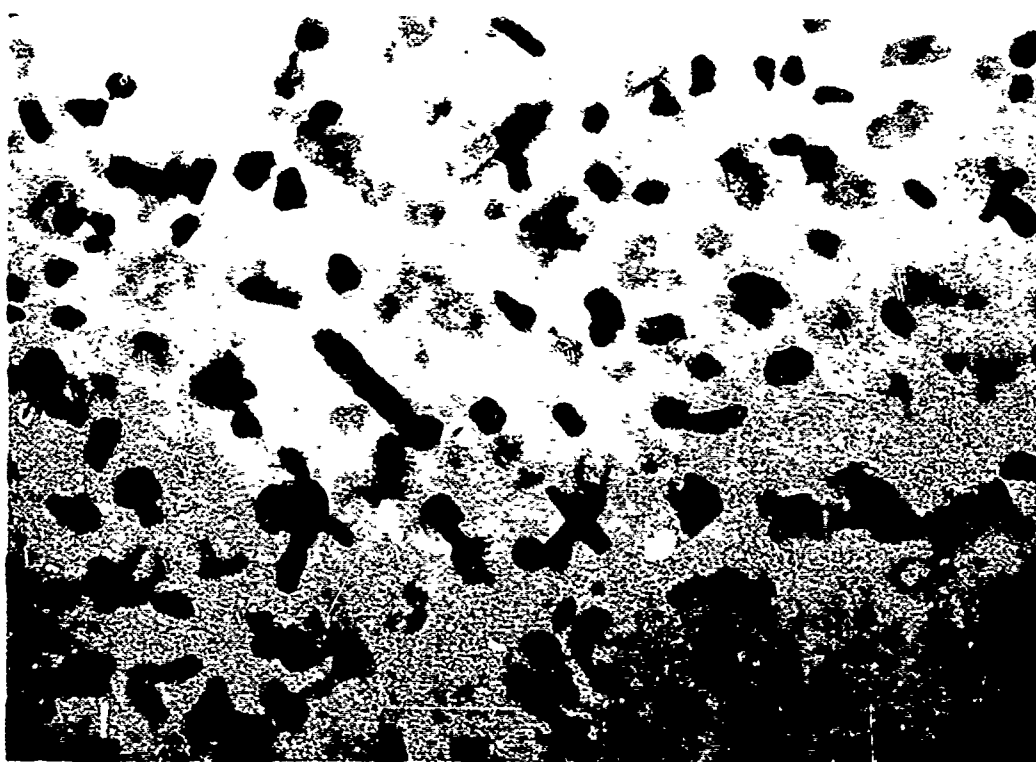
30,000X

e. B-72/850

60,000X

f. B-72/850

FIGURE 7. (CONTINUED)
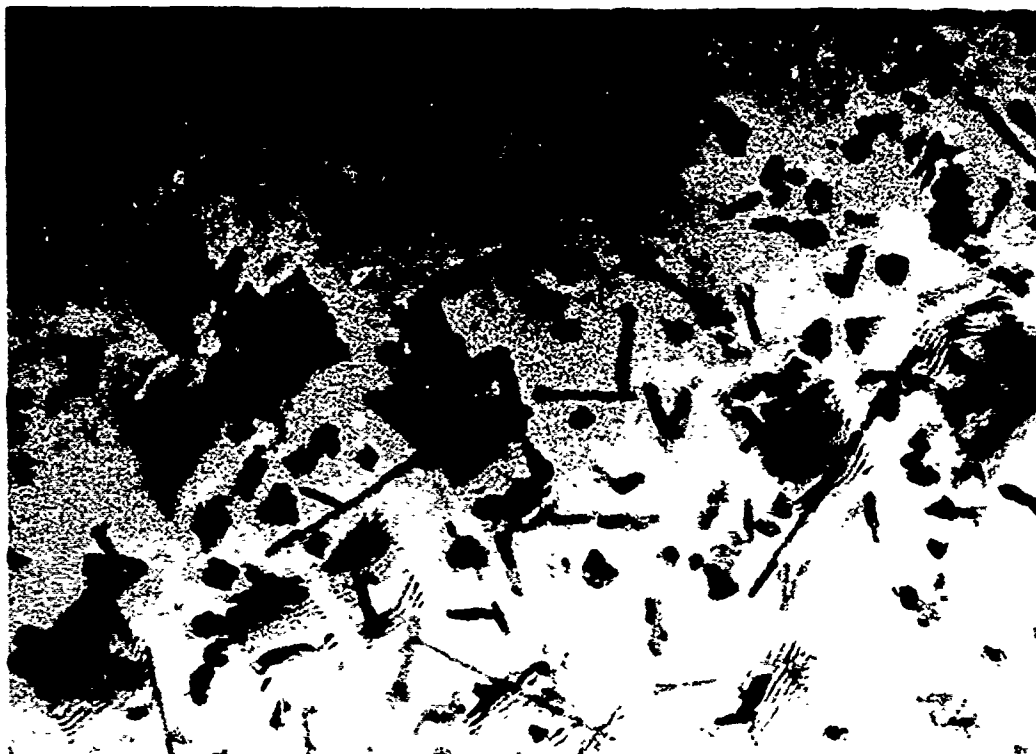
34,000X

g. B-72/850
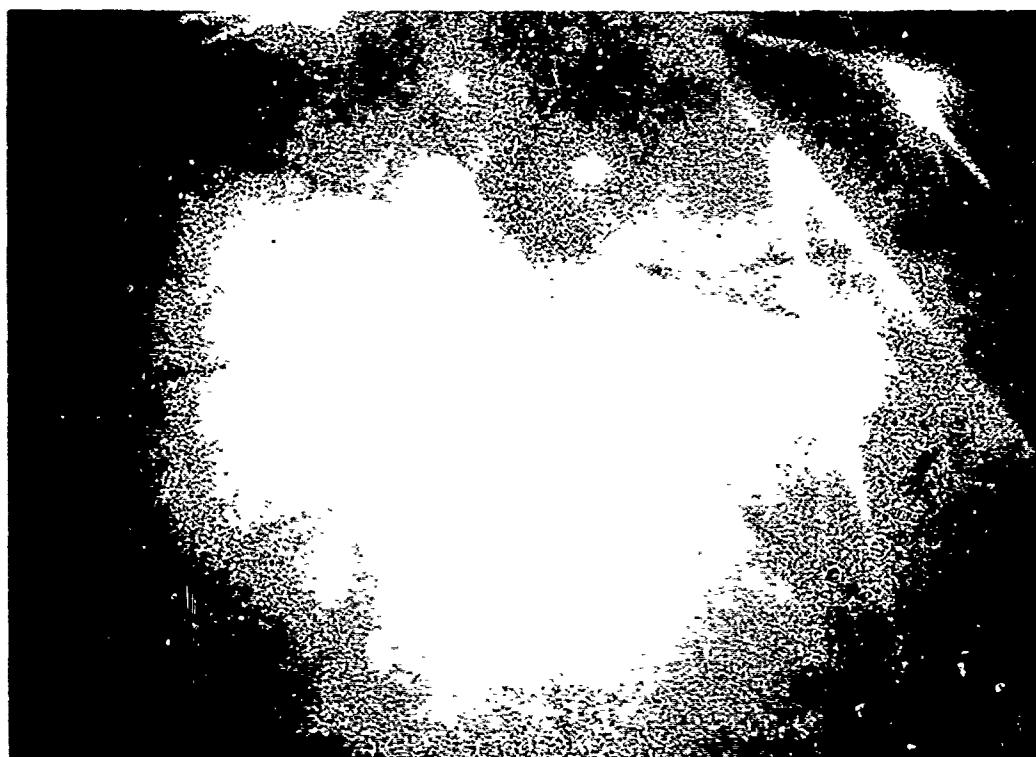
Diffraction

h. B-72/850

FIGURE 7. (CONTINUED)

22
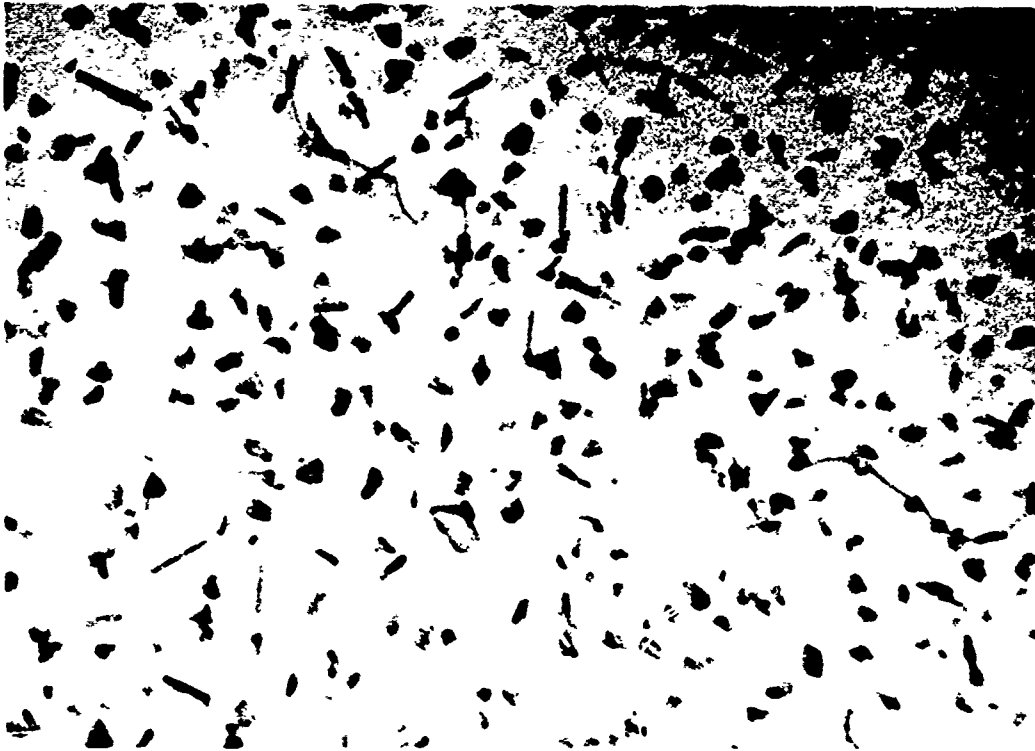
28,000X
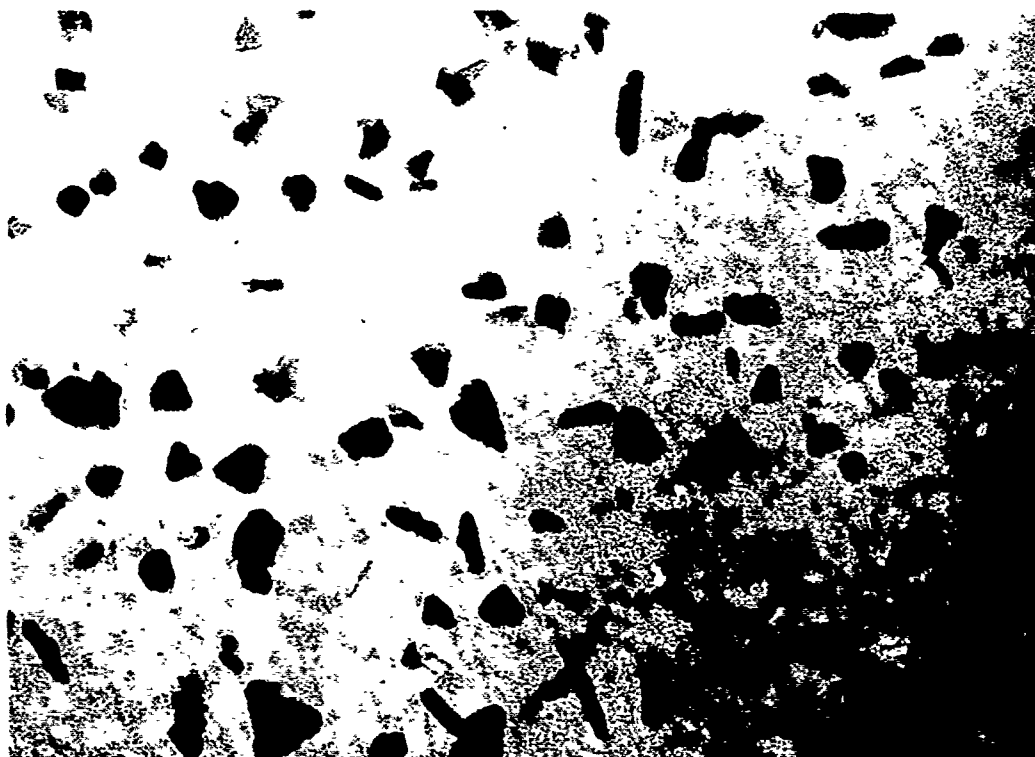
i. B-6/960

56,000X

j. B-6/960

FIGURE 7. (CONTINUED)

23
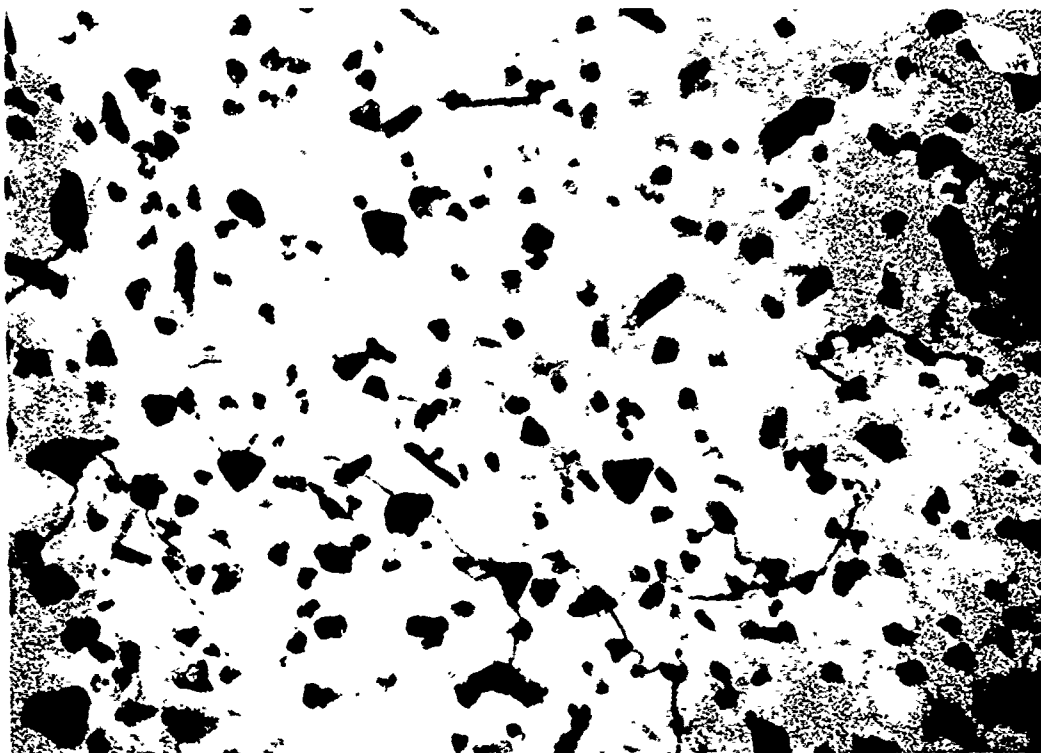
31,000X
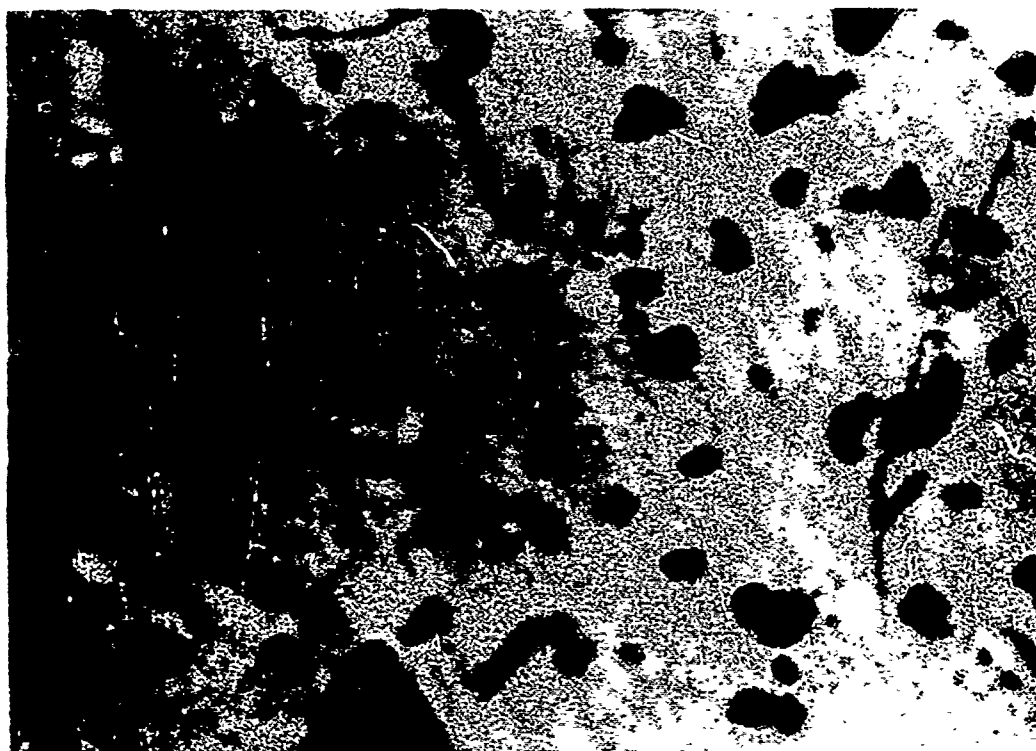
k. B-72/960

62,000X

1. B-72/960

FIGURE 7. (CONTINUED)

24
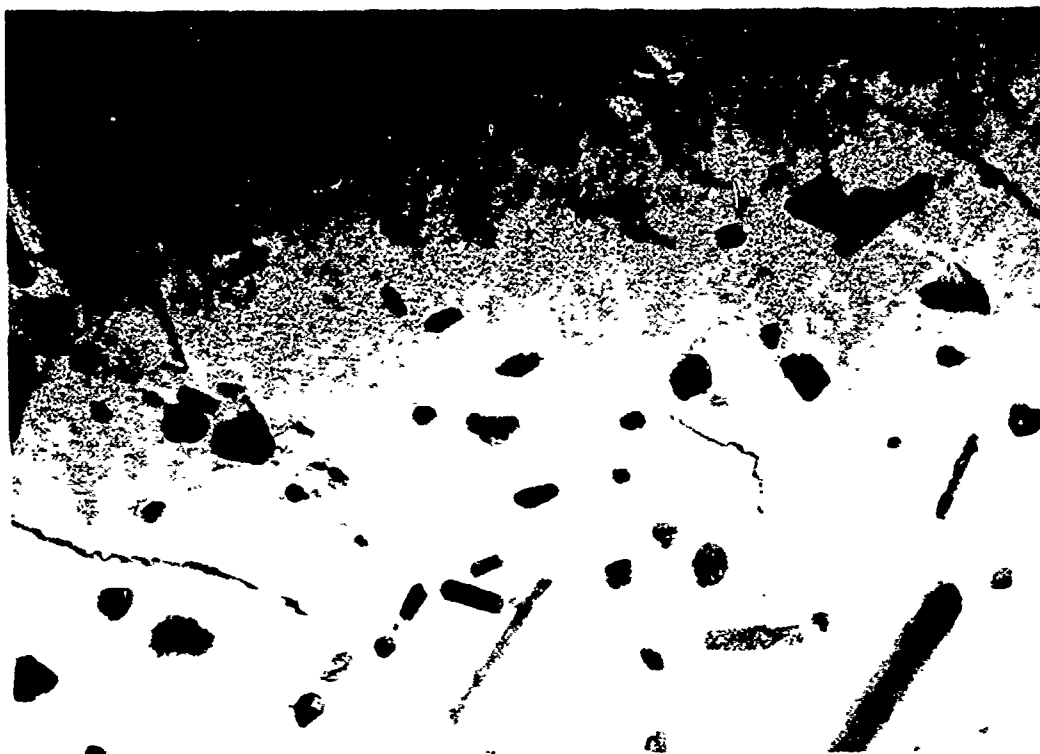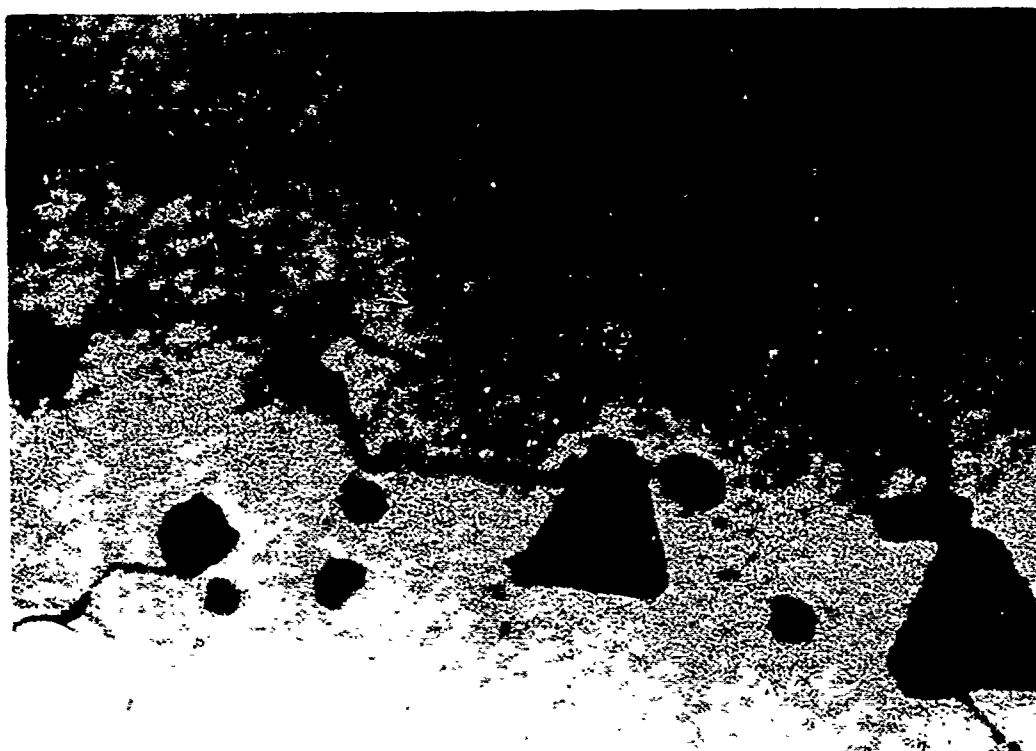
32,000X

m. B-670/960

62,000X

n. B-670/960

FIGURE 7. (CONTINUED)
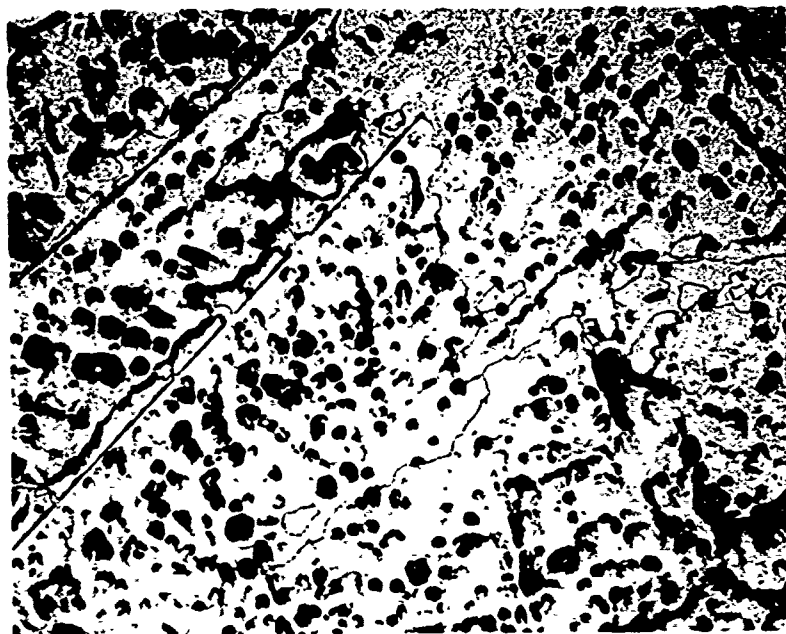
100X

a. B-72/750

500X

b. B-72/750

FIGURE 8.   OPTICAL MICROSCOPY OF ALLOY B
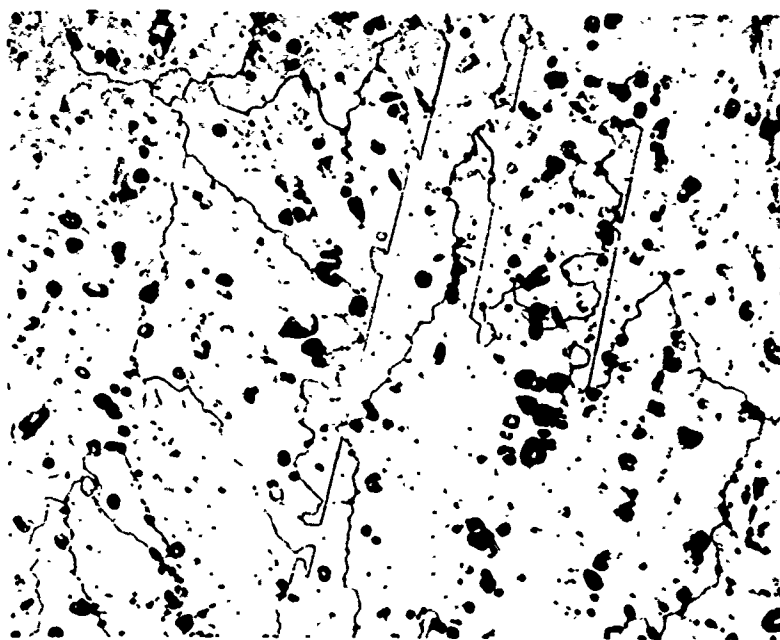
100X

c. B-6/850

500X

d. B-6/850

FIGURE 8. (CONTINUED)

27
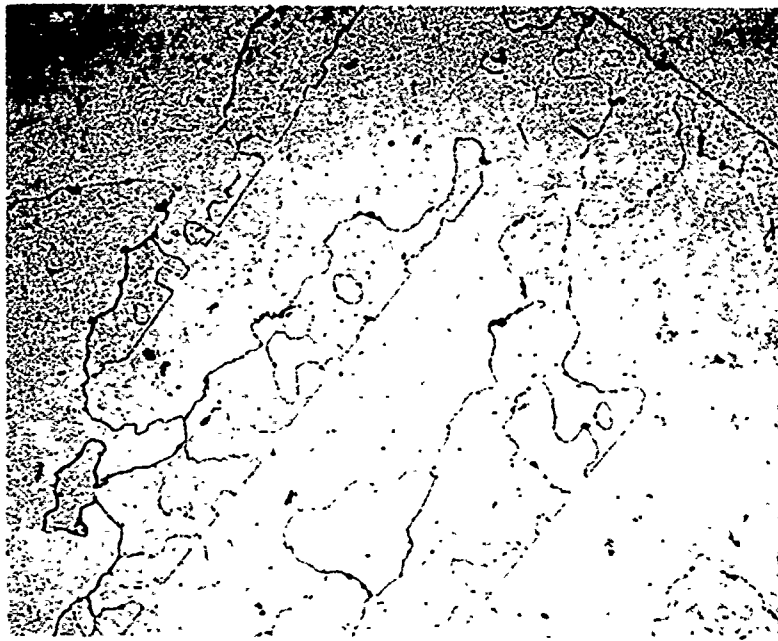
100X
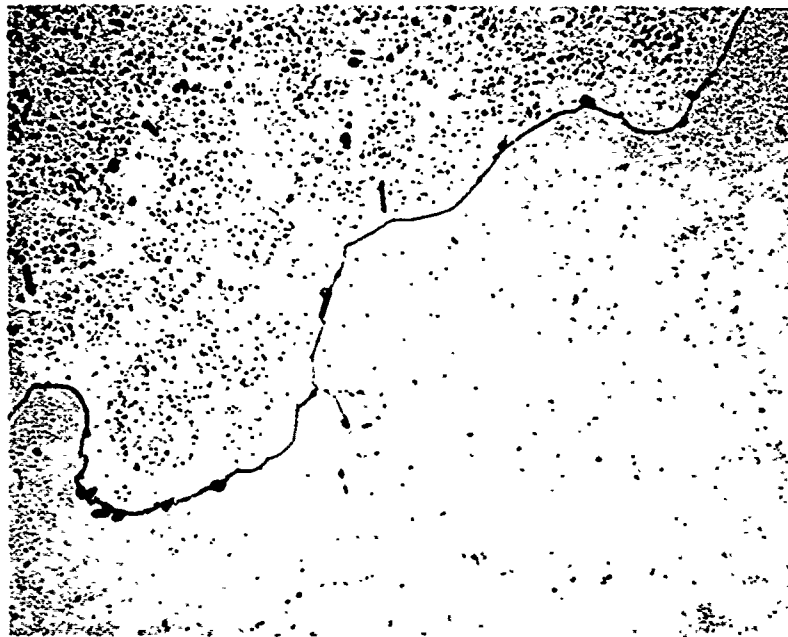
e. B-670/960

500X

f. B-670/960

FIGURE 8. (CONTINUED)
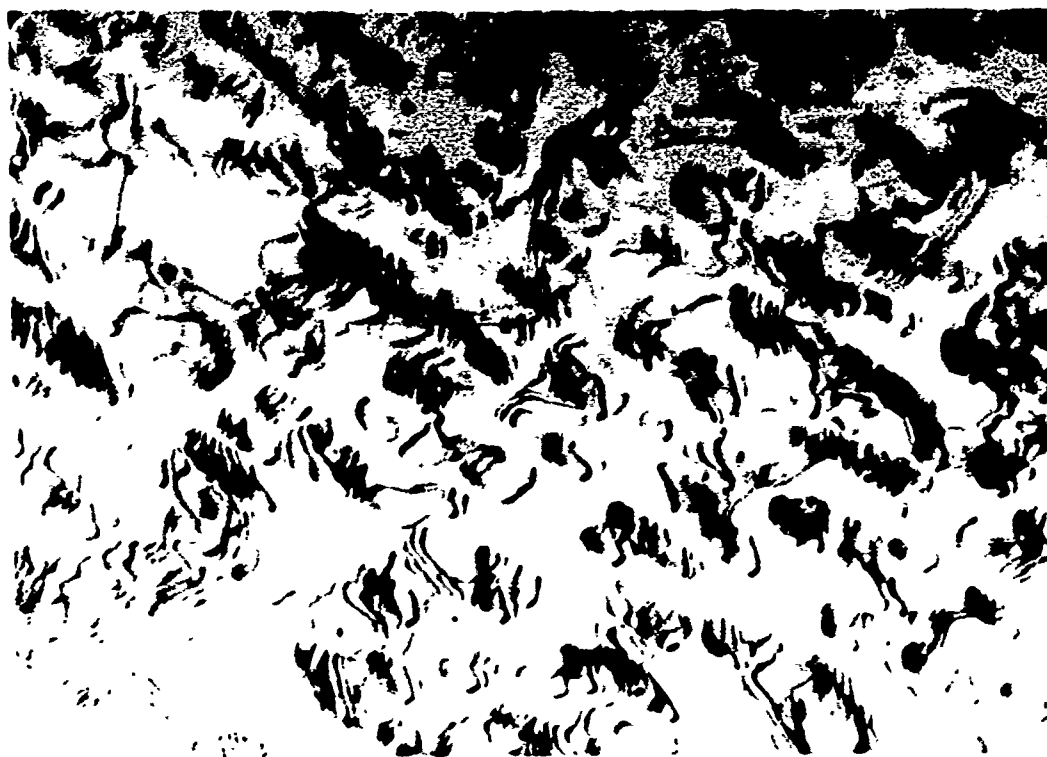
34,000X

a. J-72/750
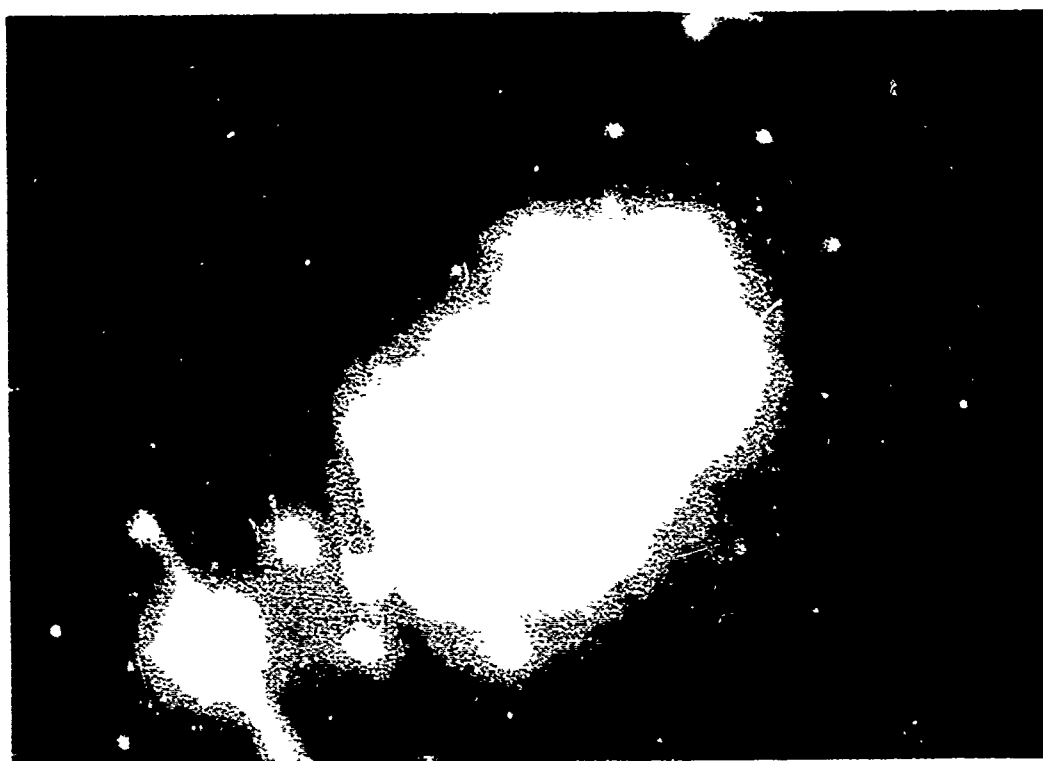
67,000X

b. J-72/750

FIGURE 9. TRANSMISSION ELECTRON MICROSCOPY OF ALLOY J

35,000X

c. J-72/750

Diffraction

d. J-72/750

FIGURE 9. (CONTINUED)
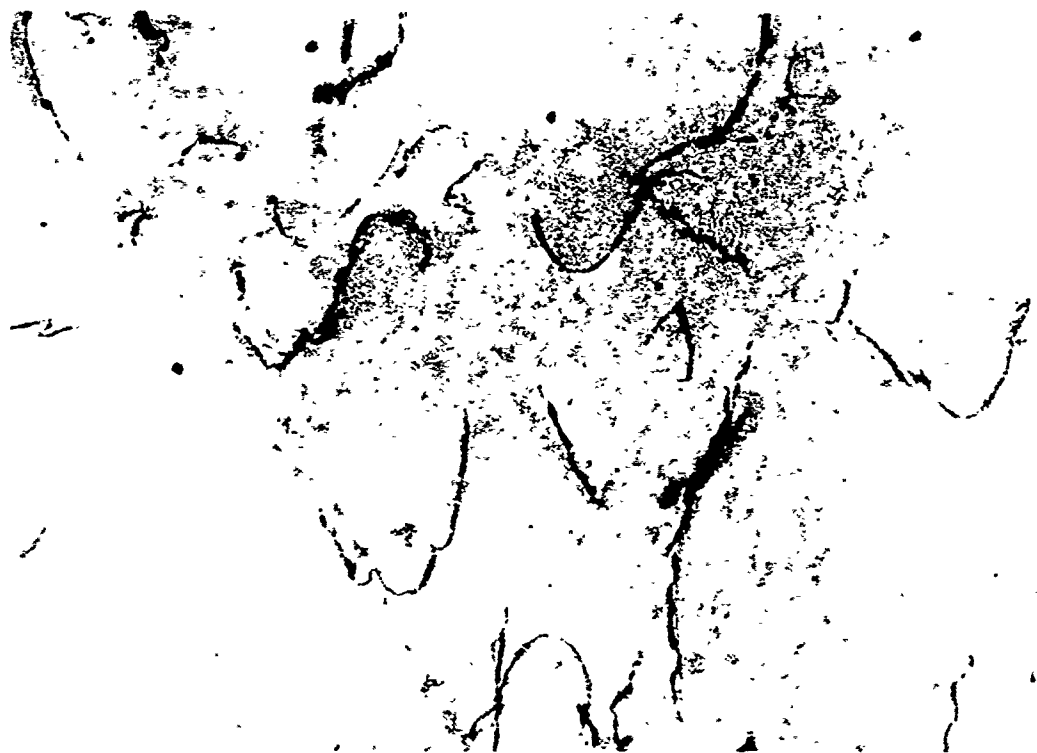
31,000X

e. J-6/850
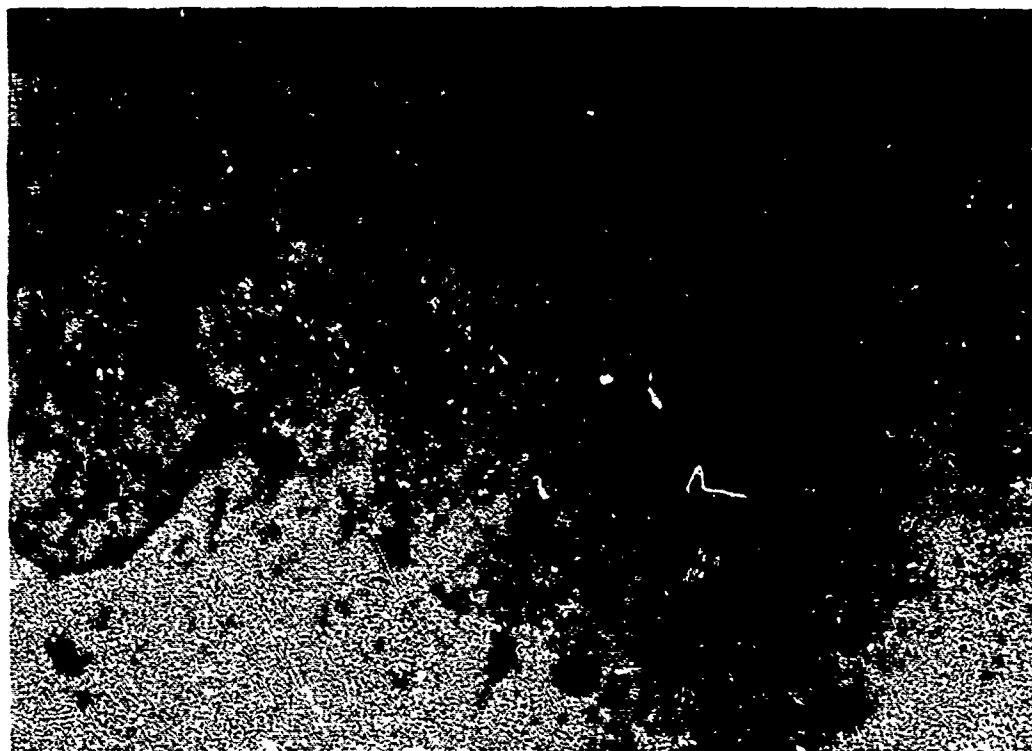
66,000X

f. J-6/850

FIGURE 9. (CONTINUED)

31
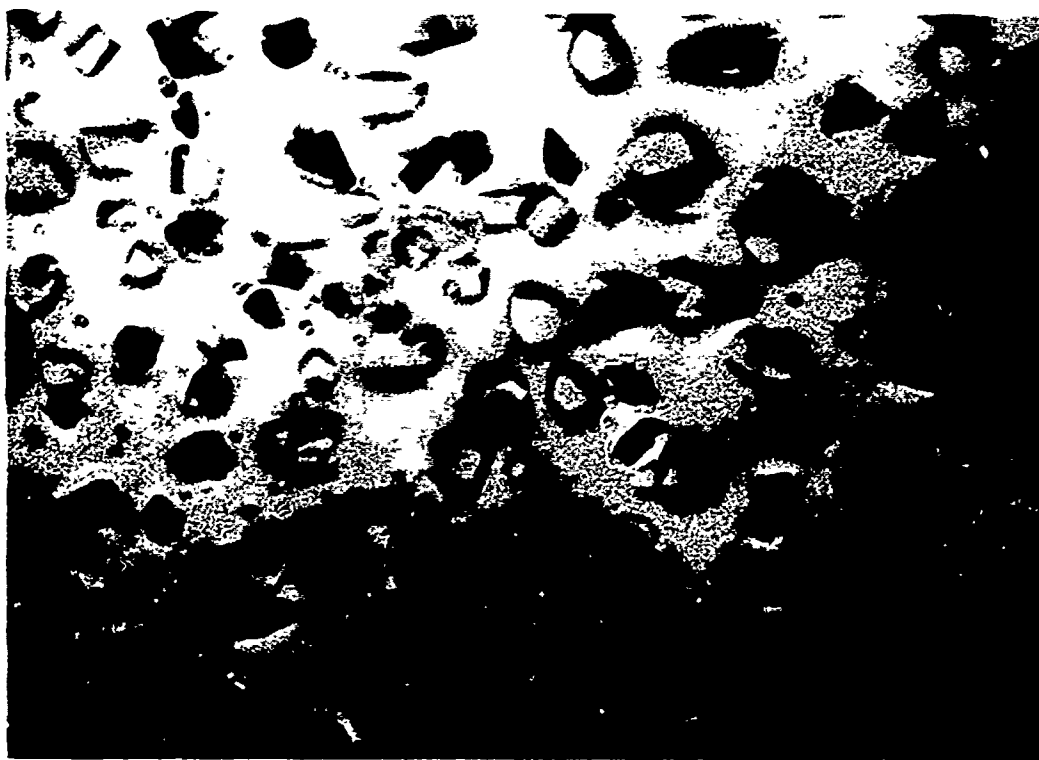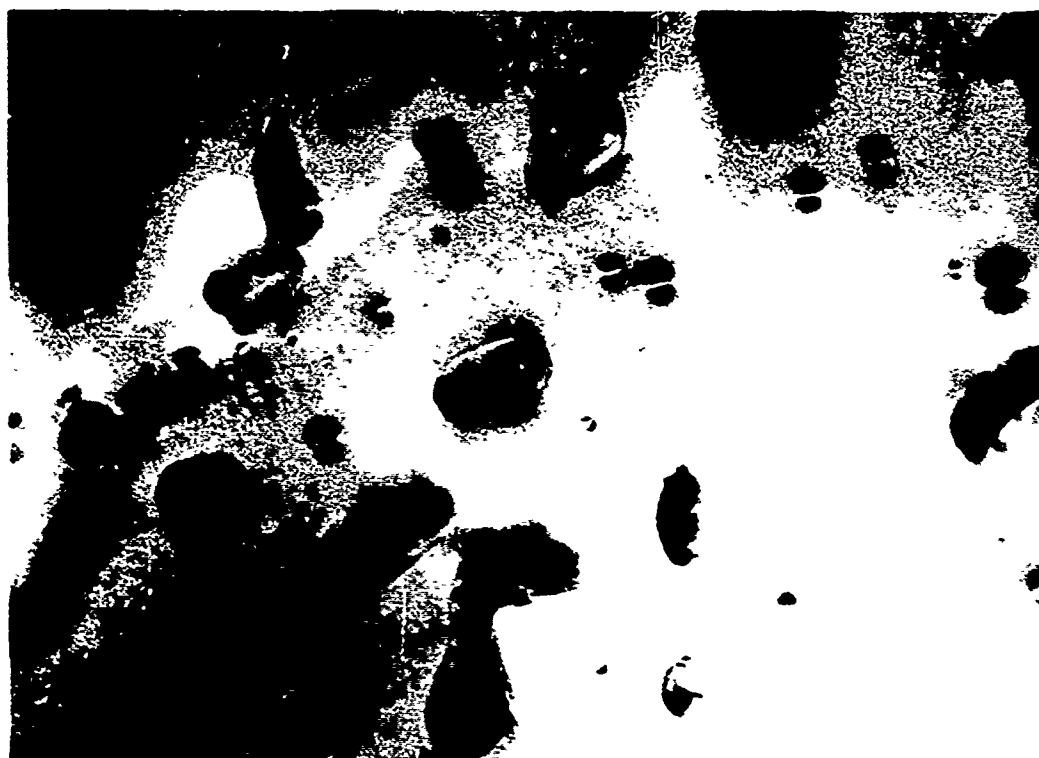
31,000X

g. J-72/960

67,000

h. J-72/960

FIGURE 9. (CONTINUED)

32
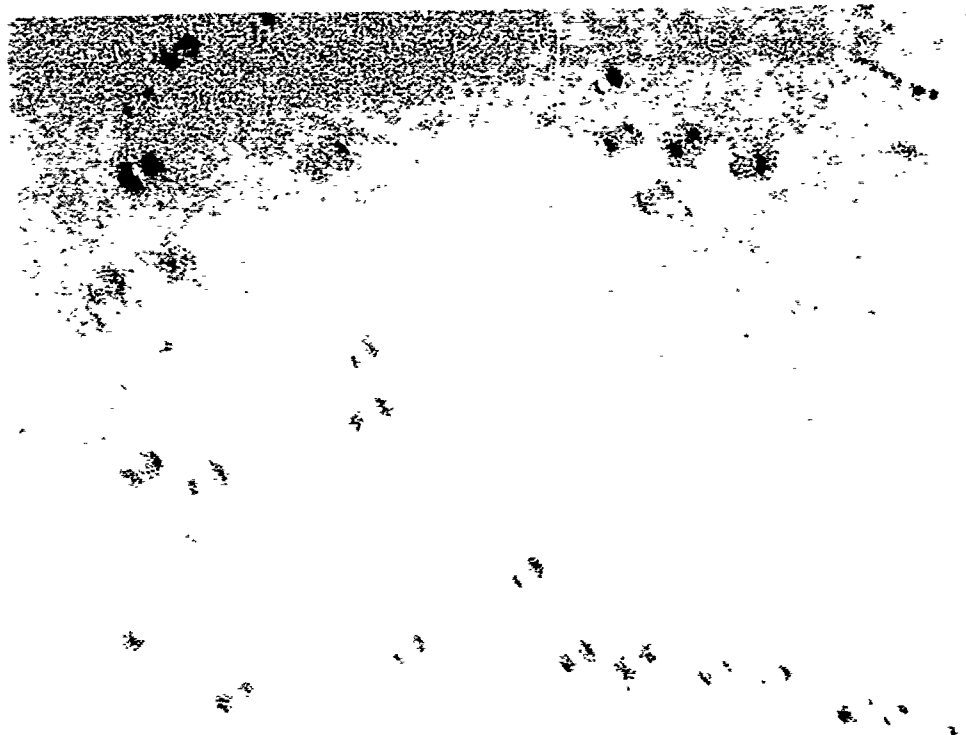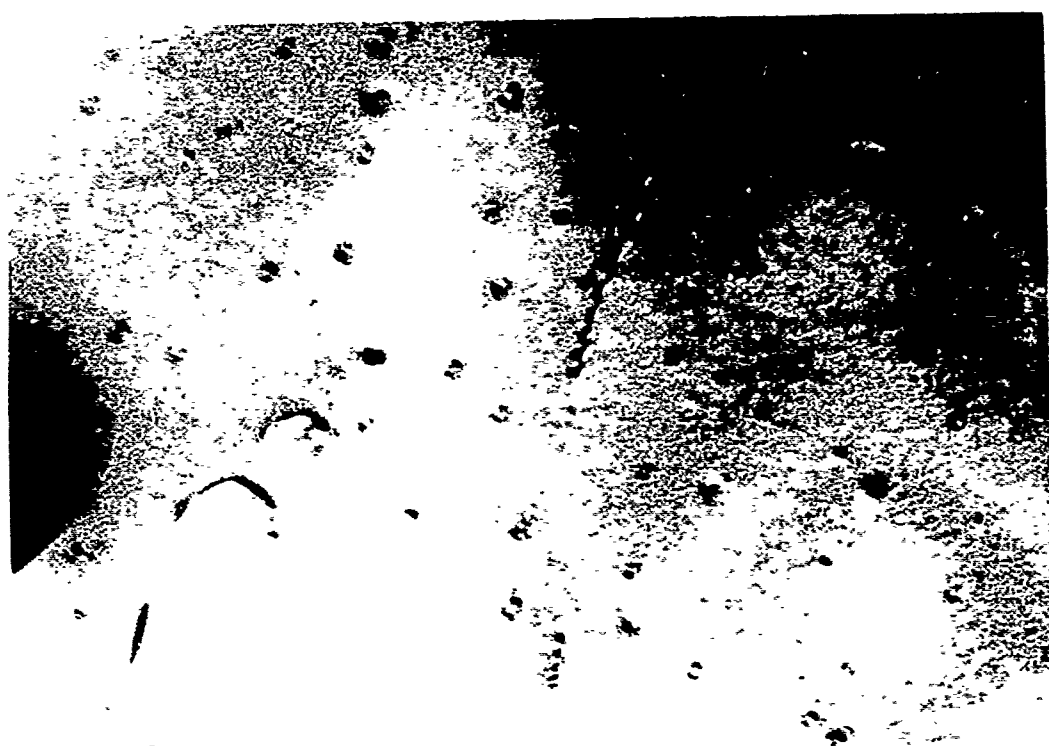
38,000X

i. J-240/960

62,000X

j. J-240/960

FIGURE 9. (CONTINUED)

33
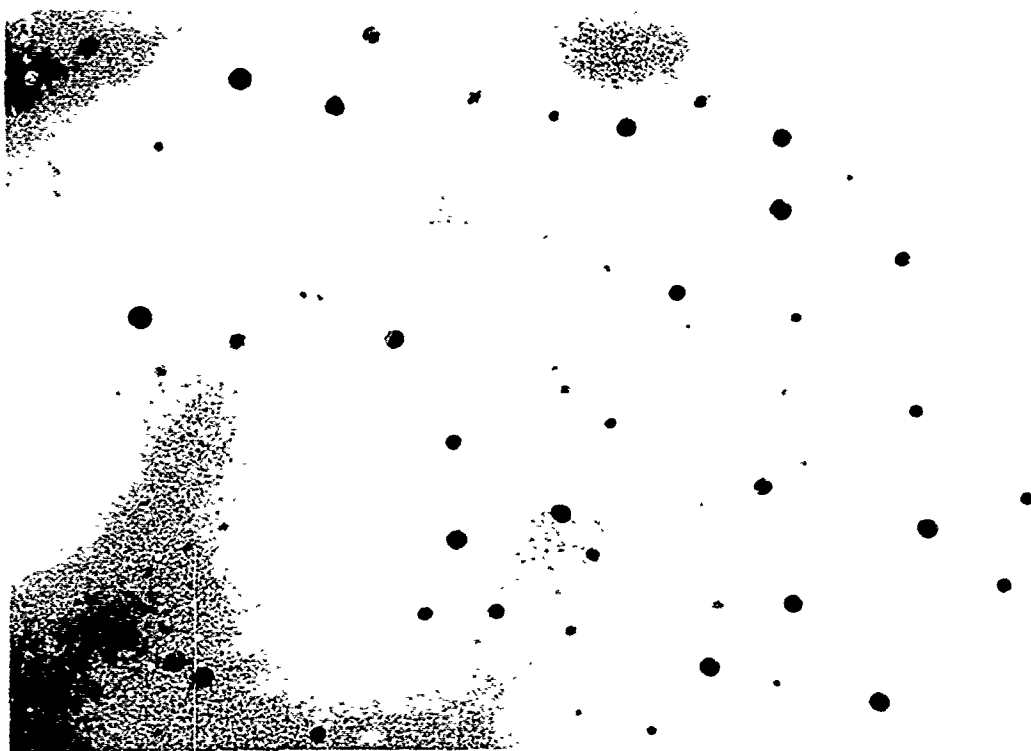
38,000X
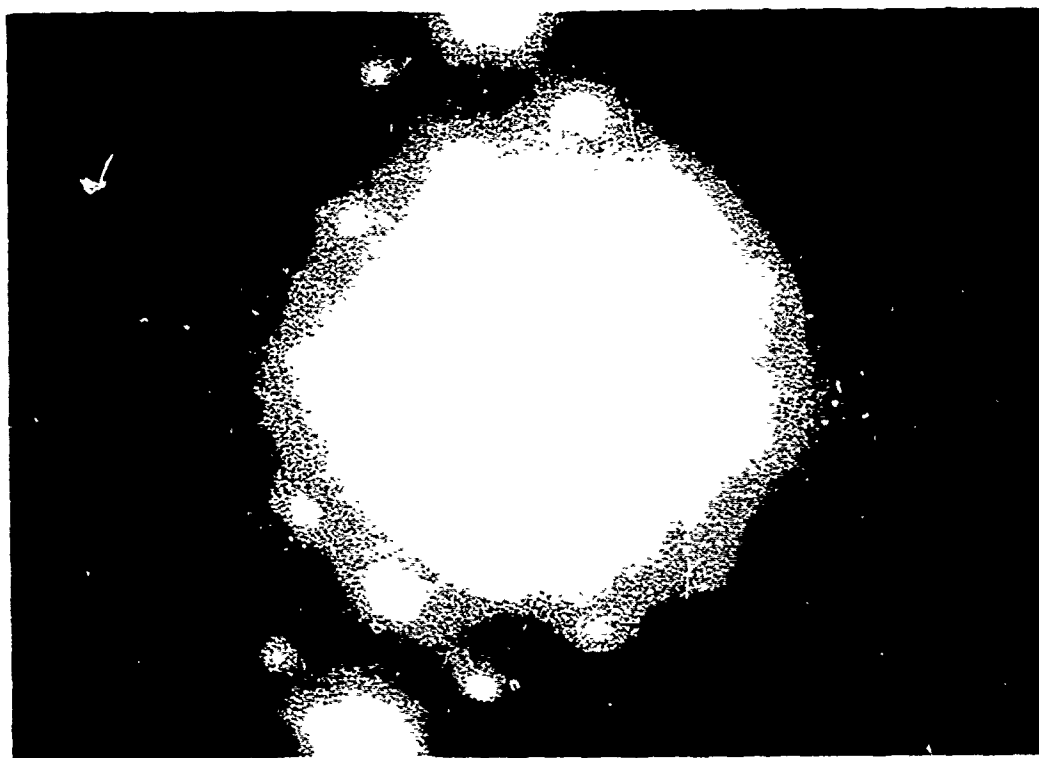
k. J-240/960

Diffraction

l. J-240/960

FIGURE 9. (CONTINUED)

34
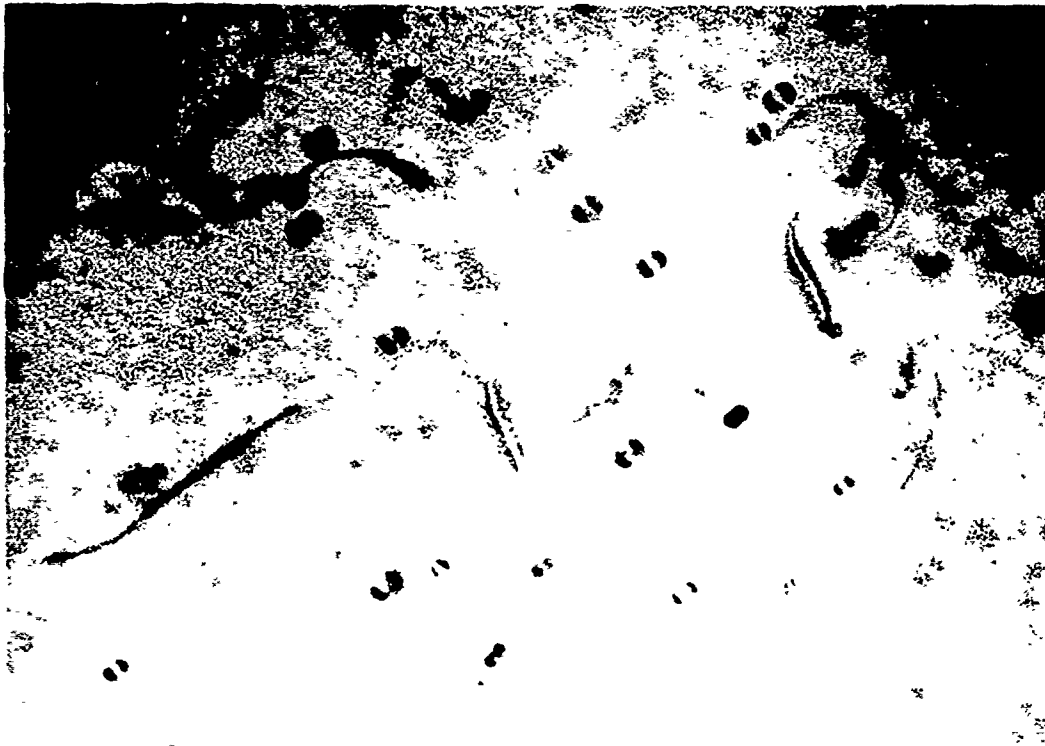
31,000X
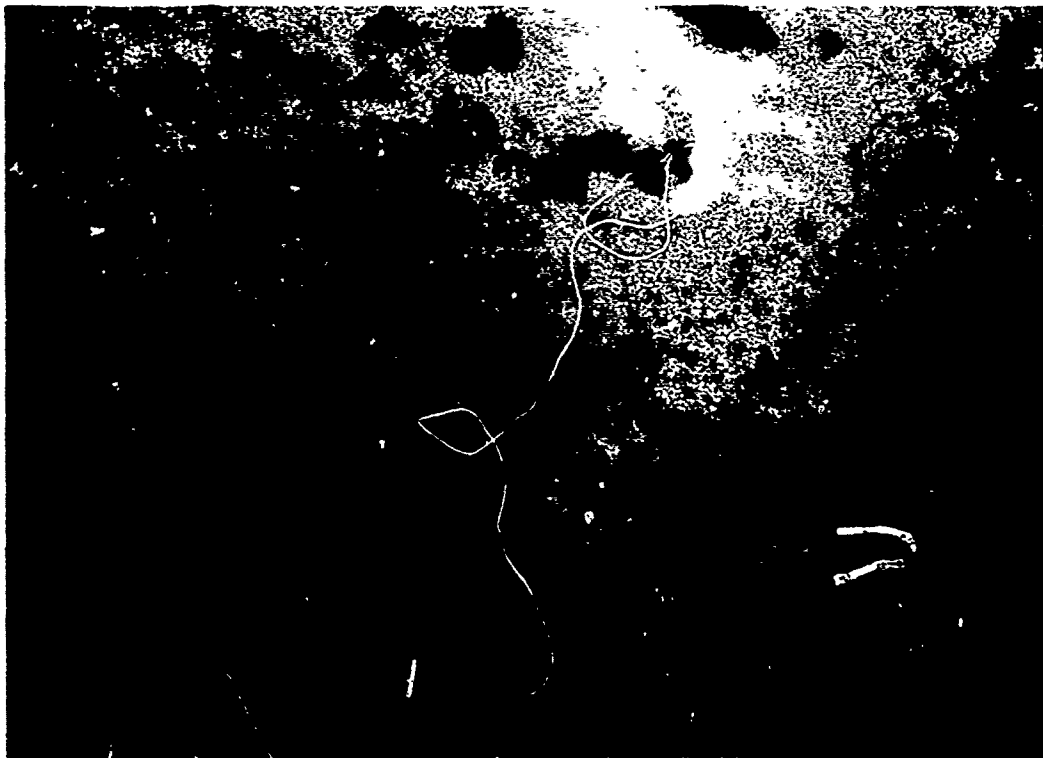
m. J-670/960

62,000X

n. J-670/960

FIGURE 9. (CONTINUED)

35
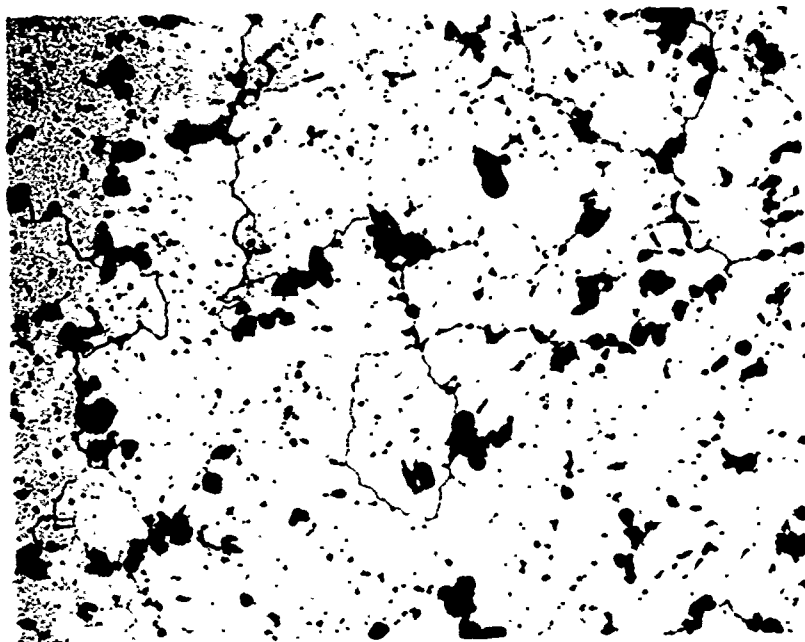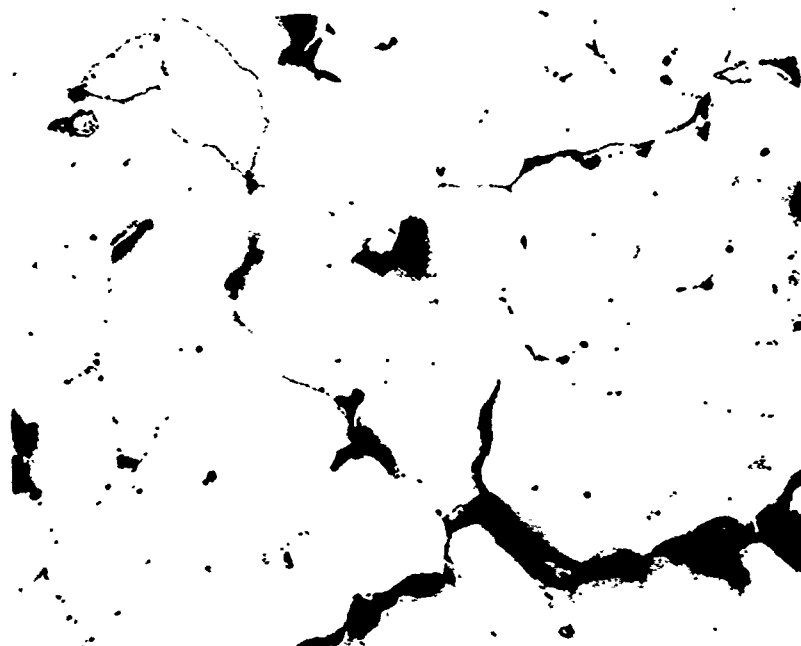
100X

a. J-72/750

500X

b. J-72/750

FIGURE 10. OPTICAL MICROSCOPY OF ALLOY J
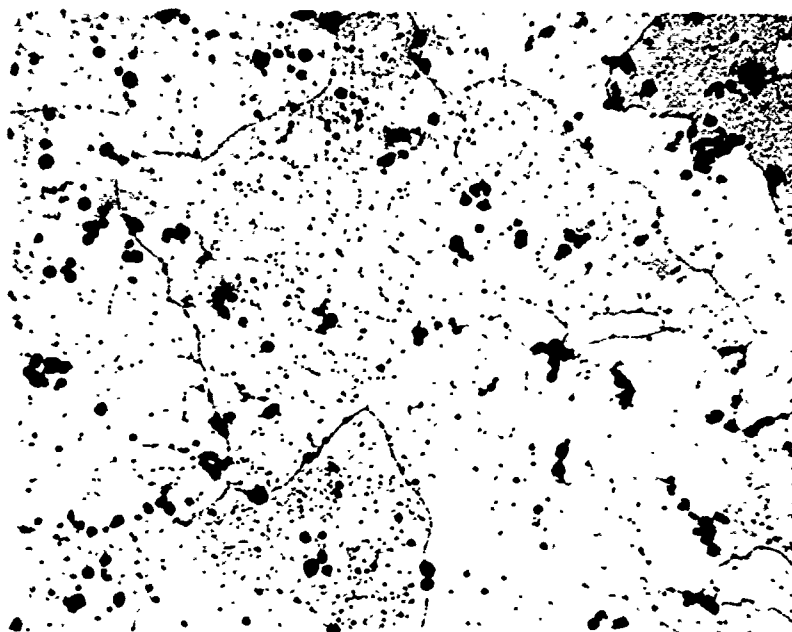
100X

c. J-72/960
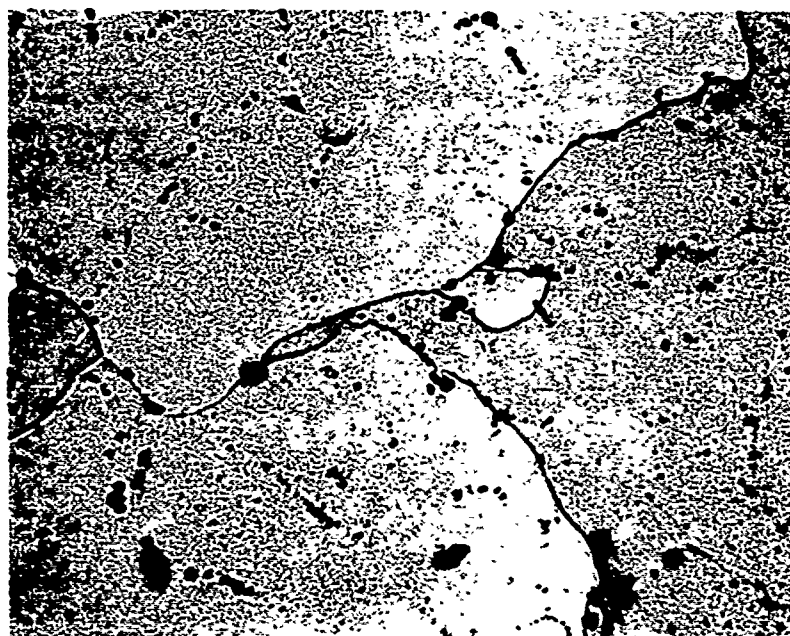
500X

d. J-72/960

FIGURE 10. (CONTINUED)

37
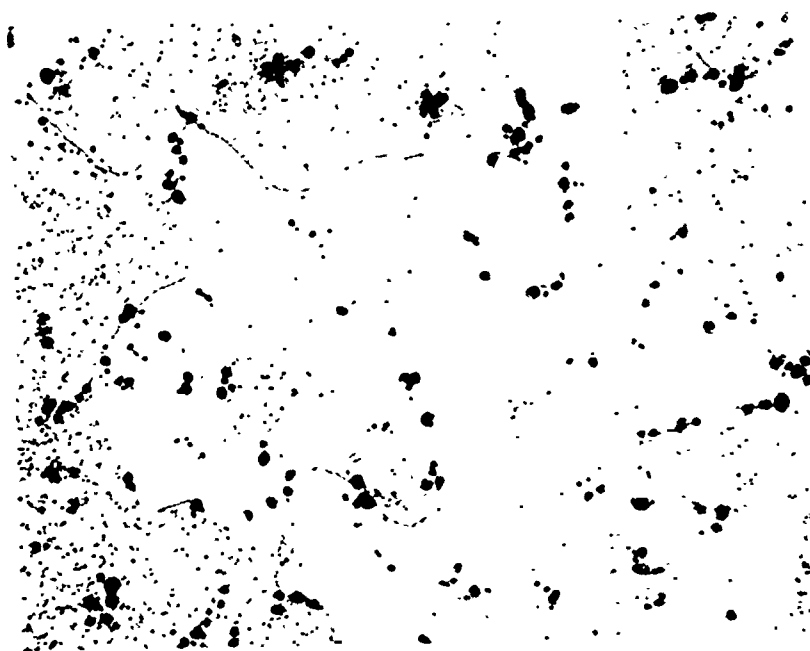
100X
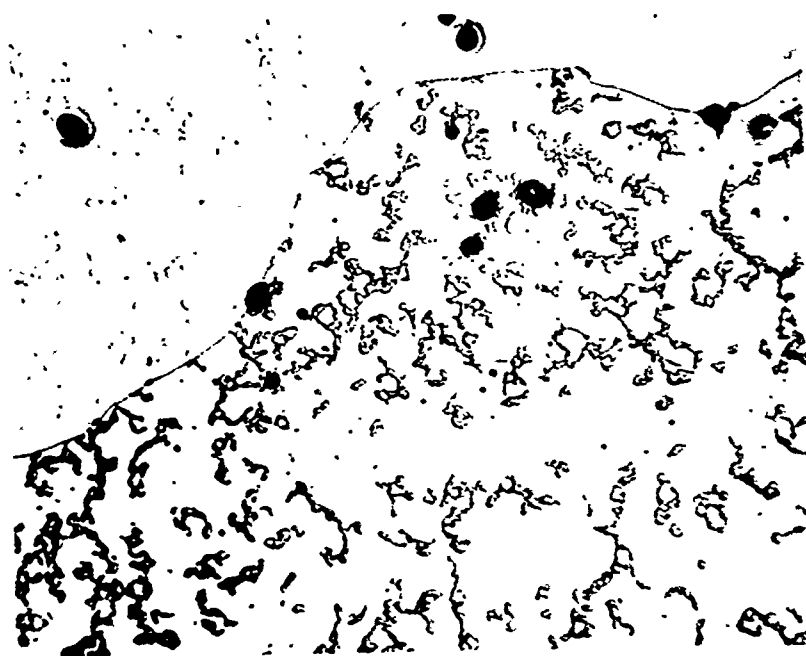
e. J-670/960

500X

f. J-670/960

FIGURE 10. (CONTINUED)

TABLE IV. HEAT TREATMENT VERSUS PARTICLE SIZE IN THE 'B' SERIES

Specimen No.	Homogenization Treatment	Solution Treatment	Average Particle Size, A
B-72/750[a]	72 hr @ 750 F (399 C)	15 min @ 910 F (488 C)	381
B-6/850	6 hr @ 850 F (454 C)	1 hr @ 850 F (454 C)+ 15 min @ 910 F (488 C)	467
B-72/850	72 hr @ 850 F (454 C)	1 hr @ 850 F (454 C)+ 15 min @ 910 F (488 C)	612
B-6/960	16 hr @ 870 F (466 C)+ 6 hr @ 959 F (516 C)	1 hr @ 850 F (454 C)+ 1 hr @ 910 F (488 C)	683
B-72/960	16 hr @ 870 F (466 C)+ 72 hr @ 959 F (516 C)	1 hr @ 850 F (454 C)+ 1 hr @ 910 F (488 C)	812
B-240/960	16 hr @ 870 F (466 C)+ 240 hr @ 954 F (513 C)	1 hr @ 850 F (454 C)+ 1 hr @ 910 F (488 C)	812
B-670/960	16 hr @ 870 F (466 C)+ 670 hr @ 954 F (513 C)	1 hr @ 850 F (454 C)+ 1 hr @ 910 F (488 C)	1224

(a) In the terminology used in this report for specimen number, "B" is the alloy designation, 72 is time in hours, and 750 is temperature, F.

## TABLE V. HEAT TREATMENTS GIVEN IN THE 'J' SERIES

Specimen No.	Homogenization Treatment	Solution Treatment
J-72/750	72 hr @ 750 F (399 C)	15 min @ 910 F (488 C)
J-6/850	6 hr @ 850 F (454 C)	1 hr @ 850 F (454 C)+ 15 min @ 910 F (488 C)
J-72/850	72 hr @ 850 F	1 hr @ 850 F
J-72/960	16 hr @ 850 F (454 C)+ 72 hr @ 959 F (516 C)	1 hr @ 850 F (454 C)+ 1 hr @ 910 F (488 C)
J-240/960	16 hr @ 870 F (466 C)+ 240 hr @ 954 F (513 C)	1 hr @ 850 F (454 C)+ 1 hr @ 910 F (488 C)
J-670/960	16 hr @ 870 F (466 C)+ 670 hr @ 954 F (513 C)	1 hr @ 850 F (454 C)+ 1 hr @ 910 F (488 C)

density and a very low count of Zr particles. J-72/960 unexpectedly formed a high density of large particles that appeared to be somewhat similar to those found in the 'B' series; small Zr particles could still be seen in the background (Figure 9g). Comparing J-72/960 (Figure 9g) and J-240/960 (Figure 9i), it appears that homogenization times over 72 hours at 954 F (513 C) are required to produce a desired microstructure for this series. In J-240/960 (Figure 9i) all the large intermediate particles appear to have dissolved and we are left with a reasonably dislocation-free matrix with a relatively even distribution of Zr particles. The average size is about 500 A. The density of these particles appeared to be higher and of more uniform distribution in J-240/960 (Figure 9i) than in J-670/960 (Figure 9m). From this characterization it would appear that the homogenization time of 670 hours would be most suitable to produce large Zr particles. The low-magnification micrographs (Figure 10) simply show a general improvement and clearing with increasing homogenization treatments.

Final Homogenization and Processing

The following homogenizations have been applied to sections of the stress-relieved [~16 hr at 525 F (275 C)] ingot:

Alloys	Low-Temperature Homogenization	High-Temperature Homogenization
M & N	6 hr @ 850 F (454 C)	240 hr @ 925 F (496 C)
A, B, & C	6 hr @ 850 F (454 C)	670 hr @ 960 F (515 C)

All these materials have been scalped and rolled to various gages. During rolling their temperature was kept above 600 F (315 C) down to approximately 0.125-in. gage. Below this gage, the high chill factor of the rolls led to essentially warm rolling, although the material was heated. Portions were retained at 1.0, 0.5, 0.25, 0.125, and 0.063-in. gage. The effects of the different intermediate particle sizes on recrystallization and grain size are shown in Figures 11-16 for alloys M and N. It can be seen that Mn particle size has a definite effect on grain size, particularly in Alloy N. An analysis of grain size and shape is given in Table VI. Very few trends can be seen in the grain-size data, except those for the much coarser grain size of the 1.0-in. material. There was a tendency for grain coarsening at the thinner gages, which was probably due to the warm working of these gages during rolling. Some dynamic recrystallization is evident in Figure 11 in the 0.063-in. material in the "as-rolled" condition. On solution heat treating of this material, considerable grain growth is evident, particularly in the material homogenized at 925 F (496 C). The same trends can be seen for Alloy N in Figure 14. Micrographs of all gages after solution heat treatment are shown in Figures 13 and 16. It is evident that Alloy N suffers more grain growth in the high-temperature homogenized condition than does Alloy M. This could be due to the presence of more Fe- and Si-bearing phases or to the higher "soluble" phase content which exceeds the solid solubility. This could be part of the reason for the

40

TABLE VI. GRAIN SIZE AND ASPECT RATIOS OF HOMOGENIZED ALLOYS M (2024)
AND N (2124)

Thickness, gage inch	Alloy M						Alloy N					
	6 Hr at 850 F (454 C)			240 Hr at 925 F (496 C)			6 Hr at 850 F (454 C)			240 Hr at 925 F (496 C)		
	l(a)	d(b)	ar(c) ~1	l	d	ar ~1	l	d	ar ~1	l	d	ar ~1
Ingot												
1.0	0.75	0.13	6	0.4	0.09	2	0.75	0.20	4	1.0	0.20	5
0.5	0.08	0.03	3	0.10	0.04	3	0.05	0.02	2	0.20	0.05	4
0.25	0.10	0.04	3	0.10	0.05	2	0.06	0.02	3	0.5	0.13	4
0.125	0.5	0.10	5	0.20	0.06	3	0.25	0.06	4	0.4	0.15	3
0.063	0.10	0.04	3	0.4	0.12	3	0.20	0.06	3	0.5	0.13	4

(a) l = average grain length (mm).

(b) d = average grain thickness (mm).

(c) ar = aspect ratio (ℓ/d).

Measurements made on 100X micrographs of a longitudinal section, i.e., a section which includes the rolling direction and the sheet or plate thickness viewed in the long transverse direction.

low-temperature homogenized material's greater resistance to grain growth (Figure 16) since Alloy N also contains considerable amounts of undissolved soluble phases (Figure 15).

Figures 12 and 15 show the "as-polished" structure after solution heat treating. It can be seen that some differences in the volume fraction of second-phase particles are still present after rolling. That is, rolling plus solution heat treating was not sufficient to return as much second phase to solution as was attained with the prolonged homogenization of the high-temperature practice. Measurements were made on an electronic particle counter of the volume percent of the second phase. The results of these counts are shown in Table VII. Note that prolonged homogenization has no systematic effect on the amount of the second phase of Alloy M, while it has a distinct effect on Alloy N. The effect of longer solution heat treatment practices on the low-temperature homogenized material will be determined.

TABLE VII. VOLUME PERCENT OF SECOND-PHASE PARTICLES IN HOMOGENIZED ALLOYS M AND N[a]

Gage, in.	Alloy M		Alloy N	
	6 Hr at 850 F (456 C)	240 Hr at 925 F (496 C)	6 Hr at 850 F (454 C)	240 Hr at 925 F (496 C)
Ingot	3.3	2.8	1.4	< 0.2 [b]
1	2.7	2.3	1.2	< 0.2 [b]
0.5	2.4 [b]	2.7 [b]	0.6 [b]	< 0.2 [b]
0.25	1.8 [b]	1.6 [b]	0.4	< 0.2 [b]
0.125	2.0 [b]	2.2 [b]	0.7 [b]	< 0.2 [b]
0.063	1.9 [b]	2.4 [b]	0.5	< 0.2 [b]

(a) Each value from 100 fields at 725X.

(b) Contained fine particles less than 2 microns in diameter which were not counted.

As Rolled

0.5 Inch

Solution Heat
Treated

As Rolled

0.063 Inch

Solution Heat
Treated
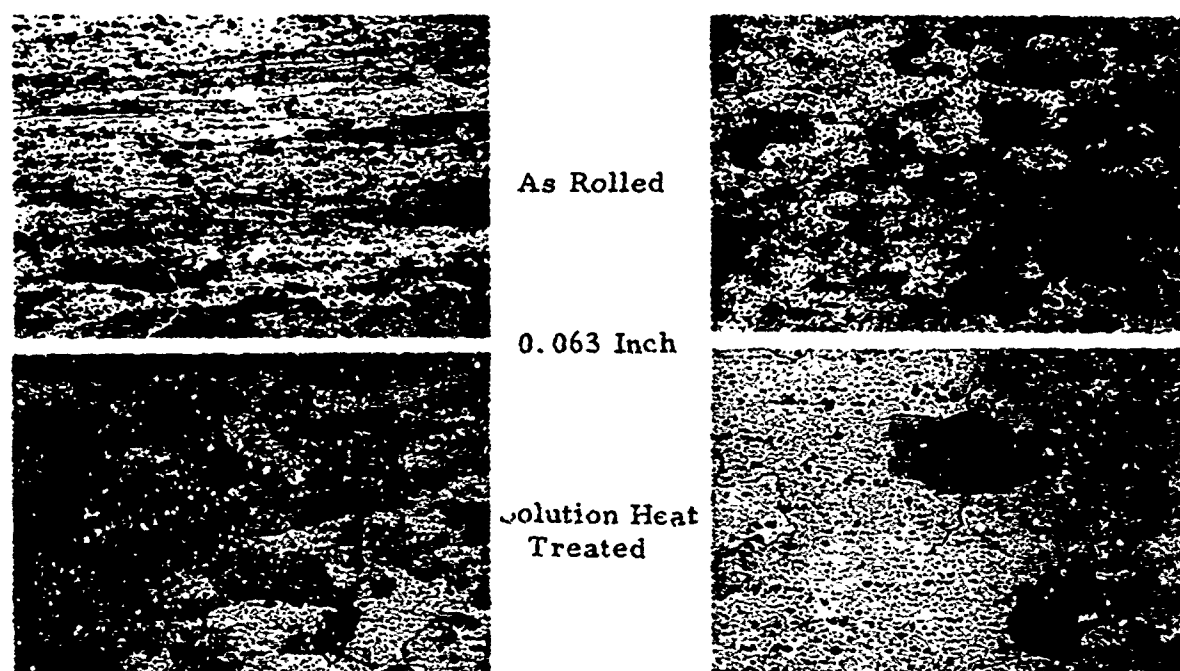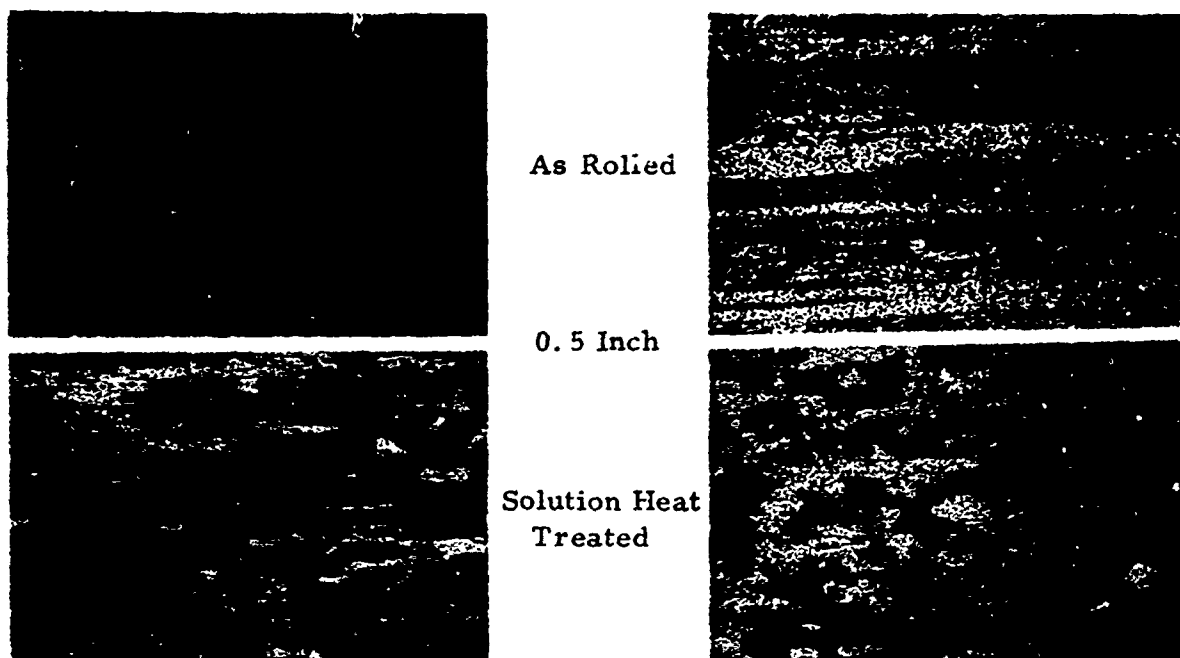
100X
Homogenized 6 hours at
850 F (454 C)

100X
Homogenized 240 hours at
925 F (494 C)

FIGURE 11.   ALLOY M (2024); KELLER'S ETCH EFFECT OF SOLUTION HEAT
TREATMENT [1 HOUR AT 925 F (496 C)] AFTER ROLLING IN
GRAIN STRUCTURE OF 0.5 AND 0.063 INCH-GAGE MATERIAL.

Ingot

0.5 Inch

0.063 Inch

250X	250X
Homogenized 6 hours at 850 F (454 C)	Homogenized 240 hours at 925 F (496 C)
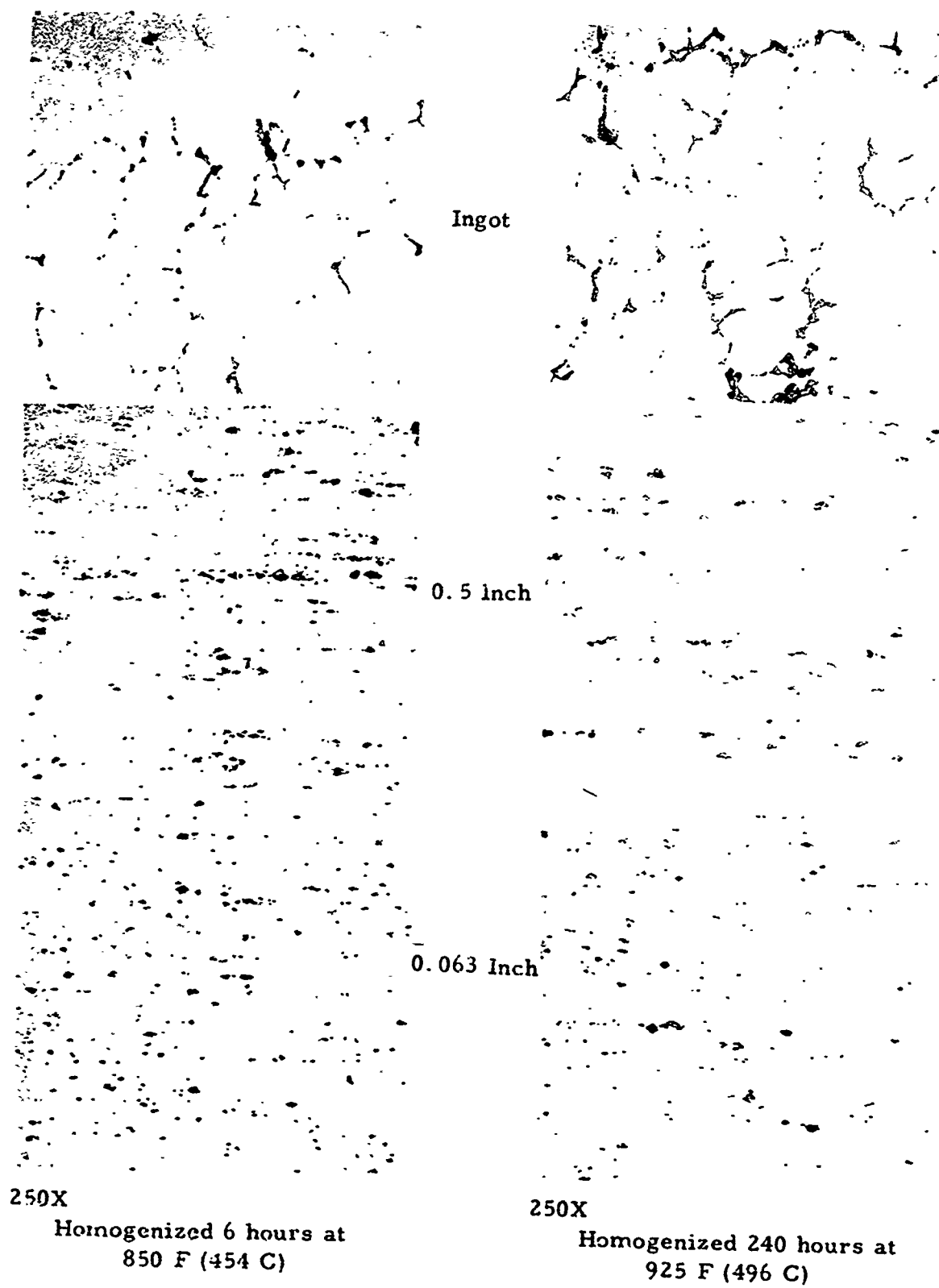
FIGURE 12.   ALLOY M (2024); AS-POLISHED EFFECT OF ROLLING ON SECOND-PHASE PARTICLE CONTENT AFTER SOLUTION HEAT TREATMENT

Ingot

1 Inch

0.5 Inch

0.25 Inch

0.125 Inch

0.063 Inch

100X Homogenized 6 hours at
850 F (454 C)

100X Homogenized 240 hours at
925 F (496 C)

FIGURE 13   ALLOY M (2024); KELLER'S ETCH EFFECT OF ROLLING
AND HOMOGENIZATION ON GRAIN STRUCTURE

Solution heat treated 1 hr at 925 F (496 C).

45

As Rolled

0.5 Inch

Solution Heat Treated

As Rolled
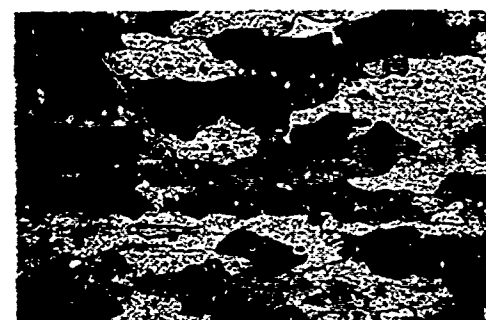
0.063 Inch

Solution Heat Treated

100X
Homogenized 6 hours at
850 F (454 C)

100X
Homogenized 240 Hours at
925 F (496 C)

FIGURE 14.   ALLOY N (2124); KELLER'S ETCH EFFECT OF SOLUTION HEAT
TREATMENT [1 HOUR AT 925 F (496 C)] AFTER ROLLING ON
GRAIN STRUCTURE OF 0.5 AND 0.063 INCH-GAGE MATERIAL

Solution heat treated 1 hour at 925 F (496 C).

46
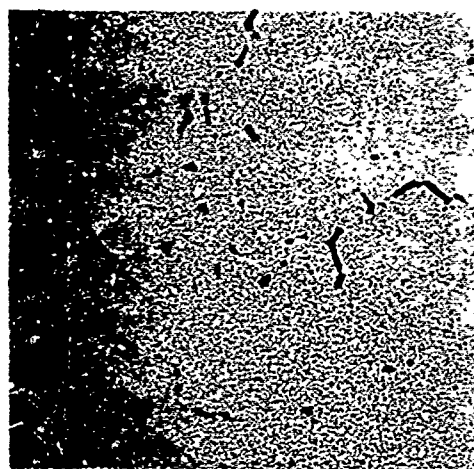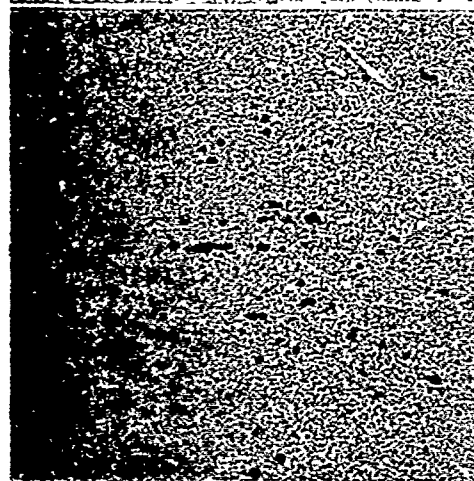
Ingot
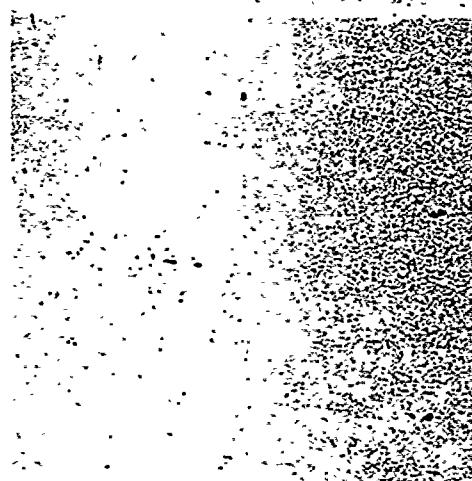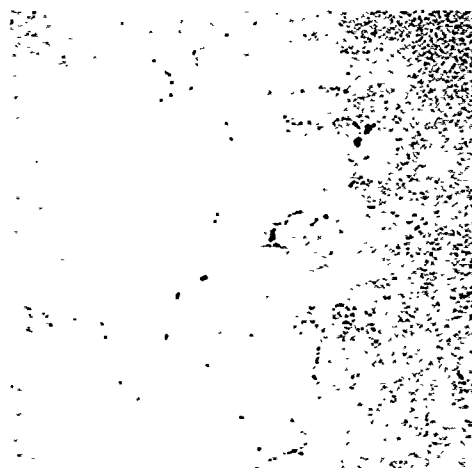
0. 5 inch

0. 063 inch

250X
Homogenized 6 hours at
850 F (454 C)

250X
Homogenized 240 hours at
925 F (496 C)

FIGURE 15. ALLOY N (2124); AS-POLISHED EFFECT OF ROLLING ON
SECOND-PHASE PARTICLES AFTER SOLUTION HEAT
TREATMENT
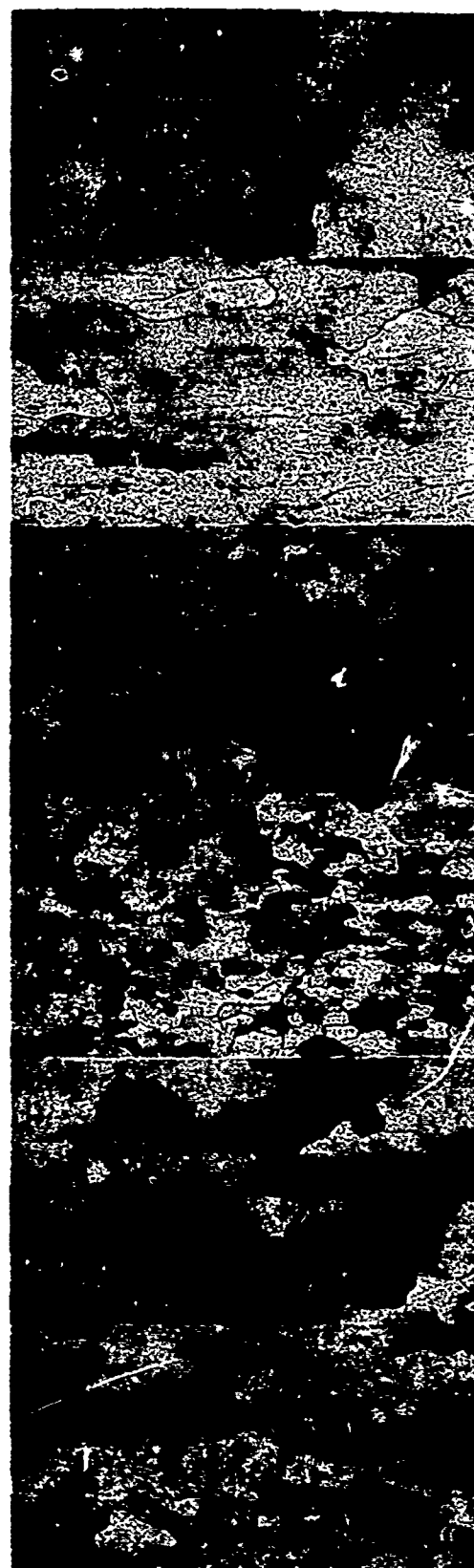
Ingot

1 Inch

0.5 Inch

0.25 Inch

0.125 Inch

0.063 Inch

100X
Homogenized 6 hr at
850 F (454 C)

100X
Homogenized 240 hr. at
925 F (496 C)

FIGURE 16. ALLOY N (2124); KELLER'S ETCH EFFECT OF ROLLING
AND HOMOGENIZATION ON GRAIN STRUCTURE

Solution heat treated 1 hr at 925 F (496 C).

Aging Practices for Alloys M (2024) and N (2124)

Prior to starting the test program, suitable aging practices must be selected. The objective will be to find two aging practices which lead to similar strengths yet have different slip modes. Initial work on Alloys M and N was carried out to determine the tensile aging curve for both homogenization practices. The results of these tests are shown in Table VIII. There is apparently a drop in yield strength at 13 hours of aging. The material aged for this time was processed separately and, since its strength doesn't fit with the adjoining data, it must be regarded as suspect; also, the T81 data [12 hr at 370 F (188 C)] do fit well with the remainder of the aging curve. It can be seen that basically neither homogenization nor composition strongly influenced aging. The high-temperature homogenized version of Alloy N has consistently higher strength, which may be due to the presence of more solute in solution (Table VII). However, the values of electrical conductivity (Table VIII), which essentially measure the amount of solute in solution, are higher for the high-temperature homogenized version of Alloy N. This is indicative of less in solution rather than more. A similar trend in electrical conductivity without any strength variations can be seen for Alloy M in Table VIII. Extended solution heat treatment practices will be employed on the low-temperature homogenized materials in an attempt to achieve increased dissolution. For the fracture toughness portions of the work it will be necessary to minimize the second-phase particle content difference between the homogenization practices if the effect of the different-size intermediate particles is to be detected.

In order to choose aging practices for the 2000 series alloys which will lead to different deformation modes, it may be necessary to use room temperature aged material. To this end, room temperature aging data are shown in Table IX. A long delay (14 days) was experienced between quenching and stretching due to a stretcher malfunction. It can be seen that little change in strength occurs between 4 and 35 days after stretching. Note that for both alloys the low-temperature homogenization version leads to greatly improved elongation. This may be indicative of toughness differences.

TABLE VIII. PRELIMINARY AGING CURVES OF HOMOGENIZED ALLOYS M (2024) AND N (2124) AS 0.063-INCH SHEET[a]

Aging Time at 375 F (191 C), hr	Grain Dir.	Alloy M (2024) 6 Hr at 850 F (454 C) S28828				240 Hr at 925 F (496 C) S28826				Alloy N (2124) 6 Hr at 860 F (454 C) S28827				240 Hr at 925 F (496 C) S28825			
		T[b]	Y	E	EC	T	Y	E	EC	T	Y	E	EC	T	Y	E	EC
2	LT	68.3	56.3	13.3	33.0	66.2	56.0	8.5	34.5	66.3	54.5	15.8	34.9	70.3	59.8	11.3	35.6
4	LT	70.9	64.0	7.0	37.9	70.7	64.8	5.3	37.8	68.6	61.8	8.5	38.9	73.1	67.4	6.5	39.4
8	LT	70.9	64.5	5.5	38.8	70.2	64.9	4.5	40.4	68.6	62.6	7.0	41.2	71.3	65.9	6.0	41.4
13	LT	66.7	56.6	7.0	41.5	66.6	57.3	5.8	42.6	65.6	56.4	6.0	43.1	67.3	57.7	6.0	43.8
36	LT	68.1	59.7	6.0	40.4	68.1	60.0	6.0	42.0	67.0	59.2	6.0	42.8	69.4	61.1	6.0	43.2
64	LT	66.7	57.2	6.0	40.8	67.4	59.0	5.5	42.2	65.8	57.0	6.5	43.0	68.3	59.0	6.0	43.4
T81 (12 hr at 170 F (188 C))	L	70.1	62.5	7.0	40.3	70.2	63.1	6.0	41.3	71.6	64.5	7.5	40.9	73.9	68.1	6.5	42.0
	LT	69.5	62.8	6.5		70.1	63.6	6.0		70.3	64.0	7.0		72.5	66.7	6.3	

(a) Solution heat treated 1 hour at 920 F (494 C), incubated 14 days at room temperature then stretched 2 percent and incubated another 29 days, at room temperature. During aging a heating rate of 25 F/hr (15 C/hr) was used.

(b) L = longitudinal
LT = long transverse
T = ultimate tensile strength (KSI)
Y = 0.2 percent yield strength (KSI)
E = elongation (%)
EC = electrical conductivity (%IACS).

50

TABLE IX. ROOM-TEMPERATURE AGING OF HOMOGENIZED ALLOYS M (2024) AND N (2124)(a)

Time After Stretching, days	Grain Dir.	Alloy M (2024)								Alloy N (2124)							
		6 Hr at 850 F (454 C) S28828				240 Hr at 925 F (496 C) S28826				6 Hr at 850 F (454 C) S28827				240 Hr at 925 F (496 C) S28825			
		T(b)	Y	E	EC	T	Y	E	EC	T	Y	E	EC	T	Y	E	EC
4	L	67.7	52.9	19.5	29.2	64.9	53.2	11.5	30.0	65.7	52.4	20.5	30.2	66.7	54.8	14.5	30.4
	LT	66.5	46.1	18.3		63.4	45.8	10.8		64.0	45.7	19.0		65.0	48.2	15.5	
13	L	69.3	54.4	19.0		66.2	53.8	13.0		67.2	53.5	20.0		68.2	55.9	14.0	
	LT	68.1	46.8	19.3		65.6	47.2	12.3		65.7	46.3	19.8		66.9	48.6	14.3	
35	L	68.0	52.8	18.5		65.7	52.7	13.5		66.4	52.3	20.3		67.0	54.7	15.5	
	LT	66.5	45.3	18.5		64.2	46.2	13.8		64.7	44.7	20.5		65.8	47.9	16.0	

(a) Solution heat treated 1 hour at 920 F (493 C), cold water quenched.
(b) See footnotes to Table 8.

51

IV

TASK B. CONTROL OF GRAIN STRUCTURE DURING HOT WORKING

Background

Aluminum alloys belong to a group of materials which dissipate strain hardening during hot working by extensive dynamic recovery as opposed to recrystallization. Recrystallization, when it occurs during hot working (or most probably, immediately following), usually introduces a coarse grain structure fairly damaging to mechanical properties. As a result, alloy compositions and processing schedules for high-strength wrought alloys have been modified to favor dynamic recovery during hot working. During fabrication, current high-strength alloys normally develop a highly elongated grain structure, which is often directly related to the cast grain size and the degree of deformation and consists of large areas of similarly oriented, highly developed subgrains separated by boundary regions containing stringered intermetallic phases. This structure can remain essentially unchanged during subsequent heat treatment. The present study is designed to determine whether this structure can be replaced by a fine equiaxed grain structure with intermetallics much more randomly distributed through control of deformation conditions and composition so as to induce recrystallization during hot working.

Benefits to properties of high-strength aluminum alloys might be expected in at least three areas if the present elongated, highly polygonized (recovered) structure were replaced by a fine-grained recrystallized structure. First, the pronounced directionality of mechanical properties might be reduced by replacing the highly preferred hot-rolling texture with a more random recrystallized texture. Second, stress-corrosion resistance in the short transverse direction might be improved by replacing a few large, continuous grain boundaries with a multitude of randomly oriented, interconnected grain boundaries. Third, fracture toughness and fatigue strength might be increased by replacing la _· regions of similarly oriented material which promote extensive localized sǐ ⎧ and easy crack extension with a random, fine-grained structure where frequent changes of slip or crack direction would be necessary.

The program presently under way is designed to determine whether a fine-grained recrystallized microstructure can be introduced into aluminum alloys during hot working by control of processing conditions and composition. Initial studies are examining the recrystallization behavior of two alloys — 2024 and high-purity Al-4.6Cu — as a function of hot-working conditions. Hot working is being accomplished by upset forging on a Gleeble unit which permits a wide variation of strain rate, temperature history, and strain. Efforts to produce the desired type of fine-grained equiaxed microstructure in two high-purity Al-Zn-Mg-Cu alloys by multiple deformation recrystallization sequences are also under way. The properties of these materials will be evaluated to determine the advantages of an equiaxed microstructure. These studies will be followed by efforts to promote

greater control of recrystallization behavior by alloy modification. Finally, fabrication of selected high-strength alloys with a fine-grained recrystallized microstructure is planned by controlled hot-working procedures using conventional primary working equipment and to evaluate the effects of this structure on the properties as heat treated.

Preliminary Upsetting Studies

In the first semiannual report the development of a Gleeble test procedure for upsetting cylindrical aluminum alloy samples between steel dies was described[1]. Samples measuring 0.25 inch in diameter and 0.5 inch long were machined from commercial 2024-T4 rod for upsetting. These samples were solution heat treated for 5 hours at 920 F and water quenched following machining to stablilize the grain structure; the structure resulting from this treatment is shown in Figure 17. A highly elongated structure was present in the 2024 alloy. The average grain thickness was about 0.04 mm, with the grain length more than ten times the grain thickness.

Initial upsetting trials were made using conical upsetting dies which it was hoped could improve homogeneity of deformation by minimizing the effects of die friction. The dies were machined to provide a 7-degree convex taper, with a matching concave taper on the sample ends. It was found that lubrication was necessary using this die shape to avoid excessive barreling. A few upsetting runs were also made using lubricated flat dies. In these runs, the sample ends were also flat.

Samples were resistance heated to the upsetting temperature in 50 seconds and were held at temperature from 210 to 420 seconds before upsetting. Following upsetting, the samples were colled to room temperature in contact with the steel dies. Heat input was stopped immediately upon completion of the upset. Cooling rate in the dies was from 7 to 10 F/second as measured between 760 and 520 F, being somewhat slower the higher the upsetting temperature.

The upsetting conditions examined during these preliminary studies are given in Table X. Several conclusions were reached on the basis of these studies which were of value in optimizing upsetting procedures. These are summarized below:

(1) A tapered upsetting die is not adequate in itself to avoid barreling. However, the use of lubricant on the die surface (Oil-Dag) greatly improved the uniformity of deformation.

(2) Although the experimental technique is satisfactory for controlling sample temperature, some arcing at the sample:die interface occasionally occurs. This lends to pitting of the die surface and

100X   1G605

FIGURE 17.   MICROSTRUCTURE OF COMMERCIAL 2024
ALLOY FOLLOWING SOLUTION HEAT
TREATMENT FOR 5 HOURS AT 920 F AND
WATER QUENCHING

Axis of upset of machined cylinders is
vertical.

TABLE X. UPSETTING CONDITIONS USED IN EQUIPMENT FAMILIARIZATION TRIALS

Run No.	Temperature, F	Upset Rate, in./sec	Die Design[a]	Reduction in Height, percent	Holding Time Before Upset, sec[c]
40	750	0.016	C	88	210
41	750	8.8	C	46	420
42	750	8.8	C	72	420
43	750	8.8	C	92	420
27[b]	800	0.016	C	33	315
28	800	0.016	C	30	210
33	800	0.016	C	47	210
29	800	3.2	C	30	210
32	800	3.2	C	50	210
34	800	8.8	C	19	210
30	800	8.8	C	26	210
31	800	8.8	C	49	210
35	800	8.8	C	75	210
36	850	8.8	C	25	210
38	850	6.8	C	87	210
37	850	8.8	C	90	210
39	900	8.8	C	88	210
44	750	8.8	F	15	420
45	750	8.8	F	70	420
46	750	8.8	F	83	420
47	850	8.8	F	50	420

(a) Conical (C) or flat (F).

(b) This sample was upset without lubrication. All others were lubricated with Oil-Dag.

(c) Samples were die cooled immediately after upsetting.

progressively less satisfactory upsetting behavior. Frequent die inspection and regrinding as necessary is desirable to maintain homogeneous deformation.

(3) Control of upset uniformity requires fairly exact sample alignment when using the conical dies. Examples of several types of non-uniform upsetting observed in these studies are shown in Figure 18. Problems in controlling upsetting increased with amount of reduction and with upset rate.

(4) The Gleeble equipment was unable to maintain a uniform upset rate (rate of ram advance) at the highest upset rate (8.8 inch per second) with the 0.25-inch-diameter sample at reduction greater than about 60 percent. This problem was apparently related to the increase in load required to continue a uniform upset rate as the sample area increased. Decreasing the load requirement by reducing the initial sample size would presumably permit a larger reduction to be developed at constant upset rate. However, since a steady-state condition is reached in aluminum alloys at relatively low strain levels in which flow stress is independent of strain[24], the inability to maintain a constant upset rate to high reductions is not considered a serious problem except insofar as it affects the strain rate obtainable in the Gleeble unit.

(5) Satisfactory upsets can be made with lubricated flat dies — thus avoiding the problems with alignment encountered with conical dies — but the homogeneity of upset is not as attractive as that obtained in properly aligned conical dies.

(6) The Gleeble unit can be programed to provide a continuous measurement of temperature, ram travel, and applied load during upsetting as a function of time as shown in Figure 19.* These values, in conjunction with measured sample dimensions, can be used to determine true strain rate and flow stress at any point in the test. Flow stress at the end of the upset process was recorded in later studies. Adiabatic heating can also be measured (at a mid-height surface location).

Four of the samples upset in these preliminary studies were sectioned for metallographic examination. Microstructure was examined both as upset and after solution heat treatment for 20 minutes at 920 F with water quenching. These structures are shown in Figures 20 and 21. (Three of the photomicrographs of the upset samples were included in the first semiannual report.) The microstructure observed after approximately 90 percent reduction in height at two temperature: rate conditions — 750 F at 0.016 inch/sec and 900 F at 8.8 inch/sec — are shown

---

*This chart is from a later run in which temperature was maintained at the upset temperature for a controlled period following upset.

56

As-Machined Sample

Run No. 35

Run No. 39

Run No. 40

Run No. 31

Run No. 38
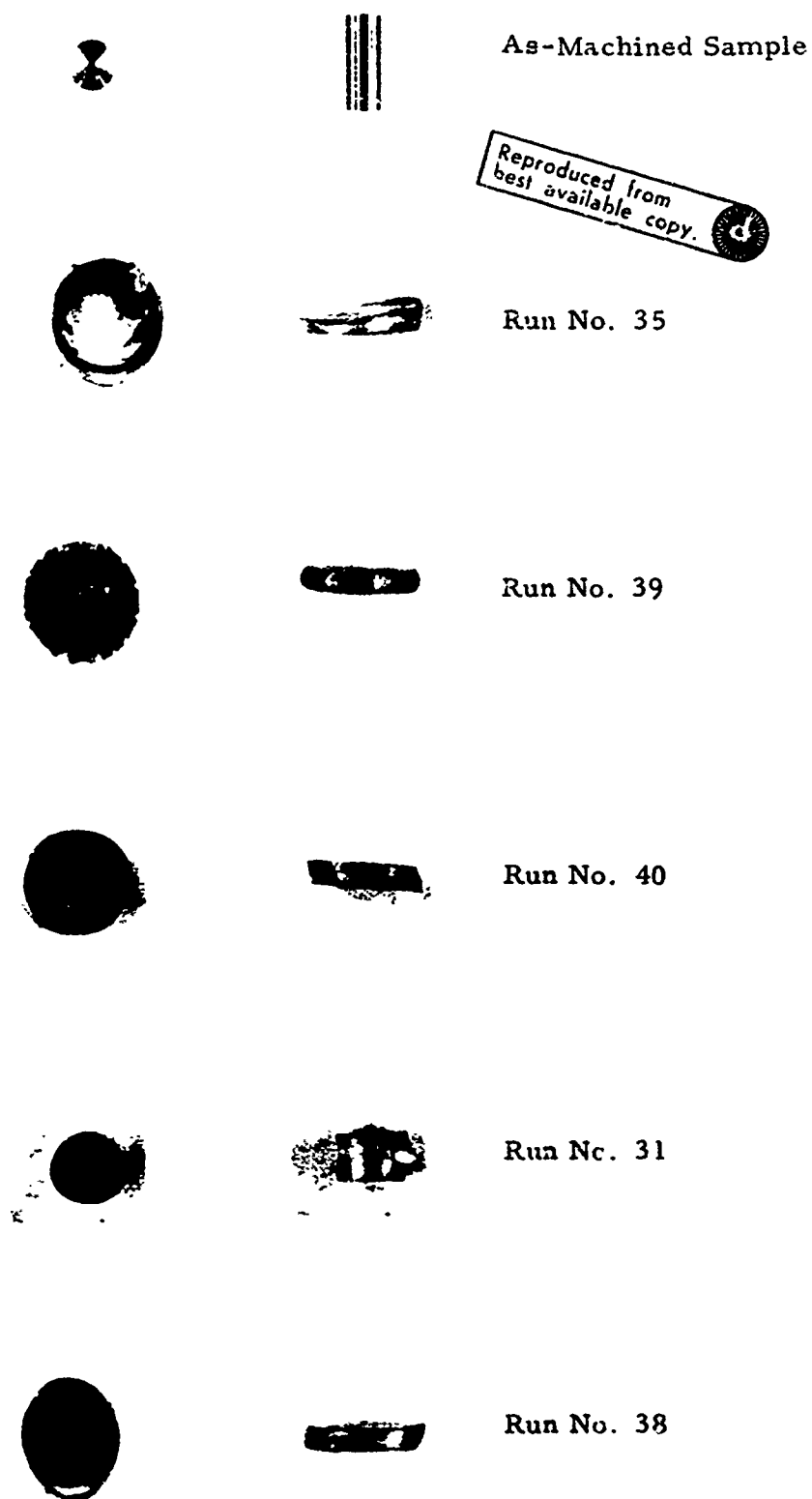
FIGURE 18.   EXAMPLES OF NONHOMOGENEOUS UPSETTING
OBSERVED IN FAMILIARIZATION TRIALS

57
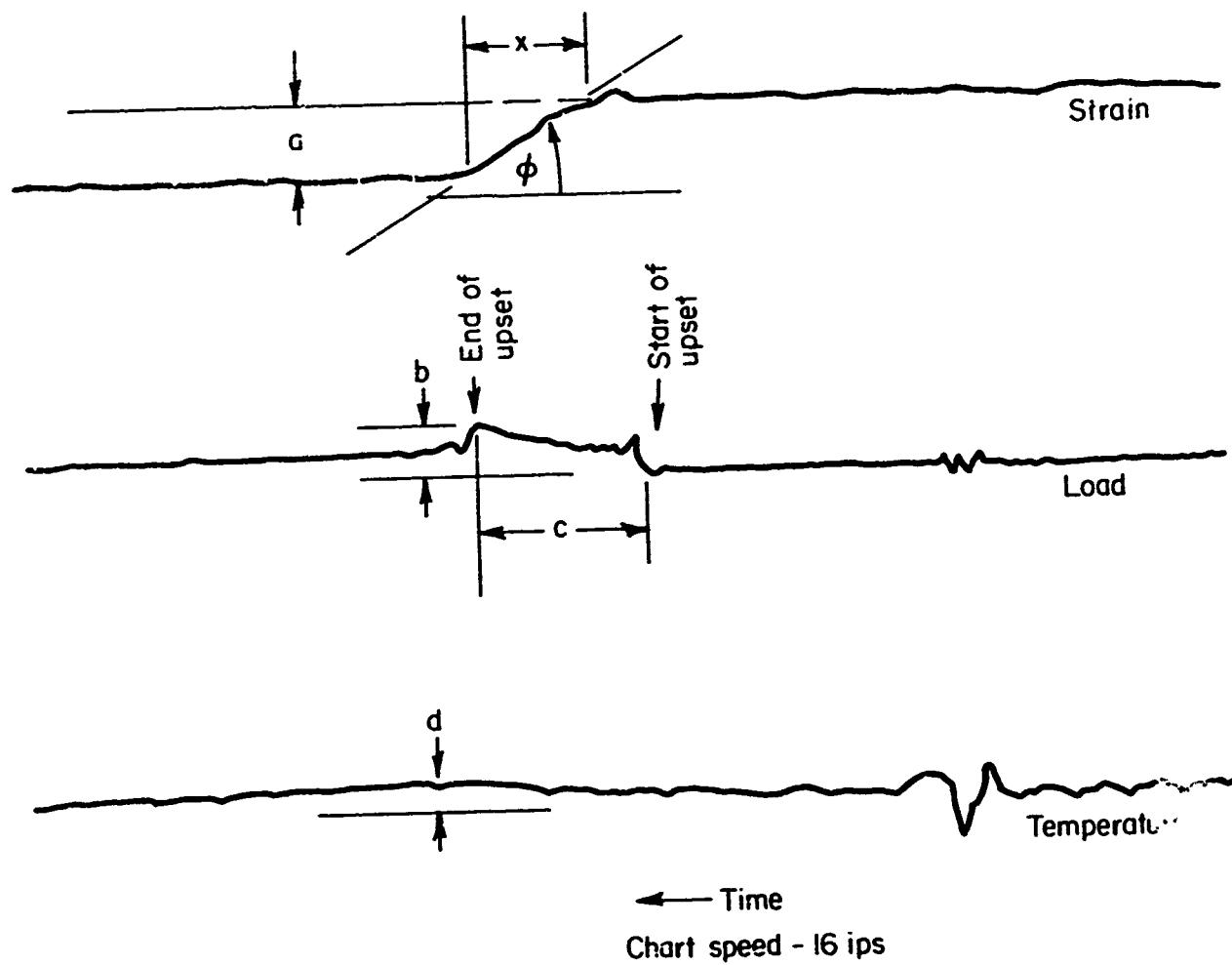
a = decrease in height
x = upset time
$\tan \phi$ = strain rate = $\dfrac{a}{x}$
b = maximum load
c = time of load application
d = temperature increase

FIGURE 19. REPRODUCTION OF TYPICAL GLEEBLE CHART

As Upset   Solution Heat Treated
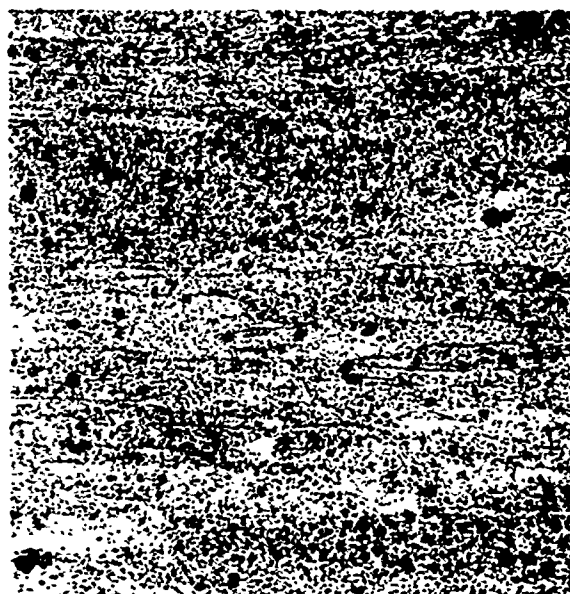
250X   9F014   250X   9F357

250X   9F015   250X   9F356

FIGURE 20.   MICROSTRUCTURE OF 2024 AFTER UPSETTING

Axis of upset is vertical.
Top: 88 percent reduction at 750 F and
         0.016 inch/sec – Run 40.
Bottom: 88 percent reduction at 900 F and
         8.8 inch/sec – Run 39.

As Upset   Solution Heat Treated

250X   9F016   250X   9F355
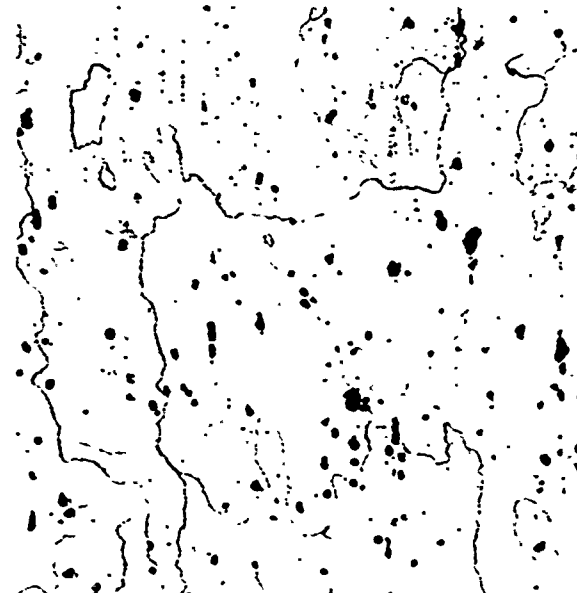
250X   9F013   250X   9F354

FIGURE 21. MICROSTRUCTURE OF 2024 AFTER UPSETTING (AXIS
OF UPSET IS VERTICAL)

Top: 20 percent reduction at 800 F and 8.8 inch/sec –
Run 34.

Bottom: 49 percent reduction at 800 F and 8.8 inch/
sec – Run 31.

in Figure 20. Neither sample showed appreciable recrystallization as upset, although upsetting at the higher temperature and upset rate resulted in some areas of fine-grained, apparently recrystallized material. Solution heat treatment, although making the structure much easier to examine by solution of precipitates, did not appear to alter the basic grain structure of either sample, suggesting both materials had recovered completely during upsetting or that recovery rather than recrystallization accompanied solution heat treatment. The elongated grain structure originally present plus the nonhomogeneous deformation encountered in these samples precluded an effort to compare final grain shape with original grain shape as altered by reduction. However, a 90 percent reduction in height would reduce the vertical grain dimension 10 times while increasing the horizontal dimension $\sqrt{10}$ times (~3.2 times), and a comparison of the structure shown in Figure 17 with those in Figure 20 suggests that the upset structure probably developed from the initial structure with no alteration in the number of grains (not including the fine, recrystallized grains in Sample 39). Figure 21 shows the structures developed after two lesser amounts of upsetting, both conducted at 800 F and 8.8 inch/sec. These structures also suggest that solution heat treatment does not alter the basic grain structure present after upsetting and that final grain shape is directly related to initial grain shape and reduction.

Selection of Upsetting Procedures

Based upon the preliminary study, it appeared that uniformity of deformation was quite sensitive to die shape and lubrication, even when limiting reduction to 50 or 60 percent. A series of 2024 alloy samples measuring 0.25-inch diameter by 0.5-inch height were upset under varying die shape and lubrication conditions to gain additional information for selecting an optimum upsetting procedure. During these runs, several experiments were also conducted to gain information about our ability to apply a controlled temperature holding period following the upset and to quench the sample following a controlled holding period. In initial studies, the samples were cooled in the dies at a moderately rapid rate, halting heat input immediately following upsetting. The Gleeble unit can be programed to maintain temperature for a finite time after upsetting, to control to a higher or lower temperature following upsetting, and to cool at a controlled slow rate. Quenching the upset sample is also possible by placing a water container below the dies, opening the dies at a preset time, and dropping the sample into the water. Several of these variables were incorporated into the upsetting schedule of the samples used to study the importance of die shape and lubrication. The studies conducted are summarized in Table XI.

Samples were upset at two temperatures, 75 and 750 F. Behavior at the two temperatures was quite different. Samples upset at 75 F in conical dies tended to deform more at the die surface if lubricated, leading to a negative barreling factor. By elimination of lubricant, fairly homogeneous deformation resulted. In flat dies, appreciable barreling occurs even when lubricated. Flow stress values correlated

TABLE XI. EFFECT OF DIE DESIGN AND OF LUBRICATION ON THE UPSETTING BEHAVIOR OF 2024

Run No.	Die Design(a)	Lubricated	Temp, F	Upset Rate, in./sec	Reduction in Height, percent	Barreling Tendency(b)	Flow Stress, ksi	Temp Increase, F	Heat-Up Time, sec	Holding Time, sec Before Upset	Holding Time, sec After Upset	Type Cooling
63	F	Yes	75	8.8	51	0.11	95.2	--	--	--	--	--
53	F	Yes	75	8.8	56	0.18	95.7	--	--	--	--	--
64	C	No	75	8.8	50	0.02	74.2	--	--	--	--	--
62	C	Yes	75	8.8	51	-0.17	51.9	--	--	--	--	--
61	C	Yes	75	8.8	(c)	-0.09	65.1	--	--	--	--	--
56	F	Yes	750	8.8	58	0.19	18.2	50	50	420	10	Water quench
55	F	Yes	750	8.8	61	0.22	19.9	45	50	420	15	Water quench
54	F	Yes	750	8.8	59	0.22	20.6	40	50	420	120	Water quench
65	C	No	750	8.8	64	0.24	19.9	40	50	420	5	Water quench
59	C	Yes	750	8.8	61	0.05	16.0	45	50	420	11	Water quench
50	F	Yes	750	8.8	51	0.22	19.3	15	50	420	1255	Slow cool
49	F	Yes	750	8.8	51	0.14	18.9	50	50	420	1255	Die cool
48	F	Yes	750	8.8	51	0.22	20.2	40	50	420	100	Die cool
52	F	Yes	750	8.8	90	-	16.4	15	50	420	680	Die cool

(a) Conical (C) or flat (F).

(b) Defined as Dc/De -1, where Dc is the final center diameter and De is the final end diameter of the upset cylin

(c) Sample was thrown out of die before upset was complete.

quite well with barreling tendencies, as would be anticipated since barreling is related to surface friction. The effect of die shape on uniformity of deformation at 75 F is shown in the macrostructures in the upper half of Figure 22. Unlubricated conical dies resulted in noticeably more uniform deformation. At 750 F, lubrication was necessary to avoid excessive barreling using the conical die. The flow behavior in unlubricated conical dies was similar to that in lubricated flat dies. The variation of deformation behavior at 750 F as a function of die shape is shown in the lower half of Figure 22.

Additional samples were upset at 750 F in lubricated flat dies to 50 percent and 90 percent reductions of height to briefly examine the behavior of material in these dies at other reduction levels. These results tended to confirm that upsetting, although easier to control in flat dies, was less satisfactory from the standpoint of homogeneity of flow.

Multiple upsets run under similar conditions tended to agree quite closely. Barreling tendencies were similar, as was flow stress. Temperature increase during upsetting, which was measured in tests at 750 F, was much more variable and did not appear to be useful data.

Considerable flexibility in designing thermal treatment following upsetting was demonstrated. Procedures were developed for quenching samples immediately following a preset holding period. With experience, it is anticipated that quenching can be conducted within 1 second after completion of the upset without undue difficulty. Quenching within 5 seconds following upsetting was successfully accomplished in three different runs (56, 59, and 65). Programed slow cooling rates can also be used if desired, although no immediate need for this type of treatment is envisioned. Control of holding time following upsetting is readily accomplished; this is expected to be of considerable assistance in determining recrystallization behavior.

As discussed earlier and illustrated in Figure 19, the Gleeble chart can be used to determine actual strain rate during upsetting. The present study confirmed that the Gleeble could not maintain the preset upset rate to 60 percent reduction at elevated temperatures, although upsets of 50 percent could be made satisfactorily. Also, measurements indicated that the actual upset rate was less than the preset upset rate, as indicated below:

Preset upset rate — 8.8 inches per second

Measured at 75 F — 3.2 to 4.7 inches per second

Measured at 750 F — 5.5 to 6.0 inches per second.

Upset rate was lowest when using flat dies and highest when using lubricated conical dies.

9F398

8X   Sample 64.   Unlubricated Coni ` Die

9F287

8X   Sample 59.   Lubricated Conical Die

9F398

8X   Sample 63.   Lubricated Flat Die

9F287

8X   Sample 56.   Lubricated Flat Die

FIGURE 22.   MACROSTRUCTURE OF UPSET SAMPLES OF 2024 ALLOY

Top: Upset ~50 percent at 75 F
Bottom: Upset ~60 percent at 750 F

64

The inability to maintain the desired upset rate beyond about 50 percent reduction and the lower than programed value when using the 0.25-inch-diameter samples indicated that the maximum strain rate attainable at the conclusion of upsetting was only 24 in./in./sec, appreciably less than our initially desired maximum strain rate of 100 in./in./sec or above. The use of smaller diameter samples (permitting upsetting at lower loads) was considered a possible way to overcome this difficulty. A group of cylindrical samples were prepared having a diameter of 0.125 inch and height of 0.25 inch to determine the usefulness of this approach. These samples were upset at 750 F after holding at temperature for 420 seconds and were released from the dies and air cooled within 1 second after upsetting. Both conical and flat lubricated dies were used. These runs are described in Table XII.

TABLE XII.   UPSET STUDIES OF 0.125-INCH-DIAMETER 2024 SAMPLES

Run No.	Die Design[a]	Temperature, F	Upset Rate, in./sec	Reduction in Height, percent	Measured Upset Rate, in./sec	Flow Stress, ksi
69	F	750	8.8	79	5.9	22.4
68	F	750	8.8	63	5.8	15.5
66	C	750	8.8	80	5.9	18.7
67	C	750	8.8	(b)	7.2	(b)
70	C	750	8.8	65	6.9	14.9

(a)   Conical (C) or flat (F).

(b)   Desired reduction was 60 percent. Loss of control caused sample to be molten near completion of upset.

Difficulty in maintaining the preset upset rate was encountered even with this smaller sample. The upset rate was somewhat higher when using conical dies. The Gleeble charts reproduced in Figure 23 showed that a constant upset rate could be maintained at 65 percent but that some decrease in upset rate occurred near the end of the 80 percent upset. A maximum useful upset of 75 percent is probably possible at 750 F using 0.125-inch-diameter samples, giving a final strain rate of 100 in./in./sec or more. Thus, it appears feasible to obtain higher strain rates by reducing the sample size if this becomes desirable as the program progresses.
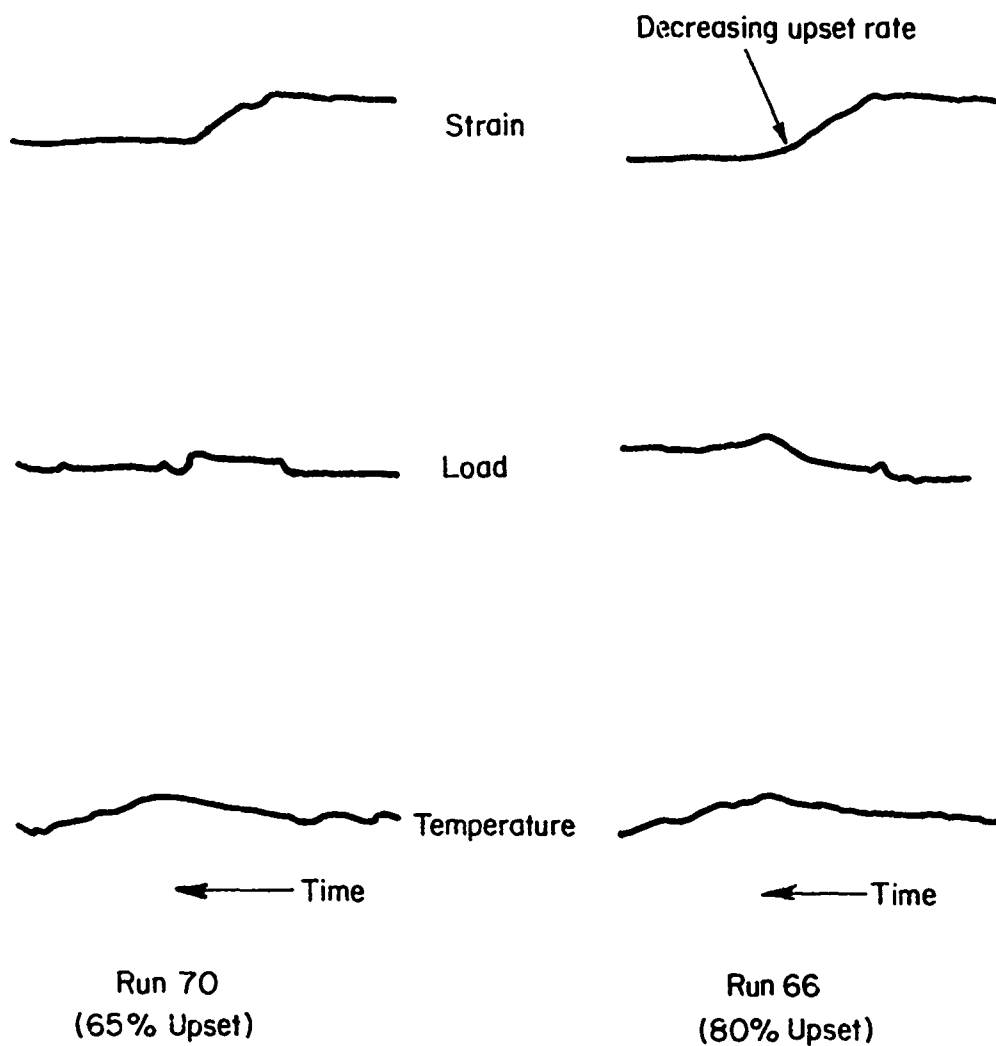
FIGURE 23. REPRODUCTION OF GLEEBLE CHARTS FOR UPSETS
AT 750 F ON 0.125-INCH-DIAMETER 2024 SAMPLES

Inducing Recrystallization During Upsetting

During conventional hot working, high-strength aluminum alloys show dynamic recovery in preference to recrystallization. Control of deformation temperature and strain rate was considered as one method of inducing recrystallization in preference to recovery during hot working. Increasing strain rate should certainly favor recrystallization, since dynamic recovery is inhibited by increasing strain rate, as shown by the effect of strain rate on flow stress[24]. The effect of deformation temperature is more difficult to predict, however, since increased temperature favors both increased dynamic recovery and recrystallization at lower levels of strain hardening. Therefore, a study of the effects of strain rate on recrystallization behavior over a fairly broad range of temperature was initiated. Post-upset holding times of 23 and 33 seconds at the upsetting temperature followed by die cooling were used. The study was conducted with 0.25-inch-diameter samples upset 50 percent in conical dies. Samples of both 2024 alloy and a high-purity Al-4.6Cu binary alloy were examined.

The high-purity Al-4.6Cu alloy was prepared from a 4-inch-diameter D.C.* ingot purchased from Reynolds Metals Company and fabricated to 0.275 inch at Battelle's Columbus Laboratories by extrusion and cold swaging. The composition of the ingot by analysis was 4.6 Cu, 0.011 Ti, and less than 0.01 Fe, Si, Zn, Mg, Mn, and Cr. The rod was solution heat treated for 1 hour at 1000 F and water quenched to develop a coarse, equiaxed grain structure essentially free of second-phase material. A photomicrograph of the structure of the binary alloy is shown in Figure 24.

The experimental conditions examined, most of which were carried out in duplicate, are summarized in Table XIII. Samples were originally planned to be upset at two upset rates, 0.016 and 8.8 inch per second, and at four temperatures, 400 F, 650 F, 800 F, and 925 F. However, it proved quite difficult to obtain satisfactory upsets at fast upset rates at 400 and 650 F, so work at these temperatures was reduced somewhat. Barreling was also more severe than anticipated, presumably the result of progressive die roughening. As a result, deformation was somewhat nonhomogeneous as illustrated for the Al-4.6Cu alloy in Figure 25.

Upset rate had an appreciable effect on flow stress and therefore presumably also affected strain hardening. The average variation of flow stress with temperature and strain rate for 2024 alloy is summarized below:

Upset Temperature, F	Flow Stress, ksi 0.016 in./sec	Flow Stress, ksi 8.8 in./sec
400	72.8	-
650	17.8	24.1
800	9.8	17.8
925	5.4	15.0

---

*Direct chill.

67

100X   9F642

FIGURE 24.   MICROSTRUCTURE OF SOLUTION HEAT-
             TREATED Al-4.6Cu ALLOY

TABLE XIII. SAMPLES PREPARED FOR A STUDY OF THE EFFECT OF TEMPERATURE
AND STRAIN RATE ON RECRYSTALLIZATION BEHAVIOR

Run No.	Alloy	Temperature, F	Upset Rate, in./sec	Reduction in Height, percent	Flow Stress, ksi	Measured Upset Rate, in./sec	Barreling Tendency
71	2024	400	0.016	42	-	-	0.00
72	2024	400	0.016	42	72.8	0.007	-0.01
78	2024	650	0.016	50	17.8	0.017	0.11
99	2024	650	8.8	48	24.1	4.8	0.25
85	2024	800	0.016	53	10.3	0.018	0.22
82	2024	800	0.016	49	9.3	0.020	0.24
91	2024	800	8.8	53	18.0	5.3	0.22
92	2024	800	8.8	54	17.5	5.1	0.22
87	2024	925	0.016	54	5.4	0.018	0.22
88	2024	925	0.016	54	5.4	0.018	0.22
95	2024	925	8.8	51	15.1	6.0	0.23
96	2024	925	8.8	52	14.9	5.9	0.23
76	Al-4.6Cu	400	0.016	52	36.0	0.013	0.23
75	Al-4.6Cu	400	0.016	50	36.7	0.013	0.24
83	Al-4.6Cu	800	0.016	53	5.4	0.018	0.22
84	Al-4.6Cu	800	0.016	53	5.3	0.018	0.22
93	Al-4.6Cu	800	8.8	54	12.4	6.0	0.22
94	Al-4.6Cu	800	8.8	50	12.0	5.5	0.24
90	Al-4.6Cu	925	0.016	54	5.1	0.020	0.22
89	Al-4.6Cu	925	0.016	55	5.0	0.019	0.21
97	Al-4.6Cu	925	8.8	53	11.4	6.0	0.22
98	Al-4.6Cu	925	8.8	54	11.8	6.2	0.22
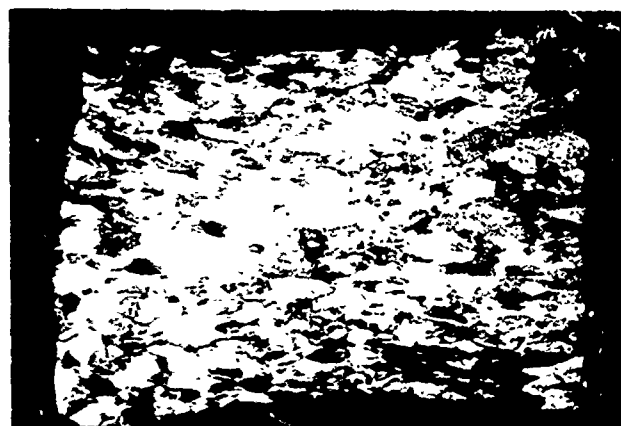
8X   1G551

Run 76 – 400 F
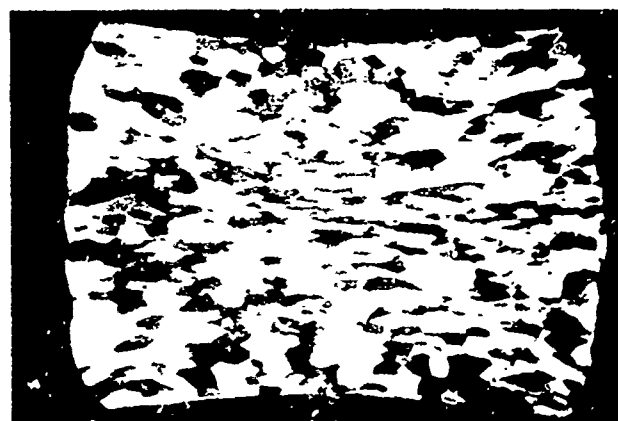
8X   1G549

Run 83 – 800 F
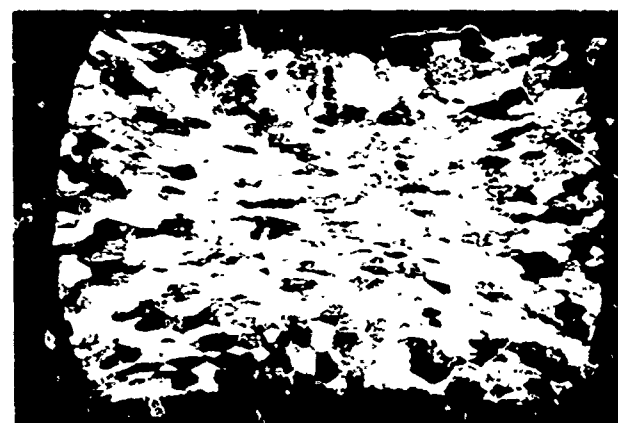
8X   1G550

Run 90 – 925 F

FIGURE 25.   MICROSTRUCTURE OF Al-4.6Cu ALLOY UPSET 50 PERCENT AT 0.016 INCH PER SECOND

Based on these results, the effect of upset rate on flow stress increased as temperature increased. The Al-4.6Cu alloy, on the other hand, did not show this trend quite so clearly:

Upset Temperature, F	Flow Stress, ksi	
	0.016 in./sec	8.8 in./sec
400	36.4	..
800	5.4	12.2
925	5.0	11.6

Despite the appreciable differences in flow stress observed as a function of upset rate, hardness measurements made following cooling to room temperature in these as well as earlier studies showed no apparent difference in hardness as a function of either upset rate or percent reduction, as shown in Table XIII. This suggests that the differences in structure present during deformation, as indicated by flow stress differences, were rapidly eliminated following upsetting. Also of interest in this respect is the similarity of hardness measured on samples cooled immediately after upsetting to that measured in samples held at temperature up to 33 seconds after upsetting. The rather pronounced variation of hardness with upset temperature shown in Table XIV is attributed largely to age hardening behavior.

Optical metallographic examination of 2024 samples tended to confirm early results as summarized in Figures 20 and 21. Recrystallization was observed only at the highest temperature and was much more obvious at the higher upset rate. It was observed only in limited regions, largely along original grain boundaries. Structures observed after upsetting at 925 F are shown in Figure 26.

Somewhat similar behavior was observed in the high-purity alloy. In this case, however, grain boundary recrystallization was fairly extensive after upsetting at 0.016 in./sec at 925 F, while the sample upset at 8.8 in./sec at 925 F appeared to show fairly large areas of essentially complete recrystallization. No recrystallization was apparent at lower temperatures. Microstructures illustrating this behavior are reproduced in Figure 27.

Further evaluation of this series of upset samples is being carried out using transmission electron microscopy. Preliminary results of these studies are given in a following section of this report.

We plan to expand this study to examine the effects of variable holding periods following upsetting on recrystallization behavior. Samples will also be examined after upsetting at one temperature, rapid heating to a second temperature, and holding for variable periods. It is believed that recrystallization is occurring following rather than during upsetting, if so, the degree of recrystallization may be highly variable as a function of the annealing condition immediately following upsetting. In these studies, samples will be water quenched upon completion of the upset-anneal sequence.

TABLE XIV. HARDNESS OF UPSET 2024 AND Al-4.6Cu ALLOY

Run No.	Alloy	Temperature, F	$\dot{\epsilon}$	R	VHN 10-Kg Load	Holding Time After Upset, second	Type of Cooling
63	2024[a]	75	8.8	51	191	-	-
64	2024[a]	75	8.8	50	174	-	-
71	2024[a]	400	0.016	42	181	40	Die cool
78	2024[a]	650	0.016	50	86	33	Die cool
99	2024[a]	650	8.8	48	90	23	Die cool
56	2024[a]	750	8.8	58	105	10	Water quench
59	2024[a]	750	8.8	61	108	11	Water quench
40	2024[a]	750	0.016	88	91	0	Die cool
85	2024[a]	800	0.016	53	106	33	Die cool
91	2024[a]	800	8.8	53	105	23	Die cool
27	2024[a]	800	0.016	33	101	0	Die cool
33	2024[a]	800	0.016	47	106	0	Die cool
32	2024[a]	800	8.5	50	109	0	Die cool
31	2024[a]	800	8.8	49	104	0	Die cool
34	2024[a]	800	8.8	19	110	0	Die cool
35	2024[a]	800	8.8	75	113	0	Die cool
36	2024[a]	850	8.8	25	121	0	Die cool
38	2024[a]	850	8.8	87	117	0	Die cool
39	2024[a]	900	8.8	88	127	0	Die cool
95	2024[a]	925	8.8	51	128	23	Die cool
87	2024[a]	925	0.016	54	127	33	Die cool
76	Al-Cu[a]	400	0.016	52	100	33	Die cool
83	Al-Cu[a]	800	0.016	53	55	33	Die cool
93	Al-Cu[a]	800	8.8	54	55	23	Die cool
90	Al-Cu[a]	925	0.016	54	60	33	Die cool
97	Al-Cu[a]	925	8.8	53	66	23	Die cool

(a) The initial hardness of 2024 was 133 VHN. That of Al-4.6Cu was 90 VHN.

100X   1G603   100X   1G602

        (Run 87)   (Run 95)

FIGURE 26.   MICROSTRUCTURE OF 2024 ALLOY UPSET AT 925 F (AS UPSET)

       Left: Upset at 0.016 inch per second
       Right: Upset at 8.8 inch per second

       (Upset direction is vertical.)

100X   1G599   100X   1G600

(Run 83)   (Run 93)

100X   1G598   100X   1G601

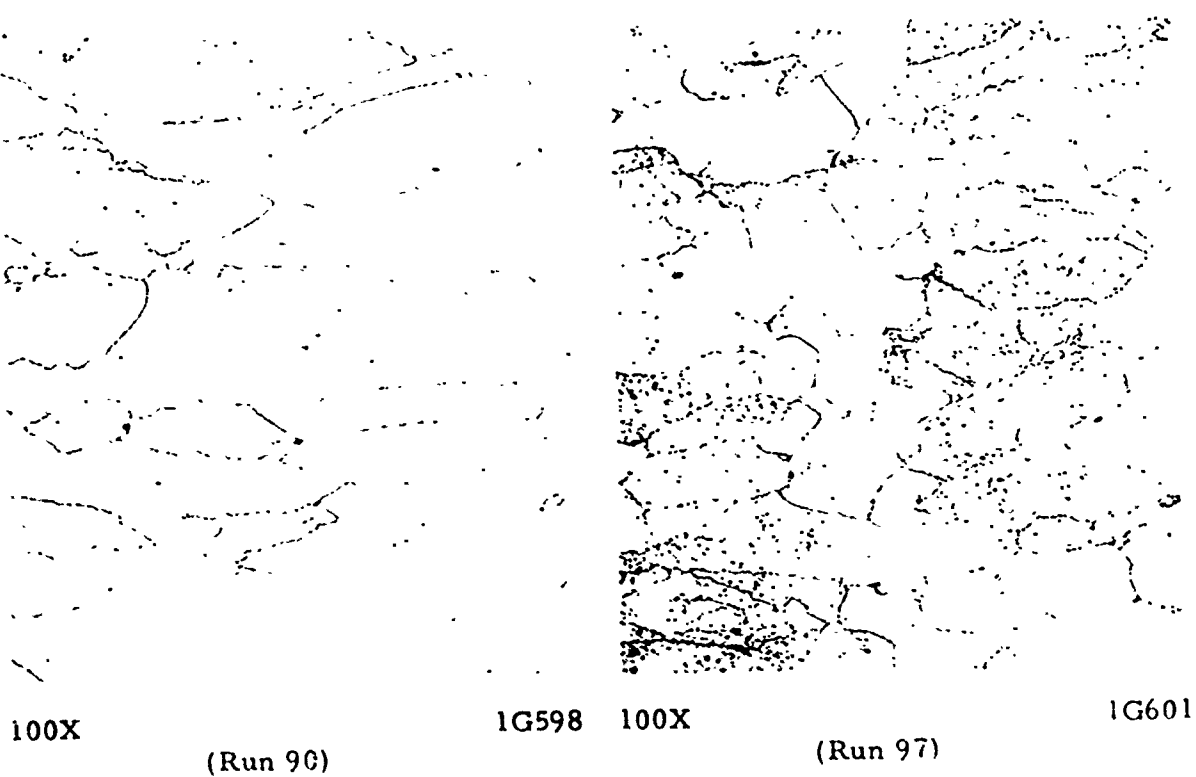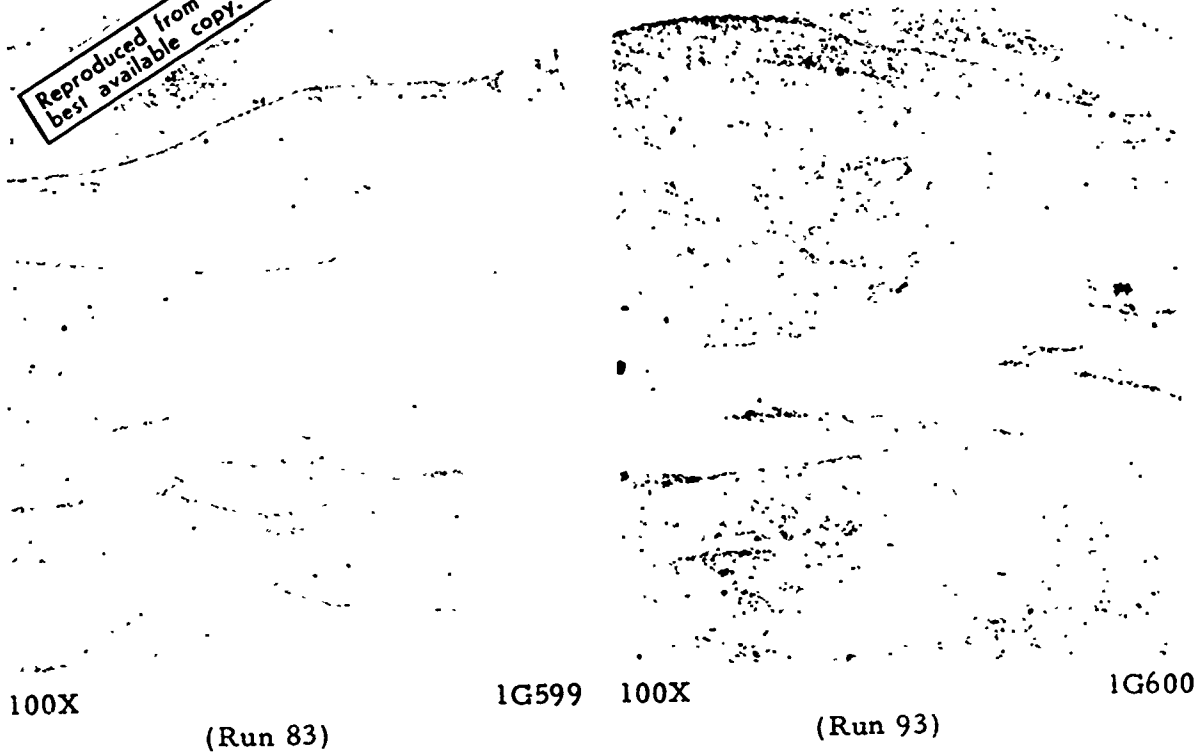(Run 90)   (Run 97)

FIGURE 27.   MICROSTRUCTURE OF UPSET Al-4.6Cu ALLOY

Upset Temperature: Top-800 F, Bottom-925 F
Upset Rate: Left-0.016 in./sec, Right-8.8 in. sec

(Upset direction is vertical.)

74

Properties of Recrystallized Aluminum Alloys

The objective of this investigation, as discussed previously, is to develop procedures for producing a fine-grained equiaxed microstructure during hot working. We anticipate that such a microstructure may favor superior stress-corrosion resistance, fatigue strength, or fracture toughness as compared with the conventional polygonized, highly directional wrought microstructure. These benefits are anticipated not only from the fine recrystallized microstructure, but also from a reduction in microsegregation. It is thought that residual alloy segregation from the casting process will be significantly reduced by recrystallization during hot working.

A structure equivalent to that sought may be available in properly processed high-purity alloys in which recrystallization is relatively easy to induce. A high-purity alloy processed by selected deformation-recrystallization sequences so as to cause recrystallization to occur several times during fabrication might simulate rather closely the type of structure which would be developed in commercial purity alloys which recrystallized during hot working.

An early indication as to whether a fine equiaxed microstructure is beneficial to properties may be available from evaluation after suitable processing of two of the high-purity alloys prepared for study in Task A. Efforts are under way to produce a fine-equiaxed microstructure in the following high-purity Al-Zn-Mg-Cu Alloys.

Alloy Number	Composition, weight percent					
	Zn	Mg	Cu	Cr	Fe	Si
X	5.60	2.44	1.43	<0.01	<0.01	<0.01
C	5.68	2.36	1.48	0.18	0.02	0.01

By multiple deformation-recrystallization operations it should be possible to destroy all traces of any residual segregation remaining from casting. Proper selection of annealing conditions should allow control of grain size. The presence of chromium in Alloy C is expected to provide added control of grain size. (Material homogenized to produce a fine dispersion of chromium phase will be studied.) Both alloys will be processed to sheet from 0.25-inch plate for preliminary evaluation of properties.

Portions of Alloy X obtained as 0.25-inch plate have been processed under varying conditions to determine how this composition responds to deformation and heat treatment. Material was solution heat treated for 20 minutes at 870 F and water quenched, following which samples were processed as follows:

(a) Cold rolled 50 percent in one pass, placed in a furnace at 370 F, held 20 minutes, and water quenched

75

(b)   Hot rolled 50 percent at 860 F in one pass, then water quenched immediately after rolling

(c)   Same treatment as (b), then placed in a furnace at 870 F, held 20 minutes, and water quenched

(d)   Same treatment as (b), then slowly heated to 870 F (3 hours between 550 F and 870 F), held 20 minutes at 870 F, and water quenched.

Photomicrographs of the microstructures resulting from these treatments are shown in Figure 28.

Several points of interest are illustrated in Figure 28. First, it is apparent that recrystallization does not occur during hot rolling. Second, it is seen that a slightly elongated microstructure is developed on recrystallization and that grain size is not appreciably different whether the sample was cold rolled or rolled at 860 F. Third, it is apparent that slow heating following hot rolling did not induce recovery instead of recrystallization, although it did favor a coarser recrystallized grain size.

Studies of methods for controlling grain size in this alloy and in Alloy C will be continued. Efforts will be made to produce a fine-equiaxed grain size from 0.25-inch plate involving at least three crystallization steps. Suitably processed material of both Alloy X and Alloy C will be evaluated to determine tensile properties, tear properties, fatigue properties, and stress-corrosion resistance.

Studies of Fine Structure

Transmission electron microscopy (TEM) is being used to study the fine structure in upset samples. Although a recrystallized microstructure is being sought which should be apparent in optical microscopy, studies of subgrain size, dislocation arrangements, and precipitate distribution as a function of hot-working conditions are expected to aid in understanding the softening processes in aluminum alloys. Preliminary studies in this area presently under way are intended primarily to learn how useful these techniques will prove in aiding our understanding of recrystallization and recovery processes.

The small size of the upset specimens dictates the use of a jet indenting technique for the preparation of TEM specimens. Specimens approximately 0.020 inch thick and 0.1 inch square are sectioned from the upset specimen, and both sides of the specimen are indented with concentric dimples using a pneumatically operated electrolytic jet[25]. The specimens are indented until approximately 0.001 to 0.005 inch of material remains between the dimples. Final thinning is accomplished in an electrolytic cell that has a collimated light source arranged on one side of the cell and a low power microscope on the other side to permit

76

100X   1G618   Initial Condition (SHT)
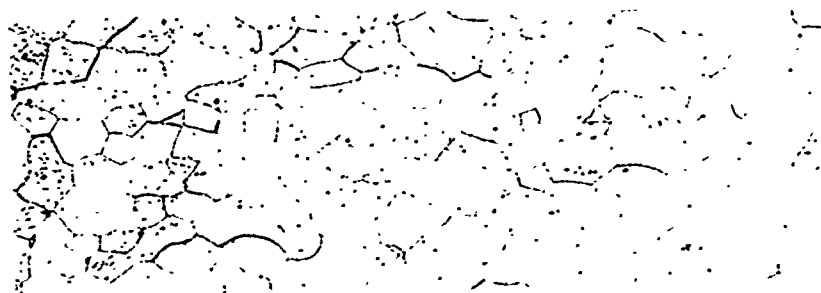
100X   9F358   Treatment A (CR + SHT)

100X   9F359   Treatment B (HR)

100X   9F360   Treatment C (HR + SHT)

100X   9F541   Treatment D (HR + Slow Heating + SHT)

FIGURE 28. MICROSTRUCTURE OF ALLOY X (Al-Zn-Mg-Cu)

77

viewing of the specimen during thinning. The current to the cell is switched off upon the first indication of a small hole in the specimen. The material at the edge of the hole formed in this manner is usually thin enough to be examined by transmission electron microscopy. One of the major advantages of this technique in addition to the small amount of material that is required is that a protective frame is left around the thinned portion of the specimen to minimize handling damage.

TEM specimens were taking from both transverse and longitudinal sections.* The transverse sections were taken near quarter-diameter positions just above the center plane of the specimen. Longitudinal specimens were taken from both the center and near the quarter-diameter position. At least two TEM specimens were examined from each position.

The following specimens have been examined:

(1) Solution heat treated 2024 starting material

(2) Run No. 62, 2024 upset at room temperature at 8.8 in./sec

(3) Run No. 82, 2024 upset at 800 F at 0.016 in./sec

(4) Run No. 92, 2024 upset at 800 F at 8.8 in./sec

(5) Run No. 91, 2024 upset at 800 F at 8.8 in./sec plus solution heat treated 1 hour at 920 F and water quenched

(6) Solution heat treated Al-4.6Cu starting material

(7) Run No. 84, Al-4.6Cu upset at 800 F at 0.016 in./sec

(8) Run No. 94, Al-4.6Cu upset at 800 F at 8.8 in./sec

(9) Run No. 93, Al-4.6Cu upset at 800 F at 8.8 in./sec plus solution heat treated 1 hour at 1000 F and water quenched.

The above specimens were all upset approximately 50 percent. Preliminary examinations were also conducted on 2024 specimens upset at 750 F to perfect the thinning technique. The results from the 750 F specimens appeared to be nearly identical to those obtained from the specimens upset at 800 F, although the former were not examined in great detail. The specimens were primarily examined for evidence of recrystallization; also, the subgrain size was determined. Evidence was also found that the intermediate precipitates in the 2024 specimens were surprisingly unstable during the upset.

---

*Specimen orientation with respect to the original rod axis. Samples are upset parallel with the longitudinal direction.

After considerable deliberation, the most convenient and reproducible technique for measuring subgrain sizes was to tilt the specimen through various angles in the electron microscope to bring all subgrains into contrast. Since all subgrains are not in contrast at the same time, this permits an average subgrain size to be determined by "mental integration". By using a standard screen magnification (5,000X and 10,000X were used most frequently), the subgrain size was compared with the standard ASTM grain size charts, and the ASTM grain size was then converted to the appropriate subgrain size. This method obviously suffers some shortcomings for elongated subgrains, but it can give some useful results if the aspect ratio is not too great.

2024 Specimens

The structure of the solution heat treated 2024 starting material is shown in Figures 29 and 30. Figure 29a is from a transverse section, and Figure 29b is from a longitudinal section. The intermediate precipitates can be seen to be in the form of rods in these figures, with the rods being parallel with the longitudinal axis. The electron diffraction patterns also showed evidence of GP zones in the natrix. A prominent distinguishing feature of the structure was the formation of helical dislocations between the intermediate precipitates, as can be seen in Figure 29. Figure 30 shows that the orientation of the intermediate precipitate was not significantly affected in the vicinity of grain boundaries and that a narrow depleted zone free of intermediate precipitates was present at the grain boundary.

Figure 31 shows the transverse and longitudinal structures in a specimen that was upset at room temperature. Although the high dislocation density tends to obliterate the intermediate precipitates, the precipitates appear to have maintained the shape and orientation of the starting material. This is an unexpected observation since the particles, even if they are not themselves deformed during upsetting, should be reoriented along the flow pattern of the matrix. The apparent stability of the particle orientation may have been characteristic only of the limited area that was available for examination in the TEM specimens; therefore, more extensive studies of intermediate precipitate alignment after upsetting are planned using scanning electron microscopy to survey larger areas of the upset sample.

The structure in the 2024 specimen from Run No. 82 that was upset at 800 F at a rate of 0.016 in./sec is shown in Figures 32 through 35. The microstructures in Figure 32 are from a transverse section and were taken from the same area at slightly different tilts to show how the subgrain size varied from the grain boundary to the center of the grain. Only some of the subgrains near the grain boundary in the lower left grain are in contrast in Figu   32a, while those near the center of the grain have been tilted into contrast in F   re 32b. The subgrain size was approximately 1.3 μm near the grain boundary and 2.5 μm toward the center of the grain. The formation of smaller subgrains near the grain boundaries appeared to occur throughout the specimen, with the subgrain size near grain boundaries generally varying between 1.3 to 2.5 μm and that toward the center of the grains
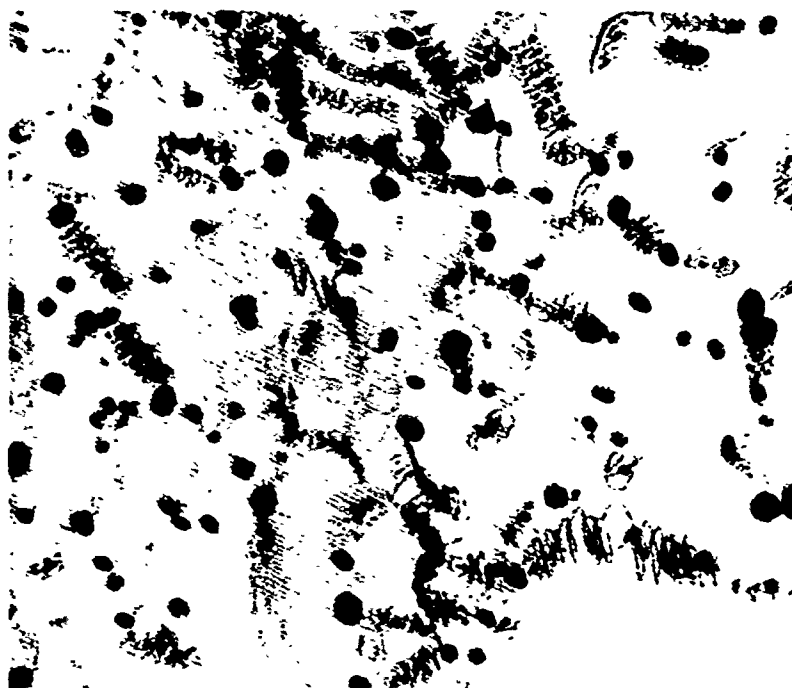
30,000X   EH3511

a.   Transverse Section
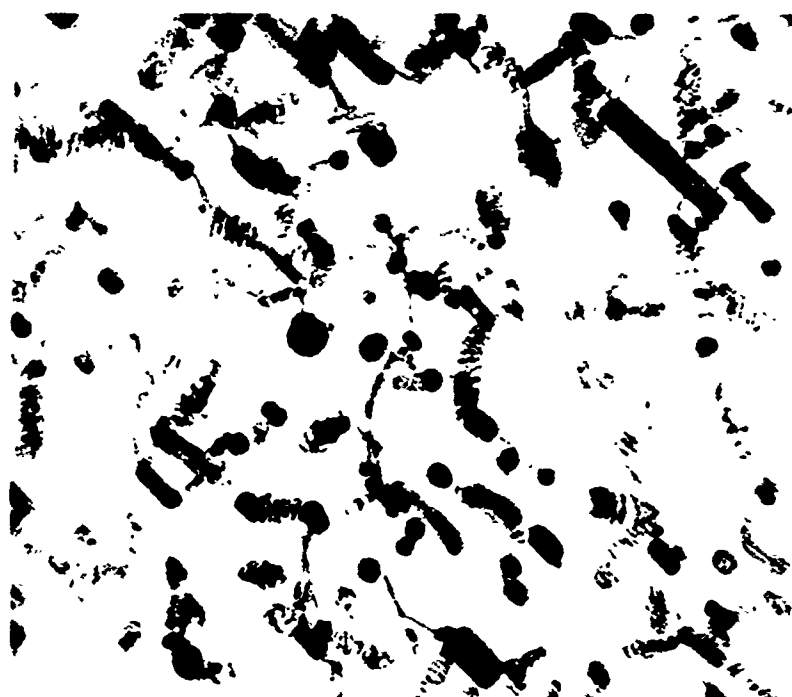
30,000X   EH3464

b.   Longitudinal Section

FIGURE 29.   SOLUTION HEAT-TREATED 2024 STARTING MATERIAL

15,000X   EH3459

FIGURE 30. STRUCTURE OF THE INTERMEDIATE PRECIPITATE IN THE
SOLUTION HEAT-TREATED 2024 STARTING MATERIAL

81
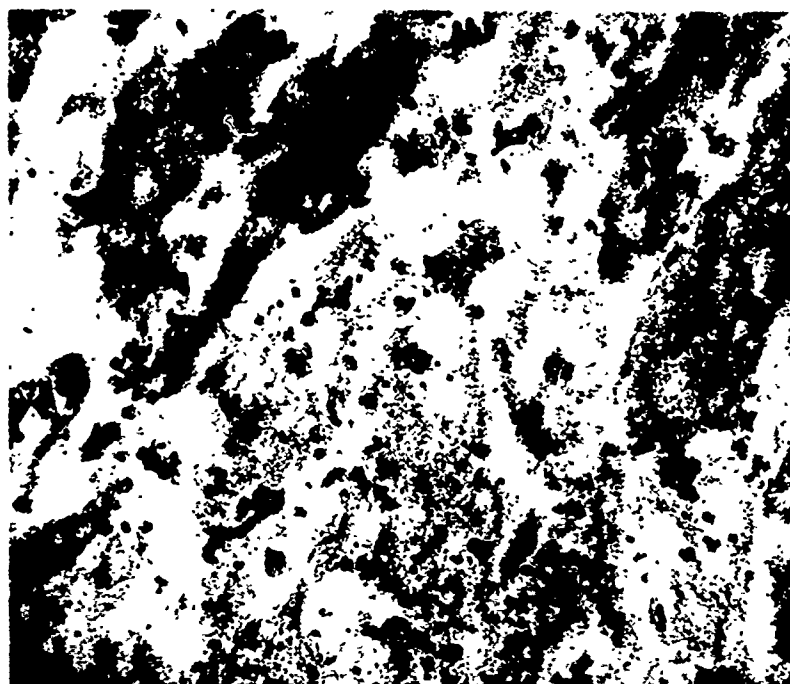
15,000X   EH3781

a.   Transverse Section
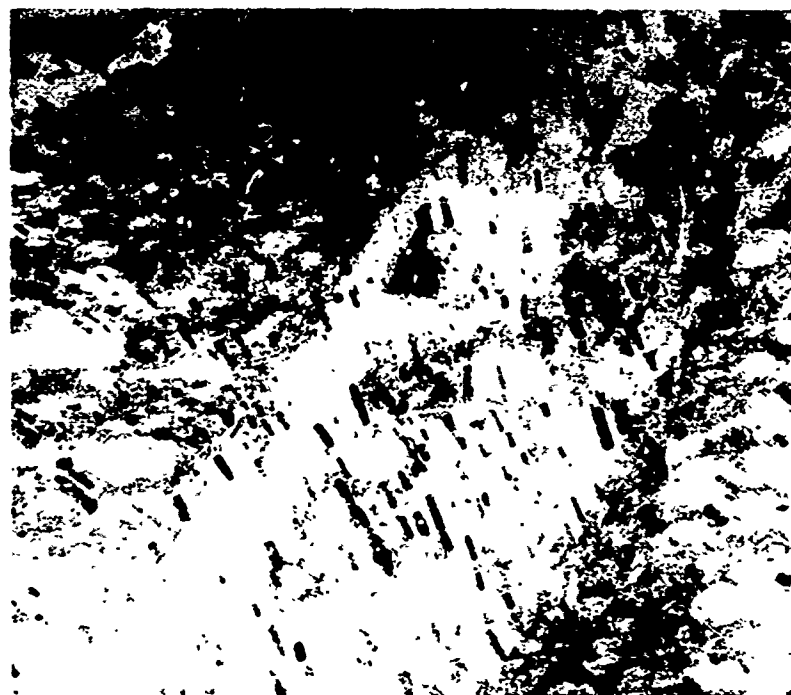
15,000X   EH3777

b.   Longitudinal Section

FIGURE 31.   RUN NO. 62; 2024 UPSET AT ROOM TEMPERATURE

7,500X   EH4069

a. Subgrains Near a Grain Boundary in Contrast

7,500X   EH4067

b. Subgrains Near the Center of the Same Grain in
    Contrast

FIGURE 32. RUN NO. 82; 2024 UPSET AT 800 F AT 0.016
            IN./SEC; TRANSVERSE SECTION

83

7,500X   EH4071

a. Subgrains in Contrast on One Side
of a Grain Boundary

7,500X   EH4072

b. Subgrains Near the Center of One of
the Grains in the Same Specimen

FIGURE 33.   RUN NO. 82; 2024 UPSET AT 800 F AT 0.016
IN./SEC; LONGITUDINAL SECTION NEAR
THE QUARTER DIAMETER

84

7,500X   EH4079

FIGURE 34.   RUN NO. 82; 2024 UPSET AT 800 F AT 0.016 IN./SEC; LONGITUDINAL SECTION NEAR THE CENTER SHOWING THE ALTERED STRUCTURE OF THE INTERMEDIATE PRECIPITATE ON ONLY ONE SIDE OF A GRAIN BOUNDARY
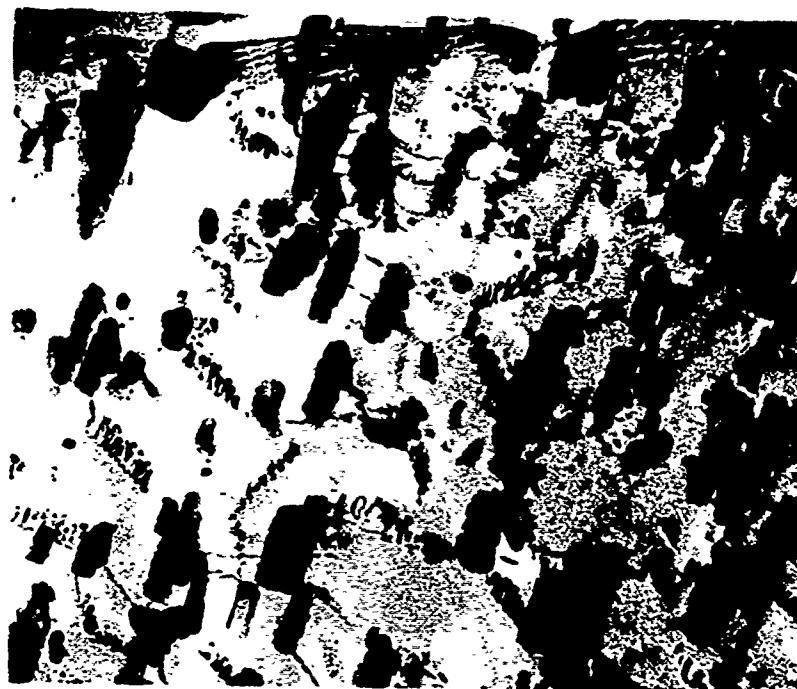
30,000X   EH4078

a. Structure of the Unaltered
    Intermediate Precipitate
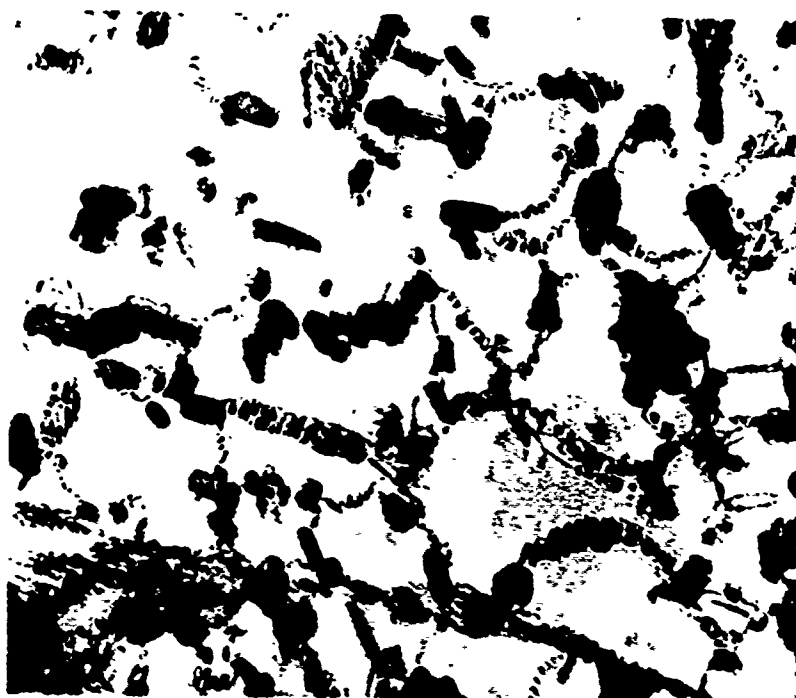
30,000X   EH4083

b. Structure of the Altered
    Intermediate Precipitate

FIGURE 35.   INTERMEDIATE PRECIPITATES IN TWO AREAS
             OF THE SPECIMEN SHOWN IN FIGURE 34

varying from 1.3 μm in small grains (which may actually have been larger grains that were intersected by the plane of the foil near a grain boundary) to 3.0 μm.

Figure 33 is from a longitudinal section near the quarter diameter in the specimen from Run 82 (the same approximate location as the transverse section shown in Figure 32), and again shows the smaller subgrain size that was usually found near grain boundaries. The subgrain size was approximately 1.5 μm in Figure 33a near the grain boundary and approximately 3.6 μm in Figure 33b near the center of a grain. Figure 33b also shows the slightly elongated subgrains that were frequently found in this specimen. The subgrain sizes varied between 1.3 and 1.5 μm near grain boundaries and between 1.3 and 3.0 μm toward the centers of grains (again, the smaller subgrain sizes toward the apparent centers of grains in the TEM foils may actually have occurred where the plane of the foil intersected a larger grain near a grain boundary).

The subgrain sizes near the center of the sample from Run 82 varied from approximately 1.3 to 7.1 μm toward the centers of the grains. As is implied by these results, several areas were observed near the center where the subgrain size was not measurably smaller at the grain boundaries, particularly for the larger subgrain sizes.

Another important feature observed in this sample in several areas was an alteration of the structure of the intermediate precipitate. Comparison of the intermediate precipitates shown in Figure 32 with those shown in the transverse section from the specimen deformed at room temperature in Figure 31a reveals that the intermediate precipitates in the specimen upset at 800 F are no longer parallel with a common direction but tend to lie along at least three different crystallographic directions. Slightly larger precipitates also appear to have formed along the grain boundaries, as is evident in Figures 32, 22, and 34. The structure of the intermediate precipitate appeared to remain unaltered in some portions of the specimens. This is shown in Figures 34 and 35. Figure 34 shows the structure along a grain boundary where the structure of the intermediate precipitate was altered in the grain to the right of the grain boundary and appeared to remain unaltered in the grain to the left. The structure of the unaltered precipitate is shown at higher magnification in Figure 35a, and that of the altered precipitate is shown in Figure 35b. Both areas show helical dislocations similar to those found in the solution heat treated starting material (Figure 29); these helical dislocations were present throughout all of the TEM specimens from the Run No. 82 upset specimen. The ends of the precipitates in Figure 35b are more rounded than those in Figure 35a. The ends of the precipitates in Figure 35a actually appear to correspond to those of the starting material in Figure 29b. This indicates that the altered and unaltered precipitates may be different types, since the round edges of the altered precipitates signifies that they may be more soluble than the unaltered precipitates. The presence of the unaltered precipitates at some locations of the Run No. 82 upset specimen may be indicative of a lower amount of upsetting in these locations. This appears to be substantiated by the somewhat larger subgrain sizes that were also found in these locations. The altered immediate precipitates have not as yet been identified. The behavior of the precipitates upon solution heat treating, which

87

will be discussed for the specimen from Run No. 91, also indicates that the intermediate precipitates formed during the upset at elevated temperatures are not the same as those in the starting material.

The structure in the upset specimen from Run No. 92, which was upset at the same temperature but at a higher strain rate than that in the upset specimen from Run No. 82, was nearly identical to that of the Run No. 82 specimen except for a smaller subgrain size. This similarity can be seen in Figure 36. Figure 36a shows subgrains along a grain boundary, while Figure 36b shows subgrains toward the center of a grain. Figure 36b is somewhat unique, however, because it resolves the fine dislocation structure in many of the subboundaries; the subboundary dislocation structure was usually difficult to resolve in the 2024 specimens. The subgrain size appeared to be fairly uniform in all of the transverse and longitudinal specimens that were examined. It varied between 0.9 to 1.5 μm along grain boundaries and between 1.3 to 3.0 μm toward the centers of the grains. Furthermore, nearly all of the subgrains in the longitudinal sections were equiaxed. The smaller subgrain size in the Run No. 92 specimen as compared with that in the Run No. 82 specimen is compatible with the different upsetting rates that were used.

The upset specimen from Run No. 91 was a duplicate of the Run No. 92 specimen that was solution heat treated for 1 hour at 920 F and water quenched. The specimen had been partially recrystallized. A boundary between a recrystallized area and an unrecrystallized area is shown in Figure 37 which is from a transverse section. The recrystallized area is free of helical dislocations, with only a few small dislocation loops around some of the intermediate precipitates. The dislocation loops were probably generated by quenching strains. Helical dislocations are still visible in the unrecrystallized area, and this along with the subboundaries provides a sharp distinction between unrecrystallized and recrystallized areas. The lengths of the intermediate precipitates have also shrunk appreciably, indicating that they are soluble at the solution temperature of 920 F. This contrasts sharply with the intermediate precipitates in the starting material which apparently withstood a 5-hour solution heat treatment at 920 F and indicates that the alteration of the structure of the intermediate precipitate during upsetting at elevated temperatures apparently involves the dissolution of the original precipitate and the formation of a different type of precipitate. Furthermore, the somewhat larger precipitates that had formed along the grain boundaries of the upset specimens appear to have been completely dissolved.

## Al-4.6Cu Specimens

Figure 38 shows the structure of the solution heat-treated Al-4.6Cu starting material. Remnants of slip traces as indicated by the band of dislocation loops and small helical dislocations in the figure were found throughout the specimen, but the matrix structure otherwise was homogeneous except for the formation of GP zones as indicated by the electron diffraction patterns.
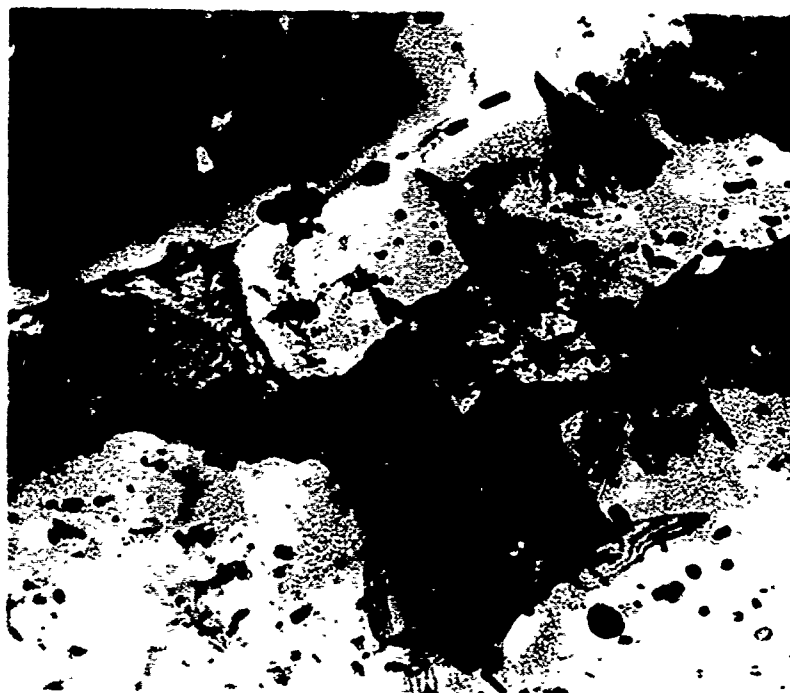
15,000X   EH3999

a. Near a Grain Boundary
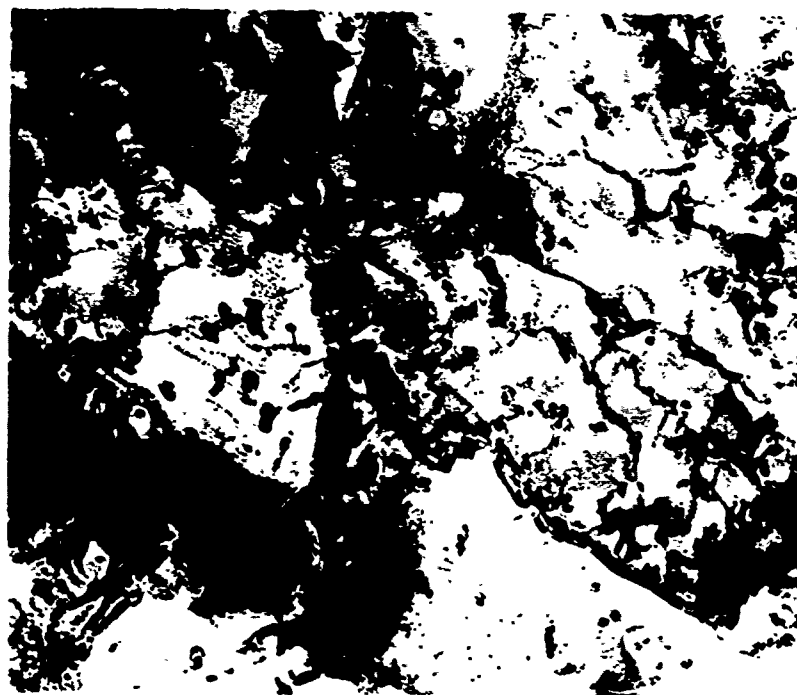
15,000X   EH3975

b. Towards the Center of a Grain

FIGURE 36.   RUN NO. 92; 2024 UPSET AT 800 F AT
8.8 IN./SEC; TRANSVERSE SECTION
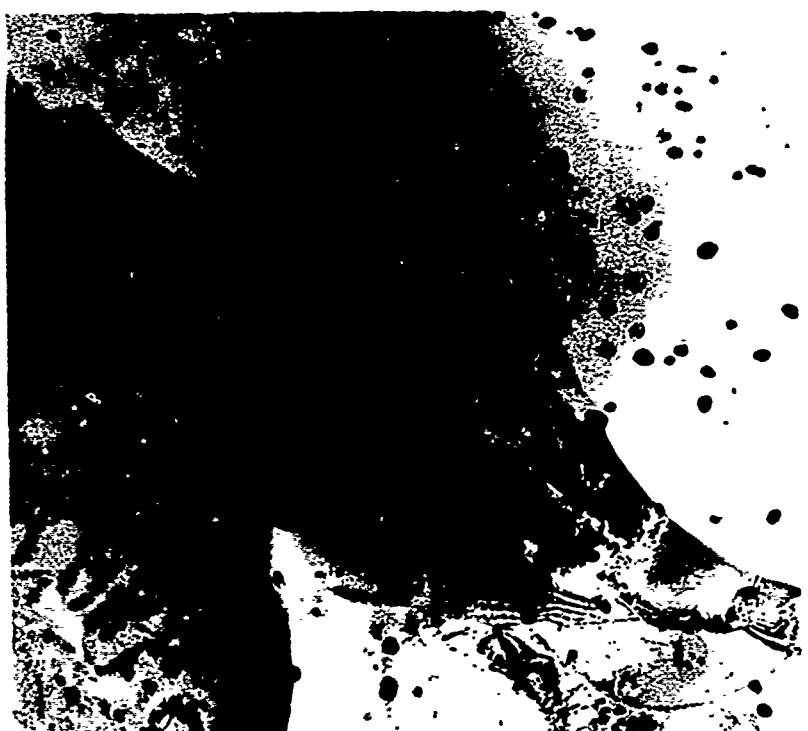
15,000X   EH3887

FIGURE 37.   RUN NO. 91; SOLUTION HEAT TREATED AFTER THE
             UPSET AT 800 F AT 8.8 IN./SEC; TRANSVERSE
             SECTION SHOWING PARTIAL RECRYSTALLIZATION
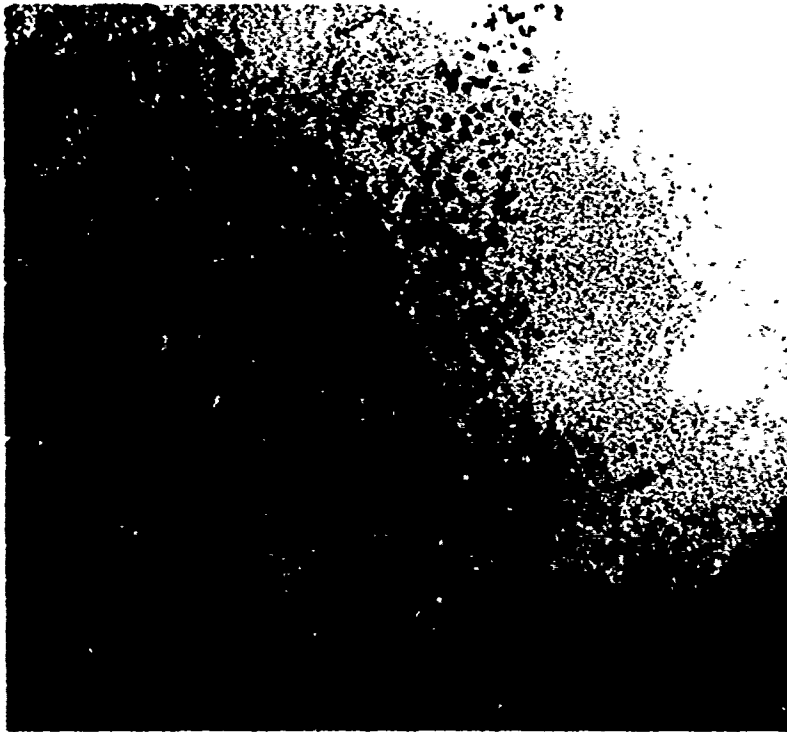
22,500X   EH3705

FIGURE 38.   SOLUTION HEAT TREATED Al-4.6Cu STARTING
                      MATERIAL: LONGITUDINAL SECTIONS

The structure in a longitudinal specimen from the Run No. 84 upset specimen is shown in Figure 39. This specimen was upset at 800 F at a rate of 0.016 in./sec. Figure 39a shows subgrains formed along a grain boundary, and Figure 39b shows the more coarse subgrains found toward the centers of the grains. Many of the subgrains in the longitudinal sections appeared to be elongated as in Figure 39b. The difference in the subgrain size along grain boundaries and toward grain centers did not appear to be as great in this specimen as in the 2024 specimens. The grain size varied between 1.8 and 2.5 μm near grain boundaries and between 2.1 and 5.1 5.1 μm toward the centers of the grains. Figure 39 also shows a coarse intermediate precipitate that formed in the upset specimen. Some of these precipitates exhibited diffraction contrast effects that were indicative of interfacial dislocations and may have been θ'; the remainder of the coarse precipitates may have been either θ' or θ. Again, the electron diffraction patterns showed evidence of the formation of GP zones in the matrix.

Transverse and longitudinal structures from the Run No. 94 specimen, which was upset at 800 F at a rate of 8.8 in./sec, are shown in Figure 40. The subgrain size in this specimen appeared to be somewhat smaller than that in the previous specimen, being approximately 1.8 μm at the grain boundaries and between 1.3 and 2.5 μm toward the centers of the grains. The subgrains in the longitudinal specimens were also equiaxed in contrast with those in the Run No. 84 specimen. The coarse intermediate precipitate again was present in this specimen as can be seen in the figures.

All of the specimens that were examined from the Run No. 93 upset specimen that had been solution heat treated after upsetting at 800 F at a rate of 8.8 in./sec were recrystallized. The structure was nearly identical to that shown in Figure 38.

No mention has been made of the dislocation structures visible in Figures 39 and 40 because of some uncertainty of their origin. The thinned material around all of the holes formed in the Al-4.6Cu specimens had a peculiar characteristic of slight buckling. Attempts were made to avoid regions that were obviously damaged by the buckling and the dislocation structures are suspected to be characteristic of the upset specimens, particularly since dislocation-free areas were easily found in the solution heat treated specimens. However, the buckling damage could be more extensive in the upset specimens than suspected. The dislocation structures should be viewed with this reservation in mind.

Future Plans

Work presently under way to define the temperature-strain rate conditions favoring recrystallization of 2024 and Al-4.6Cu material upset 50 percent on the Gleeble unit will be continued. Studies will be initiated immediately on the effects of holding upset samples at the upset temperature and at higher temperatures for

7,500X   EH4135

a.   Subgrains Near a Grain Boundary

7,500X   EH4136
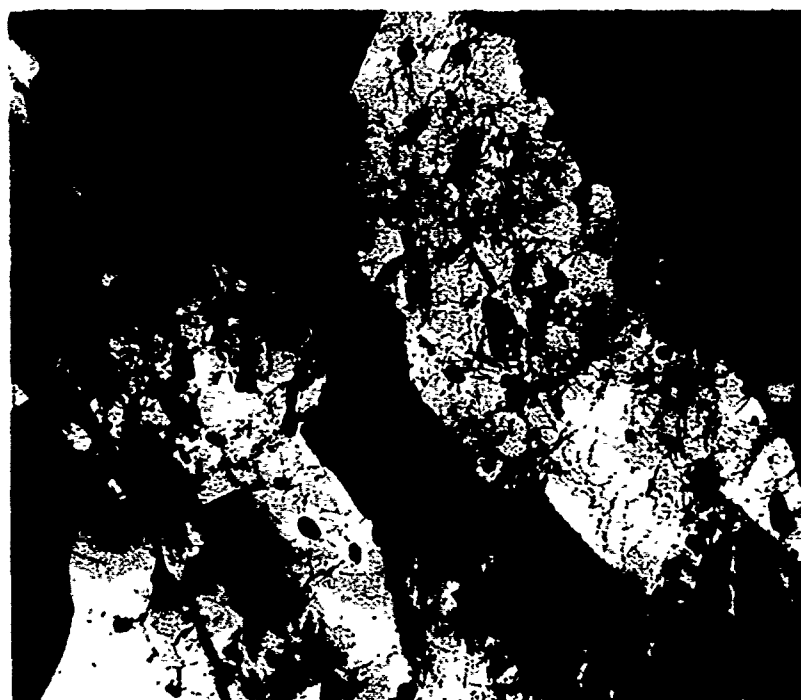
b.   Subgrains Towards the Center of a Grain

FIGURE 39.   RUN NO. 84; Al-4.6Cu UPSET AT 800 F AT
0.016 IN. /SEC; LONGITUDINAL SECTION

7,500X   EH4102

a. Transverse Section

7,500X   EH4126

b. Longitudinal Section

FIGURE 40.   RUN NO. 94; Al-4.6Cu UPSET AT 800 F
AT 3.8 IN./SEC

94

selected time intervals after upsetting on recrystallization behavior. We also plan to examine a tensile loading Gleeble procedure described in recent literature to determine if it will be of value in studying aluminum alloys[26]. In that program, steel samples were strained a fixed amount at temperature, held at temperature for various periods, and then tested to failure. Failure load was correlated with degree of recrystallization.

Processing studies of high-purity Al-Zn-Mg-Cu alloys will be continued in an attempt to develop a fine-grained, equiaxed microstructure in these materials. The properties of suitably processed material will be evaluated to determine any benefits accompanying control of grain structure.

V

REFERENCES

(1) J. D. Boyd, D. S. Thompson, D. N. Williams, and D. C. Drennan, "Research on Synthesis of High Strength Aluminum Alloy", 1st Semi-Annual Report on Contract F33615-71-C-1805, Battelle, January, 1972.

(2) D. S. Thompson and S. A. Levy, "High-Strength Aluminum Alloy Development", AFML Technical Report No. 70-171 (1970).

(3) D. Broek, "A Study on Ductile Failure", Netherlands National Aerospace Laboratory Report, 1970.

(4) J. P. Tanaka, et al., "Fractographic Analysis of the Low-Energy Fracture of an Aluminum Alloy", in Plane-Strain Fracture Toughness Testing, ASTM STP 462 (1970), p. 191.

(5) J. C. Grosskreutz, et al., "The Effect of Inclusion Size and Distribution on Fatigue of 2024-T4 Aluminum", AFML Technical Report No. 69-121 (1969).

(6) J. C. Grosskreutz and G. C. Shaw, "Mechanisms of Fatigue in 7075-T6 Aluminum", AFML Technical Report No. 66-96 (1966).

(7) K. Erhardt, "The Role of Structure, Low Strain Rates, High Strain, and Temperature on the Low-Cycle Fatigue Behavior of 2024-T4 Aluminum Alloy". AFML Technical Report, TR-69-35 (1969).

(8) F. Ostermann, "Improved Fatigue Resistance of Al-Zn-Mg-Cu (7075) Alloys Through Thermomechanical Processing", Met. Trans. 2, 2897 (1971).

(9) C. A. Stubbington, "Some Observations on Microstructural Damage Produced by Reversed Glide in an Al-7.5%Zn-2.5%Mg Alloy", Acta Met. 12, 931 (1964).

(10) M. O. Speidel, "Interaction of Dislocations With Precipitates in High-Strength Aluminum Alloys", in Fundamental Aspects of Stress-Corrosion Cracking, N. A. C. E., Houston (1969), p. 561.

(11) H. A. Holl, "Deformation Substructure and Susceptibility to Stress-Corrosion Cracking in an Aluminum Alloy", Corrosion 23, 172 (1967).

(12) P. N. T. Unwin and G. C. Smith, "The Microstructure and Mechanical Properties of Al-6%Zn-3%Mg", J. Inst. Met. 97, 299 (1969).

(13) K. G. Kent, "Microstructure and Stress-Corrosion Resistance of Al-Zn-Mg Alloys", J. Aust. Inst. Met. 15, 171 (1970).

(14) K. R. VanHorn, "Aluminum" ASM, 1967, Vol. I.

(15) H. Fredriksson and M. Hillert, "On the Mechanism of Feathery Crystalliza-
      tion of Aluminum", J. Materials Sci. 6, 1350 (1971).

(16) O. Izumi and D. Oelschägel, "On the Decomposition of a Highly Super-
      saturated Al-Zr Solid Solution", Scripta Met. 3, 619 (1969).

(17) A. Takashi and S. Komori, J. Light Metals, Japan 18, 425 (1968).

(18) A. J. Ardell and R. B. Nicholson, "The Coarsening of γ' in Ni-Al Alloys",
      J. Phys. Chem. of Solids 27, 1793 (1966).

(19) J. D. Boyd and R. B. Nicholson, "The Coarsening Behavior of θ'' and θ'
      Precipitates in Two Al-Cu Alloys", Acta Met. 19, 1379 (1971).

(20) A. J. Ardell, "The Effect of Volume Fraction on Particle Coarsening:
      Theoretical Considerations", Acta Met. 20, 61 (1972).

(21) A. J. Ardell, "Further Applications of the Theory of Particle Coarsening",
      Acta Met. 15, 1772 (1967).

(22) C. Atkinson, "Concentration Dependence of D in the Growth or Dissolution
      of Precipitates", Acta Met. 15, 1207 (1967).

(23) C. Laird and H. I. Aaronson, "Mechanisms of Formation of θ' Precipitates
      in an Al-4% Cu Alloy", Acta Met. 14, 171 (1966).

(24) H. J. McQueen, "Deformation Mechanisms in Hot Working", J. Metals,
      Volume 20, No. 4, April 1968, p. 31.

(25) C. K. H. DuBose and J. O. Stiegler, "Semiautomatic Preparation of Speci-
      mens for Transmission Electron Microscopy", Oak Ridge National Labora-
      tory, Report No. ORNL-4066, February, 1967.

(26) T. L. Capeletti, L. A. Jackman, and W. J. Childs, "Recrystallization Fol-
      lowing Hot Working of a High Strength Low Alloy (HSLA) Steel and a
      304 Stainless Steel at the Temperature of Deformation", Metallurgical Trans-
      actions, Volume 3, April 1972, p. 789.